WALKING THE LINE BETWEEN SURVIVAL AND DEATH

DROUGHT-INDUCED MORTALITY OF SCOTS PINE IS ASSOCIATED TO DISTINCTIVE GROWTH AND ECOPHYSIOLOGICAL RESPONSES

- TESI DOCTORAL -

Memòria presentada per:

Ana-Maria Hereş

Per optar al grau de Doctor

Programa de Doctorat (RD 778/1998) en DIVERSITAT I FUNCIÓ D'ECOSISTEMES MEDITERRANIS
CREAF, DEPARTAMENT DE BIOLOGIA ANIMAL, BIOLOGIA VEGETAL Y ECOLOGIA
UNIVERSITAT AUTÒNOMA DE BARCELONA

Amb l'acord dels directors de tesi:

Dr. Jordi Martínez-Vilalta
Professor Agregat
Universitat Autònoma de Barcelona

Dr. Bernat Claramunt López
Professor Titular
Universitat Autònoma de Barcelona

Bellatera, Setembre de 2013

Hereş, AM (2013)

Tesi doctoral. Programa de Doctorat (RD 778/1998) en Diversitat i Funció d'ecosistemes Mediterranis, CREAF, Universitat Autònoma de Barcelona

Tot el material grafic es de l'autora, excepte el disseny de la coberta, realitzat per Cristina Folgueira López.

Aquesta tesi s'ha dut a terme al CREAF (Centre de Recerca Ecològica i Aplicacions Forestals), Departament de Biologia Animal, Biologia Vegetal i Ecologia, Unversitat Autònoma de Barcelona

L'autora ha rebut finançament procedent d'una beca FPU (Formacion de Profesorado Universitario) concedida per el Ministerio de Ciencia e Innovacion, a l'any 2008.

„Împărat slăvit e codrul,
Neamuri mii îi cresc sub poale,
Toate înflorind din mila
Codrului, Măriei sale.”
(*Povestea codrului*, Mihai Eminescu)

“Els arbres són l’esforç sense fi de la terra per parlar amb al cel”
(Rabindranath Tagore)

Tatălui meu şi mămăiţa

CONTENTS

Chapters 2, 3 and **4** are written as scientific articles, being either published, accepted for publication or in preparation, as indicated separately for each of them when presented. Parts of the General Introduction and General Discussion and Conclusion might appear redundant due to coincidences with **Chapters 2, 3** and **4**. **Chapter 5** contains a technical report and detailed description of the software (**DACiA,** Dendrochronological Analysis on

Conifer Wood Anatomy) developed by us to measure wood anatomical features on transversal wood sections of conifer species. The **Bibliography** presented at the end of the manuscript gathers all the references from all chapters.

Chapter 1

GENERAL INTRODUCTION

DROUGHT-INDUCED TREE MORTALITY IN THE IBERIAN PENINSULA

Tree mortality episodes associated with drought and high temperatures have been reported in all the major forested biomes of the Earth over the last decades (Allen *et al.* 2010 and references therein). Considering that climatic models estimate an upcoming increase in temperature accompanied by a precipitation decrease (IPCC 2007), the frequency and intensity of severe droughts and further on climate-related tree mortality events are expected to increase. The western Mediterranean Basin is considered to be especially vulnerable to forest die-off (Giorgi and Lionello 2008; Martínez-Vilalta *et al.* 2012; Matías and Jump 2012), because here the climate is already hot and dry (during summer time) and temperatures are predicted to increase 3-4ºC (Christensen *et al.* 2007) while precipitations might drop up to 20% (Bates *et al.* 2008) during the 21st century. Indeed, the whole Mediterranean region has been identified as being a "hot spot" for climatic changes (Giorgi 2006), especially considering that the increased temperatures and low precipitations are projected to occur mostly during the summer season (Giorgi and Lionello 2008), which is already the period when plants growing in this ecosystem type undergo stressful drought conditions that limit their growth and distribution (Cherubini *et al.* 2003 and references therein; Martínez-Vilalta *et al.* 2008).

The Iberian Peninsula, where the study sites of this thesis are located, has already experienced drought-related tree decline and mortality events (e.g., Peñuelas *et al.* 2000; Martínez-Vilalta and Piñol 2002; Corcuera *et al.* 2006; Galiano *et al.* 2010). Furthermore, for this particular Mediterranean area, forest composition and distribution models estimate that, in the future (projections made for years 2020, 2050 and 2080), climatic changes are likely to induce important reductions in the potential ranges of several tree species (Benito Garzón *et al.* 2008). Nevertheless, considering that different populations of the same species are not equally vulnerable to climate changes (Ramírez-Valiente *et al.* 2009), future range shifts are expected to have a local character, depending on species plasticity, adaptation and capacity to survive stressful conditions (Benito Garzón *et al.* 2011).

Drought events have a stochastic character and can cause important damages to forest ecosystems, especially if they extend over large periods of time or if they are severe (e.g., extreme climatic events) (Bréda and Badeau 2008). As a consequence, when such conditions are met, *the acclimation capacities of the trees are challenged and likely to be exceeded* leading to severe damages from which they might not be able to recover (Gutschick and BassiriRad 2003). This depends also on species' sensitivity and/or on antecedent conditions to which trees have been exposed to (Beniston and Innes 1998) and weakened by, increasing their vulnerability to future stressful conditions (Bréda and Badeau 2008). Severe drought conditions impact on the physiology of trees (Bréda *et al.* 2006) describing a closed circle that starts by affecting water transport and photosynthesis and continues with allocation processes, root growth and thus water and nutrient uptake, and defoliation, hence further reducing photosynthesis (Pedersen 1998).

IMPLICATIONS OF FOREST MORTALITY

Forest mortality is a natural ecological process (Franklin and Shugard 1987) that can be exacerbated by extreme climatic conditions such as severe droughts or heat waves which can act directly or indirectly, through changes on insect and pathogen dynamics or increased incidence of wildfires (Allen *et al.* 2010). Although at present we lack clear understandings on the ecological implications that forest mortality have and will have, some studies are starting to explore such consequences at scales that go from local (structure, functions, services) to global (e.g., carbon sinks, climate regulation) (Anderegg *et al.* 2013*a*).

At local scales, mortality might affect selectively only some of the tree species from a mixed stand, thus perturbing the forest structure, whose community composition changes and increases the possibility, on a large time scale, of vegetation shifts. Succession processes after drought-induced mortality events are still poorly documented and understood (but see Allen and Breshears 1998), although there is an increasing interest on how understory vegetation might react when the dominant species undergoes death. Accompanying species may either be favoured or severely affected depending on their interactions with the dominant species (Galiano *et al.*

2013; Anderegg *et al.* 2013*a* and references therein), with very different implications for midterm vegetation dynamics (Lloret *et al.* 2012). Tree death also involves changes in the functions of the forest ecosystem, as both the water (soil water content and availability, run-off) and the energy (increased radiation at the floor level) fluxes are highly likely to be perturbed. Also, the risk of forest fires might be increased in the short term by the accumulated litter on the ground floor, which can provide better fuel conditions for the propagation of wildfires (Bigler *et al.* 2005). At the same time, it is clear that tree mortality episodes have the potential to affect all ecological services provided by forests to society, including provisioning (food, timber), regulating (climate control, water quality), supporting (soil, nutrient cycling) and cultural services (recreation, aesthetic benefits) (see Anderegg *et al.* 2013*a* and references therein).

At a global scale, widespread drought-induced tree mortality events are expected to weaken the role that forests have as carbon sinks (it is estimated that ≈45% of the carbon found in terrestrial ecosystems is hold by forests), as the carbon uptake and sequestration processes will be altered (Bonan 2008; Anderegg *et al.* 2013*a*). At the same time, implications on biogeochemical cycles and climatic regulation are also expected to occur as a consequence of land cover changes that involve land-surface properties (e.g., albedo, evapotranspiration, hydrologic cycles) (Bonan 2008; Anderegg *et al.* 2013*a*). Thus, although little evidence is provided by now, changes in temperature and precipitation rates are expected to take place. Nevertheless, it must be taken into consideration that all these potential changes will largely vary, depending on factors such as the type of forest, latitude, snow cover or ecosystem responses (Anderson 2011; Anderegg *et al.* 2013*a*).

MECHANISMS OF DROUGHT-INDUCED TREE MORTALITY

Under the predicted climate change scenarios, the threat of widespread tree mortality events has lead to an increased interest and debate on the mechanisms that underlie drought-induced tree mortality (McDowell *et al.* 2008; Sala *et al.* 2010; McDowell and Sevanto 2010; McDowell 2011; McDowell *et al.* 2011; Sevanto *et al.* 2013). Understanding these processes can help us predict future forests dynamics (land-

surface changes and stability) and, further on, the implications for the services and functions provided by forests (Bonan 2008; Allen *et al.* 2010; Anderegg *et al.* 2013*a*).

Manion (1991) proposed the slow-decline hypothesis that combines biotic and abiotic factors to explain tree mortality. According to his hypothesis, plants are subjected over many years to a three-stage decline, involving predisposing, inciting and contributing factors. The predisposing factors are acting over long time periods, weakening the tree. They are represented by the age, the genetic predisposition of the individuals or by factors like the site conditions. The inciting factors include defoliation, frost or severe drought events and act at a short time scale, accentuating the decline of the already weakened trees. The contributing factors, like opportunistic pathogens and/or subsequent drought events, finally kill the declining trees. However, Manion's framework does not describe the physiological processes involved in tree mortality.

More recently, McDowell *et al.* (2008) developed a hydraulically based framework to explain the physiological mechanisms that underlie drought-induced tree mortality. These authors hypothesized three mechanisms leading to tree mortality, depending on the environmental conditions (e.g., intensity and duration of water stress) and the stomatal regulation of the species involved: hydraulic failure, carbon starvation and biotic agents. We will focus on the first two here. Hydraulic failure is likely under intense drought and for species without a strict stomatal control to regulate water loss during drought (i.e., anisohydric species). In these species, xylem water potentials can reach very low negative values, causing catastrophic levels of xylem cavitation (Tyree and Zimmermann 2002), which can eventually result in irreversible desiccation of aboveground plant tissues and cellular death. On the other hand, carbon starvation is particularly likely for long-lasting droughts and for species with a tight stomatal regulation. In these isohydric species water potentials may not become negative enough to cause embolism in the xylem, but long periods of near zero assimilation, due to stomatal closure, and continued demand for carbohydrates may exhaust the plant carbon reserves (McDowell *et al.* 2008).

The mechanisms that underlie drought-induced tree mortality proposed by McDowell *et al.* (2008) have been very influential and controversial, particularly regarding the carbon

starvation hypothesis, for which we still lack conclusive evidence (Sala *et al.* 2010; McDowell and Sevanto 2010). According to Sala *et al.* (2010), this mechanism of drought-induced tree mortality is difficult to explain in the absence of the hydraulic failure one and/or contingent related biotic factors (e.g., pathogens) attack. This is due in part to the fact that carbon mobilization may be limited under water shortage conditions, due to phloem transport impairment. Sala *et al.* (2010) and McDowell and Sevanto (2010) highlighted that a tree could actually die without having completely depleted its carbon pools, because part of the stored carbohydrates may in fact not be available for metabolism, especially under drought conditions. Later on publications have shown that the two mortality mechanisms proposed by McDowell *et al.* (2008) are actually highly interdependent (McDowell 2011; McDowell *et al.* 2011; Sevanto *et al.* 2013). Under drought conditions, tree mortality seems to be determined by a complex set of interrelated changes in the carbon and water economy of plants, involving differential effects on photosynthesis and respiration, hydraulic deterioration and, possibly, phloem impairment (Galiano *et al.* 2011; McDowell 2011; Anderegg *et al.* 2013*b*; Sevanto *et al.* 2013).

A RETROSPECTIVE APPROACH TO STUDY TREE MORTALITY

Most studies of tree and forest mortality use experimental or observational approaches to characterize forest responses to current drought events. However, retrospective analyses of how trees reacted to severe droughts in the past can also help us understand their functioning and give us clues about how they might react in the future (Fritts 2001; Vaganov *et al.* 2006). Tree rings are widely used proxies to study long time tree-growth climate relationships, as they faithfully register events to which trees' have been exposed during their lifetime. Thus, they represent natural archives of information based on which the past responses to environmental events can be reconstructed (Fritts 2001; Vaganov *et al.* 2006). Dendrochronological studies are based on the concept that trees growing in the same area are similarly influenced by external factors' variability (Fritts 2001; Vaganov *et al.* 2006). Thus, tree individuals can be combined and compared among them looking for patterns that might explain their differential sensitivity to environmental variability or severe climatic events, such as drought episodes. By comparing trees that perished as a result of a given drought event with surviving

individuals, tree ring width dynamics can be used to characterize the growth patterns of trees that are likely to die in the future (Ogle *et al.* 2000; Suarez *et al.* 2004; Bigler *et al.* 2006; Levanič *et al.* 2011; Eilmann and Rigling 2012; Matías and Jump 2012).

Besides their width, tree rings contain valuable information that can be used to infer the trees' past physiological performance and responses to stressful conditions. Carbon isotope composition ($\delta^{13}C$) is commonly used as a proxy to retrieve physiological information from wood records (Fritts 2001; McCarroll and Loader 2004; Vaganov *et al.* 2006). Wood is mainly formed by carbon, oxygen and hydrogen, and each of these three elements has different stable isotopes (non-reactive). Carbon (C) has two stable isotopes, ^{12}C and ^{13}C. Each of these two isotopes has six protons, but different number of neutrons: six for ^{12}C and seven for ^{13}C, respectively. Due to these atomic weight differences, physical, chemical and biological processes discriminate between these isotopes, usually favouring the lighter one (i.e., ^{12}C). Nevertheless, most of these processes are tightly dependent on climatic conditions and, thus, by analyzing the variation of the isotope composition (i.e., $\delta^{13}C$) in tree rings, the variation and effects of environmental signals can be estimated.

During carbon fixation, plants discriminate against ^{13}C (McCarroll and Loader 2004) both during diffusion through stomata (4.4‰; O'Leary 1981) and carboxylation by Rubisco and PEP carboxylase (27‰; Farquhar and Richards 1984). Under dry conditions, when stomata close in order to avoid water loss, the discrimination against ^{13}C is reduced as the relative importance of diffusion versus Rubisco and PEP carboxylase discrimination changes (McCarroll and Loader 2004 and references therein). This is a frequent situation in seasonally-dry climates areas, like the Mediterranean, where $\delta^{13}C$ depends tightly on water availability due to the impact of drought on stomatal conductance (Warren *et al.* 2001; Ferrio *et al.* 2003). Thus, $\delta^{13}C$ in tree rings can be used as an estimator of intrinsic water-use efficiency (WUE_i; the ratio of assimilation to water loss through the stomata), a key component of plant drought responses (Farquhar *et al.* 1982).

Wood anatomical features are another proxy used to analyze the past physiological behaviour of plants, having the advantage of a higher temporal resolution than tree

rings themselves (Fritts 2001). The production of xylem conduits (tracheids in gymnosperms and mostly vessels in angiosperms) and the subsequent processes of enlargement and cell-wall thickening have a strong genetic control. Nevertheless, all those processes, which can last from days to weeks, are also affected, directly or indirectly, by environmental conditions (Denne and Dodd 1981; Wimmer 2002; Schweingruber 2007; Fonti *et al.* 2010). These environmental effects on wood formation are both species- and site-specific (Tardif *et al.* 2003).

Environmental conditions can determine important aspects such as the forming period of a tree ring (Camarero *et al.* 1998), and they can also influence the photosynthesis process by inducing stomatal closure under drought conditions, and thus potentially limiting the available carbon for growth (McDowell *et al.* 2008). Further on, cell enlargement processes are driven by turgor and, therefore, the water status of the xylem plays a critical role on final cell size (Boyer 1985). At the same time, the hydraulic conductivity of a xylem conduit is a function of the fourth power of its lumen diameter, which determines a very tight dependence between conduit dimensions and hydraulic function (Tyree and Zimmermann 2002). Finally, the relative dimensions of the conduits' lumen and cell wall thickness determine important biomechanical properties, including resistance to implosion under high tension, such as those experienced by plants under drought. This resistance to implosion has been related to the vulnerability to xylem embolism across species (Hacke *et al.* 2001). The anatomical properties of xylem conduits are faithfully registered in growth rings and can be studied through image analyses of wood micro-sections.

TREE SPECIES GROWING AT THEIR SOUTHERN LIMIT OF DISTRIBUTION

Plant species' geographical distribution is limited to areas where biotic and abiotic factors allowed them to colonize and further on grow and reproduce (Woodward 1987). These conditions are being altered by ongoing climate change (IPCC 2007). The impact of these changing conditions is likely to be especially apparent at species' range edges, as it is in theses areas where species normally grow at their tolerance limits (Hampe and Petit 2005), being prone to suffer high mortality rates and reduce their area of distribution (Benito Garzón *et al.* 2008, 2011).

Species growing close to the southern distribution limit, where drought and high temperatures usually represent their main constraining factors (Hampe and Petit 2005), are particularly interesting as they provide the opportunity to study the species' behaviour under the conditions that will presumably become common at more northern latitudes in the future (Martínez-Vilalta *et al.* 2012). Also, as such populations many times represent refuges of species' genetic diversity (Petit *et al.* 2003; Hewitt 2004), their study can help us estimate and understand the implications for overall genetic diversity loss (García López and Allué Camacho 2010). At the same time, populations at the dry limit of a species distribution may have specific adaptations that increase their resistance and resilience to future drought, an aspect that needs to be studied and considered when projecting future vegetation dynamics (e.g., northward migrations) (Benito Garzón *et al.* 2011; Lloret *et al.* 2012) that may be imposed by predicted climatic changes (IPCC 2007).

OUR STUDY SYSTEM: SCOTS PINE UNDER MEDITERRANEAN CONDITIONS

Scots pine (*Pinus sylvestris* L.) is a Eurosiberian tree species considered to be the conifer with the widest distribution in the world (Nikolov and Helmisaari 1992). Although especially common in northern latitudes, where it finds its optimal growth conditions, it has a wide ecological niche. Its distribution range spans from Southern Spain (Sierra Nevada) to Northern Europe (the Scandinavian Peninsula, Siberia) and from Western Spain (Galicia) to Eastern Russia (Yacutia) (Figure 1.1). Thus it tolerates a broad range of climatic conditions that vary from dry to extreme cold and from oceanic to continental climates (Carlisle and Brown 1968). In the Iberian Peninsula it reaches its south-western (and dry) distribution limit (Barbéro *et al.* 1998), usually occupying mountain environments at relatively high altitudes (Ceballos and Ruiz de la Torre 1971; Boratynski 1991) (Figure 1.1).

Figure 1.1 – Distribution map of Scots pine (*Pinus sylvestris* L.). Original source: EUFORGEN 2009 (www.euforgen.org).

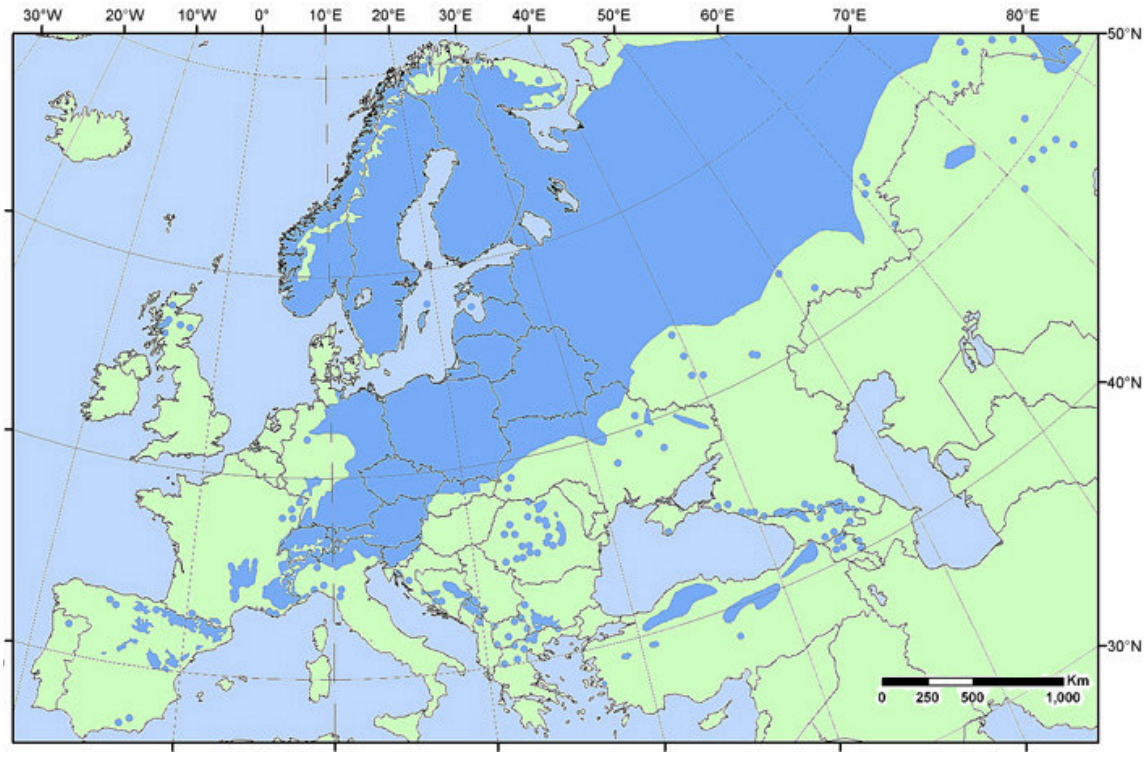

In Spain, Scots pine is the third most abundant trees species and it is estimated that ≈50% of its range is represented by natural populations (Catalan Bachiller *et al.* 1991; Martín *et al.* 2010). In this area, summer drought is considered its main limiting environmental factor (Castro *et al.* 2004; Mendoza *et al.* 2009; Matías *et al.* 2011*b*). It is here and in the dry Swiss alpine valleys, where Scots pine has experienced important mortality rates over the last decades, especially following extremely dry years (Martínez-Vilalta and Piñol 2002; Galiano *et al.* 2010; Eilmann *et al.* 2006; Bigler *et al.* 2006; Rigling *et al.* 2013). Although drought conditions might not lead directly to tree mortality, they can weaken the trees making them more sensitive to future drought events or pathogen attacks (Dobbertin *et al.* 2005; Giuggiola *et al.* 2010). Despite recent advances in understanding the spatial determinants of tree mortality in this species (Galiano *et al.* 2010; Vilà-Cabrera 2011, 2013), as well as on the physiological mechanisms underlying mortality (Galiano *et al.* 2011; Poyatos *et al.* 2013), the fine scale determinants of mortality and the reasons why some individuals succumb to death while some co-occurring individuals survive are still unknown. From the water use point of view, Scots pine is an isohydric species that closes stomata

rapidly when water shortage conditions are met (Irvine *et al.* 1998; Poyatos *et al.* 2013), thus limiting carbon uptake. Ongoing research at the same sites studied in this thesis has confirmed that carbon starvation (cf. McDowell *et al.* 2008) is likely to be involved in the mortality process (Galiano *et al.* 2011; Poyatos *et al.* 2013), although other mechanisms can not be discarded.

The relatively high drought-related mortality rates observed in several Scots pine populations in Spain, together with the low regeneration rates that have been reported (Castro *et al.* 2004; Mendoza *et al.* 2009; Galiano *et al.* 2010; Vilà-Cabrera *et al.* 2011), suggest that this species may not be able to cope with ongoing climate change in some areas, especially at its southern distribution limit (Reich and Oleksyn 2008; Matías and Jump 2012). This prediction is consistent with the results of climate envelope models suggesting that the potential habitat for this species in Spain might shrink substantially by the end of the current century (Benito Garzón *et al.* 2008, 2011). As current climatic changes are occurring faster than in the past (e.g., after glaciations), it is estimated that Scots pine species will require a faster rate of biotic response in order to cope with climate change (Savolainen *et al.* 2011). In this context, it is critical to determine which populations are at greater risk and what determines the differential susceptibility of individuals within populations, as Scots pine is a valuable tree species both from ecological and economical point of view (Matías and Jump 2012 and references therein). Furthermore, Iberian Scots pine populations are genetically different from other European ones, which involves potential loss of genetic diversity (García López and Allué Camacho 2010).

OBJECTIVES AND STRUCTURE OF THE THESIS

This thesis contributes to the study of drought-associated tree mortality. More specifically, in this thesis I study Scots pine mortality at two sites located in NE Iberian Peninsula, where this species started to suffer high mortality rates following severe drought episodes during the 1990s and 2000s. In order to do this, co-occurring now-dead and living Scots pine individuals were sampled and their growth rings were investigated in detail with regards to radial growth patterns, carbon isotopic composition and wood anatomy. The general objective was to compare surviving and

now-dead trees to see why some of the individuals survive while others perish following drought events, given that they lived under similar environmental conditions.

The specific objectives were to: (**A**) test if a direct association could be established between tree mortality events and drought episodes, as characterized by climatic variables; (**B**) determine whether now dead trees presented a distinctive growth pattern than surviving ones, which could be eventually used to assess the future vulnerability of individuals and populations; and (**C**) characterize the physiological performance of now-dead trees during the period preceding death, in terms of water-use efficiency, water transport capacity and carbon availability and use, in order to contribute to the current debate on the mechanism of drought-induced mortality.

Several hypotheses concerning the trees that had increased susceptibility to undergo death by comparison with the ones that survived stood at the base of this thesis (Diagram 1.1). A first one was that mortality would especially affect Scots pine trees with low growth rates and increased climatic sensitivity. Growth rates (e.g., annual tree rings) are indicators of trees' vigour (Pedersen 1992). They can be considered as sensitive indicators of stress conditions (e.g., climatic events such us droughts) as stem growth has low priority for resource allocation (Waring and Pitman 1985) by comparison with other organs (e.g., buds, needles, roots) (Waring 1987), when such conditions are met. A second hypothesis was that now-dead Scots pine trees had limited intrinsic water-use efficiency (WUE_i) responsiveness to raising atmospheric CO_2 conditions while alive. Trees have the ability to increase their WUE_i as the atmospheric CO_2 concentrations rise. Nevertheless, this increase can be restricted under limited water conditions that can counterbalance the stimulating effect of increasing CO_2 concentrations on the plant carbon budget (Waterhouse *et al.* 2004). Finally, a third hypothesis was that death would affect Scots pine individuals with reduced hydraulic conductivity and low carbon investments in tissue formation and tree defence. As hydraulic conductivity can be estimated from measurements of wood anatomical features, a reduced tracheid production or the formation of small size (e.g., lumen diameter) tracheids due to water shortage conditions would indicate its limitation (Tyree and Zimmermann 2002). At the same time, this would imply low

carbon allocations to tissues' formation due to their unavailability or to their preferential use for other organs (Waring 1987; Eilmann *et al.* 2009).

Diagram 1.1 – Structure and hypothesis of the thesis

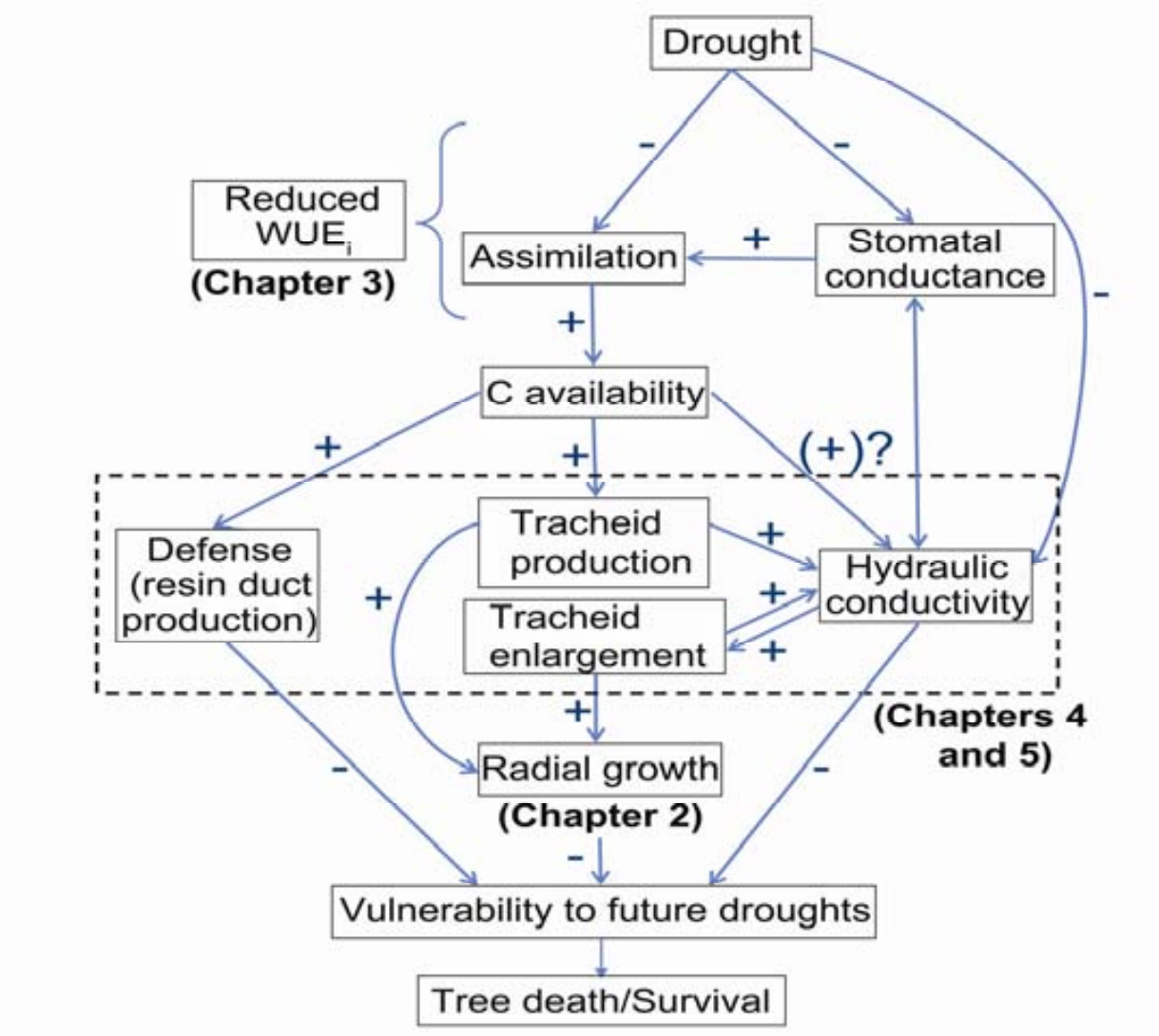

SHORT DESCRIPTION OF MAIN CHAPTERS:

Chapter 2: **Growth patterns in relation to drought-induced mortality at two *Pinus sylvestris L.* sites in NE Iberian Peninsula**

In this chapter we investigate the association between episodes of Scots pine mortality and the drought conditions that preceded them at two different sites in NE Spain. In addition, the radial growth and climatic sensitivity of the trees that managed to survive is compared to that of those that died.

Chapter 3: **Drought-induced mortality selectively affects *Pinus sylvestris* L. trees that show limited intrinsic water-use efficiency responsiveness to raising atmospheric CO_2**

In this chapter we study the ecophysiological differences between surviving and now-dead Scots pine trees at the same two sites, in terms of intrinsic water-use efficiency (WUE_i). Carbon isotopic composition ($\delta^{13}C$) and discrimination ($\Delta^{13}C$) are analyzed at an annual resolution in tree rings, for a 34 years period. We focus on the factors that might underlie predispositions to mortality. In order to do so, the relationship between previously measured growth rates (see **Chapter 2**) and WUE_i is also assessed.

Chapter 4: **Declining hydraulic performances and low carbon investments predate Scots pine drought-associated mortality at its south-western distribution limit**

In this chapter we use wood anatomy features to compare the physiological performance of now-dead and surviving trees, particularly in terms of carbon use and xylem hydraulic properties and for the period immediately preceding tree mortality. Wood anatomical features were measured in the earlywood and latewood at an annual resolution (34 years period) using a novel software developed by us for this purpose (see **Chapter 5**).

Chapter 5: **Measurements of wood anatomical features in conifer species. Image analyses with DACiA. Technical Report**

All wood anatomical measurements on transversal wood section of Scots pine wood were carried out with a novel software (**DACiA,** Dendrochronological Analysis on Conifer Wood Anatomy), developed for this purpose. This chapter provides a detailed description of this software and of its functioning. Technical information is also provided together with a comparison with other available softwares that are used for similar purposes.

Chapter 2

GROWTH PATTERNS IN RELATION TO DROUGHT-INDUCED MORTALITY AT TWO *PINUS SYLVESTRIS* L. SITES IN NE IBERIAN PENINSULA

A modified version of this chapter is published in *Trees Structure and Function* **26**, 621-630

Hereş AM, Martínez-Vilalta J, Claramunt López B, 2012

ABSTRACT

Drought-related tree mortality has become a widespread phenomenon. Scots pine (*Pinus sylvestris* L.) is a boreal species with high ecological amplitude that reaches its south-western limit in the Iberian Peninsula. Thus, Iberian Scots pine populations are particularly good models to study the effects of the increase in aridity predicted by climate change models. A total of 78 living and 39 dead Scots pines trees were sampled at two sites located in the NE of the Iberian Peninsula, where recent mortality events have been recorded. Annual tree rings were used to (1) date dead trees; (2) investigate if there was an association between the occurrence of tree death and severe drought periods characterized by exceptionally low ratios of summer precipitation to potential evapotranspiration (P/PET); and (3) to compare the growth patterns of trees that died with those of surviving ones. Mixed models were used to describe the relationships between tree growth (in terms of basal area increment, BAI, and the percentage of latewood, LW%) and climate variables. Our results showed a direct association between Scots pine mortality and severe drought periods characterized by low summer water availability. At the two sites, the growth patterns of dead trees were clearly distinguishable from those of the trees that survived. In particular, the BAI of dead trees was more sensitive to climate dryness (low P/PET_{summer}, high temperatures) and started to decline below the values of surviving neighbours 15-40 years before the time of death, implying a slow process of growth decline preceding mortality.

INTRODUCTION

Climatic models estimate that mean annual temperatures in the western Mediterranean Basin will rise ≈3-4ºC in the next century (Christensen *et al.* 2007), while the annual precipitations will decrease up to 20% (Bates *et al.* 2008). These predicted climatic conditions will probably result in reduced summer soil moisture (Douville *et al.* 2002; Christensen *et al.* 2007) and more frequent and intense drought episodes (Bates *et al.* 2008). These changes are likely to affect vegetation and have the potential to transform landscapes at regional scales (Allen and Breshears 1998; Allen *et al.* 2010). Several studies suggest that coniferous species may be particularly vulnerable to drought-induced decline both in the Mediterranean Basin (Martín-Benito *et al.* 2008; Linares *et al.* 2010) and other regions of the world (Ogle *et al.* 2000; Guarín and Taylor 2005; Bigler *et al.* 2006; van Mantgem *et al.* 2009).

Tree rings have been widely used to study climate–tree growth interactions, based on the fact that each ring registers fluctuations of the environmental factors that influence tree growth, and assuming that the trees growing in the same area are influenced in a similar way by climatic variability (Fritts 2001; Vaganov *et al.* 2006). In particular, tree rings have been used to reconstruct past climate fluctuations (e.g., Helama *et al.* 2002; Grudd *et al.* 2002; Helama *et al.* 2009) and to study the sensitivity and variability of tree growth in response to climate (e.g., Guarín and Taylor 2005; Bigler *et al.* 2006; Martín-Benito *et al.* 2008). In that respect, they provide a powerful tool to characterize trees that are particularly likely to die (Ogle *et al.* 2000; Suarez *et al.* 2004; Bigler *et al.* 2006).

The mechanisms that lead to tree mortality during drought events are complex and still to be completely understood (McDowell *et al.* 2008; Sala *et al.* 2010; McDowell 2011) due to the multiple intrinsic and extrinsic contributing factors (Pedersen 1998). Predisposing factors, like competition or air pollutants, can affect a tree during long periods of time and can increase its sensitivity to short-term stressors such as insect defoliation or drought (Bigler *et al.* 2006). Depending on the tree's condition and the severity of the stress factor, a tree may be able to recover its previous state or not (Dobbertin 2005; Bigler *et al.* 2006). Trees that don't completely recover are likely to be more susceptible to die (Pedersen 1998; Drobyshev *et al.* 2007), and their death

might emerge as a delayed effect years after the immediate impact of the stress factor (Guarín and Taylor 2005; Bigler *et al.* 2007; Galiano *et al.* 2011). Isohydric species, like most pines, are known to reduce stomatal conductance during periods of low water availability, lowering carbon uptake (and eventually growth) and running the risk of starving to death if dry conditions last long enough (McDowell *et al.* 2008).

Scots pine (*Pinus sylvestris* L.) is one of the most widely distributed tree species on Earth, with populations ranging from Boreal to Mediterranean regions (Barbéro *et al.* 1998). The sites in the Iberian Peninsula represent the south-western limit of the distribution of this species and include some of its driest populations. Iberian Scots pine populations are thus particularly good models to study the effects of predicted future climate change (Martínez-Vilalta *et al.* 2008). Due to its isohydric regulation with efficient stomatal control of water loss (Irvine *et al.* 1998), Scots pine is considered as being a relatively drought resistant species (Ellenberg 1988). In spite of this, drought-induced Scots pine mortality has been reported in many populations over the last decades, particularly towards the southern end of its distribution (Martínez-Vilalta and Piñol 2002; Bigler *et al.* 2006; Galiano *et al.* 2010).

In this study we use tree rings to date dead trees, to investigate Scots pine mortality following severe droughts and to compare the patterns of radial growth of dead and living individuals from two sites located in the North East of the Iberian Peninsula. Our main objectives were: (1) to determine if the occurrence of mortality of the Scots pine trees sampled at the two study sites was associated with severe drought periods; and (2) to compare the growth patterns of the trees that died with those of the trees that survived. We hypothesized that mortality would affect preferentially the trees with low growth rates and high growth sensitivity to dry climatic conditions (Pedersen 1998; Ogle *et al.* 2000; Suarez *et al.* 2004).

MATERIALS AND METHODS

Study sites and field work

Two Scots pine sites were selected in the North East of the Iberian Peninsula (Catalonia), one situated in the Prades Mountains (41°33´N, 1°01´E, 800-1000 m

a.s.l.) and another one in Arcalís, Central Pyrenees (42°34´N, 1°09´E, 1000-1300 m a.s.l.) (Table 2.1). At these two sites, important mortality rates have been recently observed and current standing mortality is about 20%: in Prades after severe droughts in 1994, 1998 and the early 2000s (Martínez-Vilalta and Piñol 2002) and in Arcalís particularly after a drought episode registered in 2005 (Galiano *et al.* 2010). The two study sites are located in protected areas (Prades is in the National Interest Site of Poblet and Arcalís is in the Alt Pirineu Natural Parc), where forest management has been minimal for the last decades.

The climate in Prades is typically Mediterranean, with an annual mean temperature of 11.2°C and an annual mean rainfall of ≈611 mm (Climatic Digital Atlas of Catalonia, period 1951-2006) (Pons 1996; Ninyerola *et al.* 2000). The substrate is composed by Paleozoic slates and metamorphic sandstones with microconglomerates (Piñol *et al.* 1991), while the soils are xerochrepts with clay-loam texture (Hereter and Sánchez 1999). The vegetation follows the climatic gradient, with holm oak (*Quercus ilex* L.) forests at lower altitudes and Scots pine at altitudes above ≈800 m a.s.l. (Gutiérrez 1989).

In Arcalís, the climate is sub-humid Mediterranean, characterized by an annual mean temperature of 9.7°C and an annual mean rainfall of ≈653 mm (Climatic Digital Atlas of Catalonia, period 1951-2006) (Pons 1996; Ninyerola *et al.* 2000). The soils are calcareous with a predominantly clay-loam texture. Scots pine forests occur at altitudes above ≈600 m a.s.l. (Galiano *et al.* 2010).

Field work was conducted in late autumn 2008 (Prades) and in early spring 2009 (Arcalís). At each site two linear sampling transects, perpendicular to the same slope, were established within the same valley. These transects differed between them in altitude and in water availability. A lower and wetter transect situated ≈800 m a.s.l., and an upper and dryer one, situated ≈1000 m a.s.l. were selected in Prades (Table 2.1). As for Arcalís, the lower and dryer transect was located ≈1000 m a.s.l., while the upper and wetter one was at an altitude of ≈1300 m a.s.l. (Table 2.1). The gradient of water availability with altitude was determined by local characteristics and had opposite directions at the two sites, as described in previous studies. In Prades, the

water availability gradient is determined by the bedrock characteristics, which do not allow water loose by seepage, and by the differences in runoff and in the water holding capacity of the soil along the slope (Piñol *et al.* 1991). Instead, in Arcalís the water availability gradient along the slope is mainly determined by the higher temperatures and therefore greater potential evapotranspiration towards the valley bottom (Galiano *et al.* 2010).

Transects were established always on north-facing slopes. They started at a random location within the slope and progressed at a constant altitude until the required number of trees had been sampled. All sampled trees were of a similar size (around 30 cm of diameter at breast height, DBH) (Table 2.1) to reduce unwanted variation. Trees were sampled within 5 m of the central transect line so that the distance between sampled trees was always >5 m. Depending on tree density at each sampling location, total transect length varied between 240 and 400 m. Overall, 153 Scots pine trees were sampled, including living and dead individuals. Of those, only 117 were used in the final analyses as some of the ring series did not correlate well with the other trees in the area and some of the dead trees could not be properly dated (Table 2.1).

From the wet transects, where mortality was low, only living trees were sampled, while from the dry transects, wood cores were extracted from both living and dead trees (Table 2.1). Two wood cores were sampled to the pith from each tree at breast height and orthogonal to the slope. The wood core used here was obtained with a Suunto© (Vantaa, Finland) 5 mm Pressler borer. A second core was obtained for each tree from the other side of the stem with a Haglöf© (Haglöf Sweden AB, Långsele, Sweden) 12 mm Pressler borer. This latter core was used for isotopic analyses reported in **Chapter 3**. However, when doubts arose on the dating of specific samples, these second cores were used to aid the dating process. The cores were fixed into wood supports for drying and posterior processing. In Arcalís, 14 whole stem discs were sampled using a chainsaw from trees that died and had been fallen by local managers after the mortality event to avoid outbreaks of insect pests.

Sample preparation and growth measurements

The wood cores and sections were slowly dried at room temperature, glued and sanded progressively until all the rings were clearly visible under a binocular scope (Fritts 2001). All samples were visually cross-dated using skeleton plots for each of them (Pilcher 1990). In order to measure total ring (RW) and latewood widths (LW) to the nearest 0.01 mm, both for living and dead trees, the samples were scanned and the images were analyzed using the WinDENDRO^{TM} software (Régent Instruments Inc Quebec Canada 2004*c*). To identify locally absent rings, eliminate measurement errors and ensure dating accuracy, the quality of cross-dating was repeatedly checked with the COFECHA software (Holmes 1983). Only the living trees that had a positive correlation with the master dating series ($r>0.1$) were kept for further analyses. The final dataset had 78 living trees: 38 for Prades and 40 for Arcalís, spanning from 1861 to 2008 and from 1908 to 2008, respectively (Table 2.1). Basal area increment (BAI) and latewood percentages (LW%, as a measure of autumn tree growth) were used in further analyses. Transition from earlywood to latewood was established visually based on darkening and tracheid structure (Fritts 2001; Vaganov *et al.* 2006).

Dating of the dead trees

The years of tree death were established by attributing calendar years to the outermost annual rings. Cores from the dead trees were visually cross-dated with the ones sampled from the living individuals from the same site. For this, pointer calendar years corresponding to narrow (1986, 1991, 1994, 2005) and wide (1975, 1977, 1992, 2004) rings, were used. The cross-dating process was then repeatedly checked with COFECHA (Holmes 1983) by running dead trees samples against the master chronologies built from the living trees at the corresponding site. The confidence of the dating process was influenced by the conservation status of the samples and by the fact that trees might not develop growth rings the years immediately before death (Amoroso and Daniels 2010). In some cases, the oldest parts (pre 1950) of the cores from dead trees were discarded, as our main purpose was to have the year of death and the growth characteristics from 1951 onwards. The final dataset had 14 dated dead trees from Prades (spanning from 1923 to 2008) and 25 from Arcalís (spanning from 1906 to 2008) (Table 2.1).

Table 2.1 – Main characteristics of the six chronologies from Prades and Arcalís. Values in brackets represent standard deviations. Abbreviations: *DBH,* diameter at breast height; *correlation with master (COFECHA),* mean correlations of the total period

	Prades wet living	Prades dry living	Prades dry dead	Arcalís wet living	Arcalís dry living	Arcalís dry dead
Altitude (m a.s.l.)	800	1000	1000	1300	1000	1000
Total period covered by the samples	1865-2008	1861-2008	1923-2008	1908-2008	1920-2008	1906-2008
Common period of all trees	1965-2008	1968-2008	1966-1997	1977-2008	1962-2008	1957-1994
Initial number of sampled trees	25	25	26	25	25	27
Final number of analyzed trees	19	19	14	21	19	25
DBH average (cm)	29.51 (3.09)	28.73 (3.39)	30.56 (10.98)	30.93 (2.57)	30.63 (3.38)	31.11 (5.35)
Correlation with master (COFECHA)	0.468 (0.19)	0.468 (0.10)	0.453 (0.16)	0.524 (0.14)	0.511 (0.16)	0.464 (0.15)

Calculation of BAI

The measured ring widths (RW) (Supplementary Figures 2.1 and 2.2) of both living and dead Scots pine trees were converted into annual basal area increment (BAI, cm^2/year) assuming concentrically distributed tree-rings, according to the formula

$$BAI = \pi(R^2_t - R^2_{t-1})$$

where *R* is tree radius and *t* is the year when the ring was formed. BAI is considered a relatively age-independent measure of radial tree growth and, therefore, it can be used without the need of detrending to remove age trends (Biondi 1999).

Climatic data and variables

The main climatic dataset used in this study included monthly temperature and precipitation values, modeled at a spatial resolution of 180 m from discrete climatic data provided by the Spanish weather-monitoring system (cf. Ninyerola *et al.* 2007*a, b*). This data series covered a period of 56 years, from 1951 to 2006. A second database was provided by the Catalan Weather Service (SMC) and included monthly temperature and precipitation data from two weather stations: Prades (situated at ≈3 km of the study plots) and La Pobla de Segur (situated at ≈15 km from Arcalís), for the 1996-2008 period. This information was used to fill in the temperature and precipitation values for the years 2007 and 2008, which were missing in our main climatic dataset. This was accomplished by using regression models relating temperature (Prades: R^2=0.99; Arcalís: R^2=0.78) and precipitation (Prades: R^2=0.81; Arcalís: R^2=0.85) between the two climate datasets for the common period (1996 - 2006).

Mean annual temperatures (T) and yearly indexes of summer drought stress (P/PET_{summer}) were calculated and used as climatic variables in further analyses. The mean annual temperatures corresponded to twelve months periods, covering August previous year to July current year. P/PET_{summer} was calculated from precipitation (P) and potential evapotranspiration (PET) data corresponding to June, July and August of the year of ring formation. Monthly potential evapotranspiration (PET) was calculated using the Thornthwaite method (Thornthwaite 1948). The periods used to calculate the two climatic variables were chosen based on previous studies conducted on Scots pines growing in dry areas (Gutiérrez 1989; Rigling *et al.* 2001; Weber *et al.* 2007; Martínez-Vilalta *et al.* 2008; Gruber *et al.* 2010) and were also consistent with the relationships obtained using our own data (Supplementary Figure 2.3).

Definition of drought periods

Severe drought periods of three consecutive years were defined for each study site for the time intervals that corresponded to the periods when mortality was observed

(1998-2008 and 1995-2008). In order to do this, the four driest years were selected at each site (corresponding to P/PET_{summer} values < ≈0.2 for Prades and < ≈0.3 for Arcalís). These years were: 2001, 2006, 2007 and 2008 for Prades and 2000, 2001, 2004 and 2006 for Arcalís (Figure 2.2). It was considered that each three year period starting in any of those years corresponded to a period where drought effects could be expected. In this way we accounted for delayed drought effects on tree mortality (Pedersen 1999; Guarín and Taylor 2005; Bigler *et al.* 2007).

Data analyses

The analyzed variables were checked for normality (Kolmogorov-Smirnov test) and logarithm or arcsine squared root transformations were applied when necessary. Association between tree-death dates and severe drought periods was evaluated by means of Chi-square tests. Mixed linear models were used to assess how climatic variables and different site conditions influenced Scots pine growth at the two studied sites. The response variables were log BAI (named BAI) and the arcsine of the square root of LW% (named LW%). The predictor variables were P/PET_{summer}, temperature (T), a categorical variable coding for transect and tree state (Condition), the interaction between P/PET_{summer} and Condition and the interaction between T and Condition. The variable Condition had three levels (wetL, dryL and dryD) corresponding to the transect humidity condition (wet or dry) and the state of the trees (Living or Dead). The predictor variables were introduced as fixed effects. Tree identity and year (from 1952 to 2008) were introduced into the models as random effects to account for tree-level effects and temporal autocorrelation (first-order autoregressive), respectively. All statistical analyses were carried out with SPSS for Windows (version 15.0 SPSS Inc Chicago IL 2006).

RESULTS

Temporal trends of climatic variables

Mean annual temperature increased significantly at the two studied sites from 1951 to 2008 (R^2=0.25, P<0.001 for Prades; R^2=0.52, P<0.001 for Arcalís) (Figure 2.1*a*). The average rate of temperature increase was ≈0.02 ºC/year in Prades and ≈0.04 ºC/year in Arcalís. For the same time period, annual precipitation (Figure 2.1*b*) registered a

significant decline (Prades: R^2=0.08, P<0.05; Arcalís: R^2=0.22, P<0.001), with an average reduction of 2.2 mm/year in Prades and of 4.4 mm/year in Arcalís. P/PET_{summer} (Figure 2.1*c*) also decreased significantly at both sites (R^2=0.22, P<0.001 for Prades; R^2=0.32, P<0.001 for Arcalís).

Figure 2.1 - Temporal (1951-2008) trends of temperature (*a*), precipitation (*b*) and P/PET_{summer} (*c*) in Prades and Arcalís study sites.

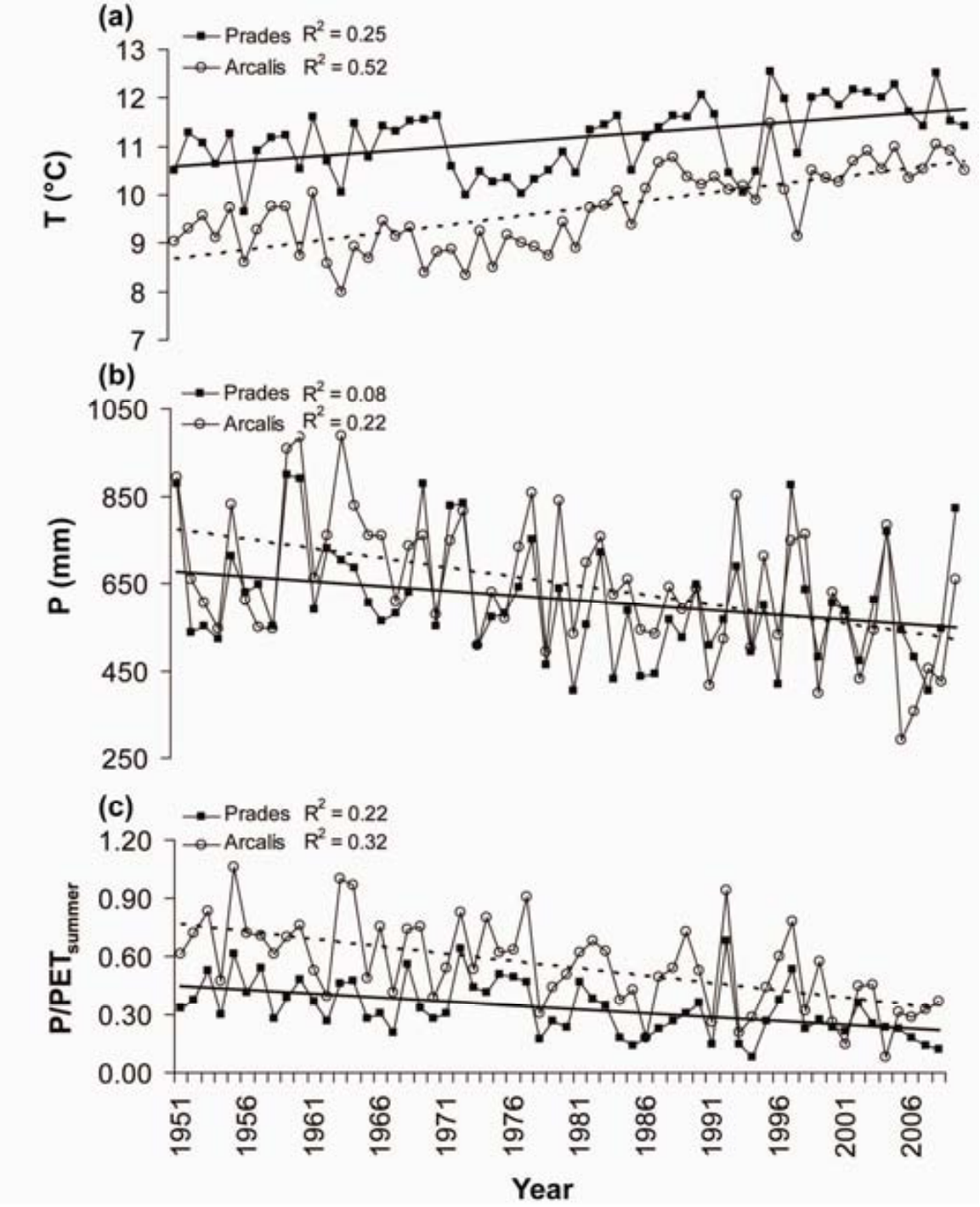

Occurrence of dieback events and association with drought

At both study sites tree mortality was episodic, being typically grouped in periods of consecutive years (Figure 2.2). The years of tree death dated back to 1998 in Prades and to 1995 in Arcalís. In Prades, tree mortality concentrated mainly in the periods 2001-2003 and 2005-2008 (Figure 2.2). The defined severe drought periods at this site included 86% of the dead trees. In Arcalís, mortality was also concentrated in two periods: 1995-1996 and 2000-2008. All 25 dead individuals sampled here corresponded to these two mortality periods, with a peak of 6 dead individuals in 2005 (Figure 2.2). The defined severe drought periods at this site included 92% of the dead trees. A clear association was found between the death years of Scots pine trees and the severe drought periods registered between 1998 and 2008 in Prades (X^2=5.49, P<0.05), and between 1995 and 2008 in Arcalís (X^2=8.36, P<0.01). Overall, ≈90% of dead trees died within the specified severe drought periods (Figure 2.2).

Figure 2.2 - Number of the dead trees per year and annual P/PET_{summer} values in Prades and Arcalís. Horizontal lines mark the 0.2 and 0.3 P/PET_{summer} values. Solid circles indicate the driest years that defined severe drought periods (see text).

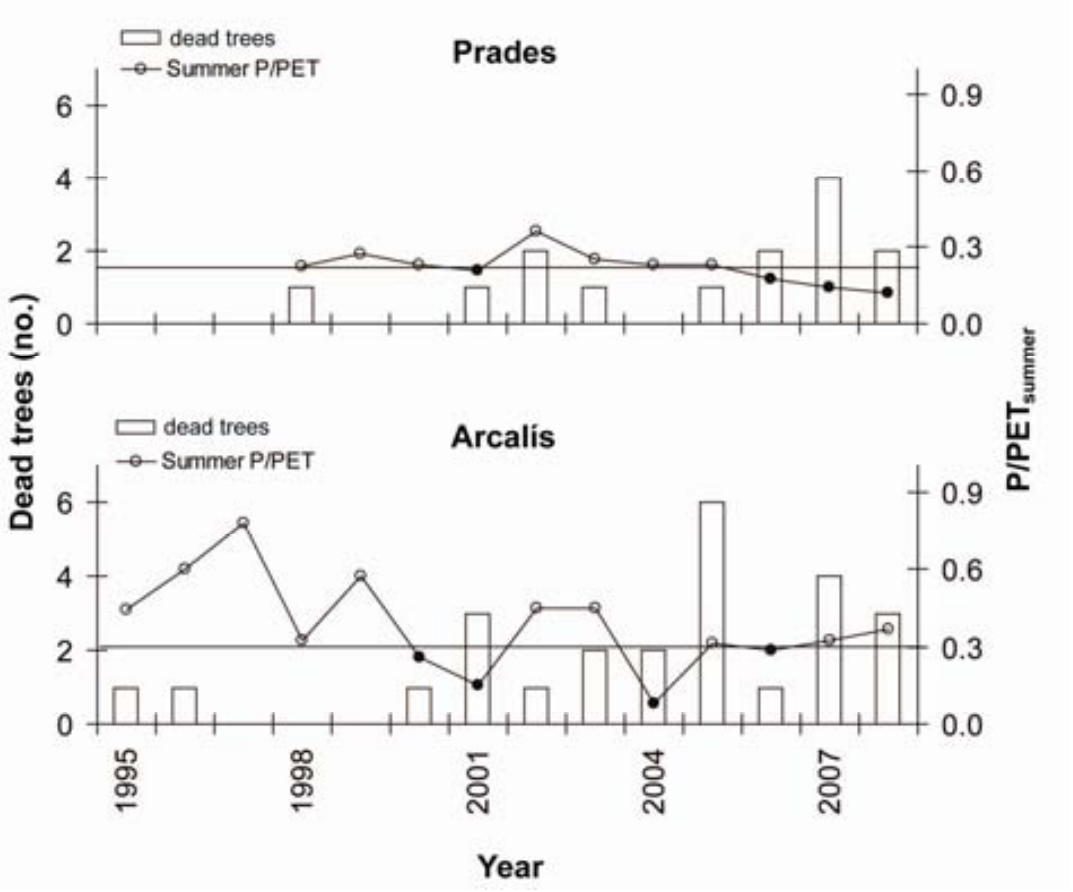

Growth trends and influence of climate

Between 1951 and 2008, BAI of the Scots pines from both study sites was highly variable and lacked any clear overall time trend (Figure 2.3*a, b*). In Prades, BAI of living and dead trees peaked in the mid 1970s. The BAI of trees that were going to die was lower than that of living trees since the late 1960s (Figure 2.3*a*). In Arcalís, BAI showed similar patterns, except for living trees from the wet transect, which experienced a marked BAI increase in the 1980s. Again, BAI tended to be lower for dead trees in recent years (Figure 2.3*b*). The BAI of now-dead trees relative to the average BAI of living trees sampled at the dry transect started to decline almost 40 years before tree death in Prades and around 15 years before tree death in Arcalís (small panels in Figure 2.3*a, b*), indicating that death was the culmination of a long term declining process.

Figure 2.3 - Temporal (1951-2008) growth trends (BAI) of Scots pine trees from Prades (*a*) and Arcalís (*b*). Bottom panels indicate the sample size (number of trees per year). Top panels represent relative BAI (%) of the dead trees from Prades and Arcalís as a function of time before death. Each value corresponds to the average of the ratio of the BAI of trees that were going to die and the BAI of surviving trees for any given year, multiplied by 100 to turn it into a percentage. Error bars show standard errors.

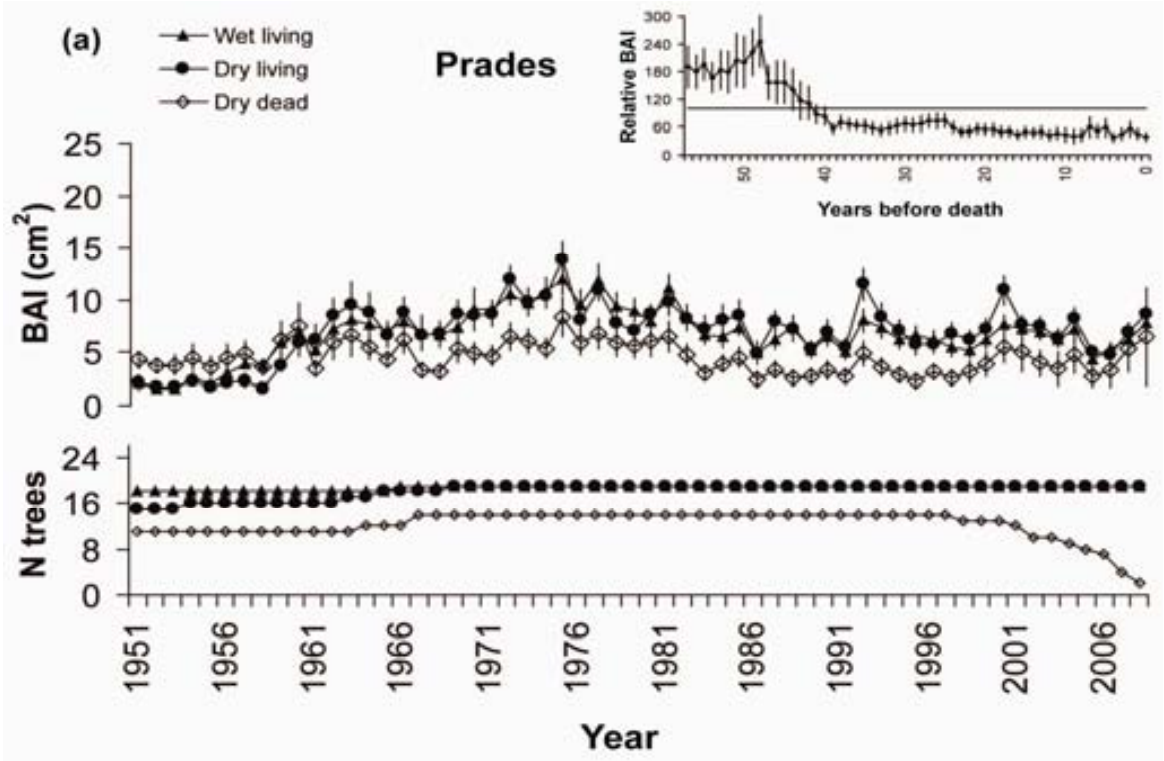

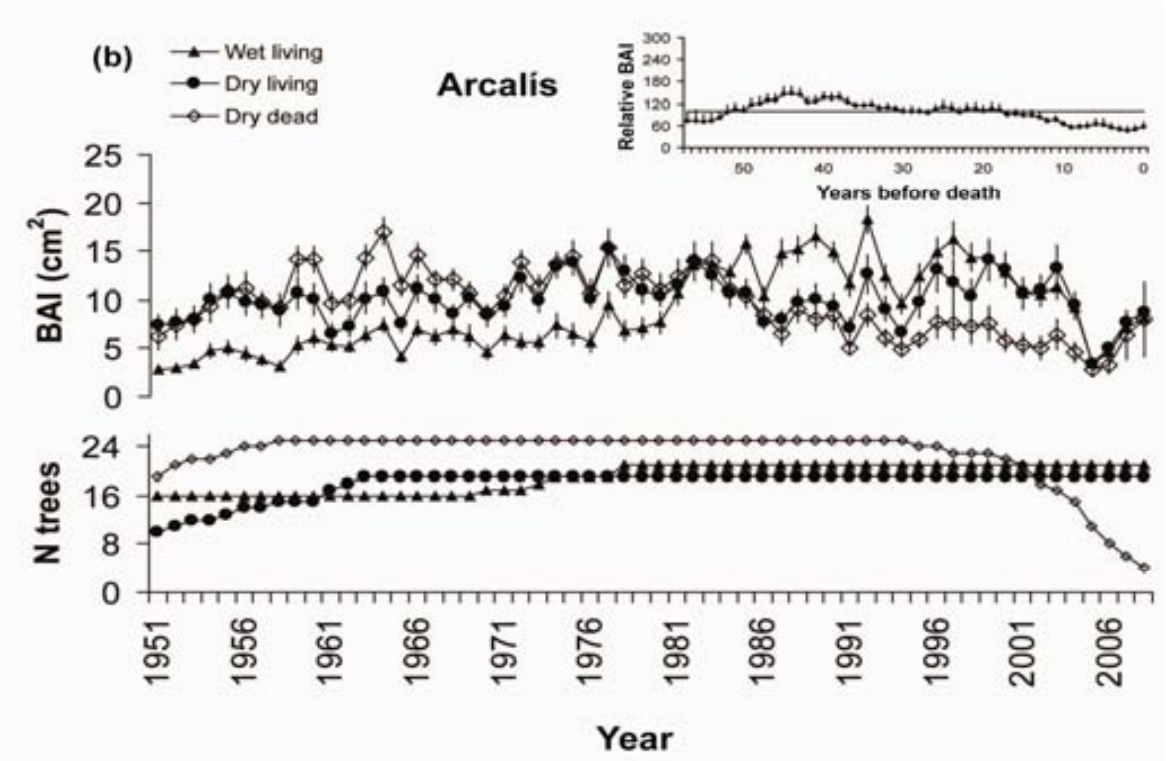

According to the mixed model results, both P/PET_{summer} and T significantly drive BAI growth at the two study sites, and their effects differed depending on Condition (Table 2.2; Figures 2.4 and 2.5). The effect of P/PET_{summer} on BAI was particularly marked in now-dead trees, for which high P/PET_{summer} values always promoted growth. A smaller but significant positive effect of P/PET_{summer} on BAI was also observed for the living trees from the dry transect at Arcalís (Table 2.2 and Figure 2.4). The effect of T on BAI was significant and negative for the trees that were going to die both at Prades and Arcalís, indicating that these trees were also sensitive to high temperatures (Table 2.2 and Figure 2.5). At the same time, a positive significant effect of T was registered for the living trees from the wet transect at Arcalís (Table 2.2 and Figure 2.5). No significant interaction was found between the effects temperature and P/PET_{summer} (not shown). The previous results imply that the lower growth rates of now-dead trees occurred mostly during years of low summer water availability and/or high temperatures (Figures 2.4 and 2.5).

Table 2.2 – Summary of the mixed linear models with log BAI as a response variable. Bold values indicate significant relationships (P<0.05)

	Fixed effects	Estimate	SE	*t*-value	*P*-value
Prades	Intercept	**0.9817**	**0.3089**	**3.178**	**0.003**
	Condition dryL	-0.2167	0.2315	-0.936	0.349
	Condition dryD	0.1674	0.2556	0.655	0.513
	P/PET_{summer}*Condition wetL	0.0602	0.0935	0.644	0.521
	P/PET_{summer}*Condition dryL	-0.0032	0.0942	-0.034	0.973
	P/PET_{summer}*Condition dryD	**0.4346**	**0.1030**	**4.220**	**<0.001**
	T*Condition wetL	-0.0308	0.0239	-1.291	0.200
	T*Condition dryL	-0.0101	0.0240	-0.422	0.674
	T*Condition dryD	**-0.0783**	**0.0255**	**-3.066**	**0.003**
Arcalís	Intercept	**-0.8102**	**0.2445**	**-3.314**	**0.001**
	Condition dryL	**1.7033**	**0.1926**	**8.844**	**<0.001**
	Condition dryD	**2.9055**	**0.1832**	**15.864**	**<0.001**
	P/PET_{summer}*Condition wetL	0.1049	0.0583	1.800	0.074
	P/PET_{summer}*Condition dryL	**0.1756**	**0.0591**	**2.973**	**0.003**
	P/PET_{summer}*Condition dryD	**0.3097**	**0.0548**	**5.652**	**<0.001**
	T*Condition wetL	**0.1605**	**0.0234**	**6.862**	**<0.001**
	T*Condition dryL	-0.0120	0.0236	-0.509	0.612
	T*Condition dryD	**-0.1513**	**0.0230**	**-6.576**	**<0.001**

Figure 2.4 - Effect of P/PET_{summer} on Scots pine growth (Basal Area Increment, BAI, and percentage of latewood, LW%) at the two study sites (Prades and Arcalís) according to the mixed effects models reported in **Tables 2.2** and **2.3**.

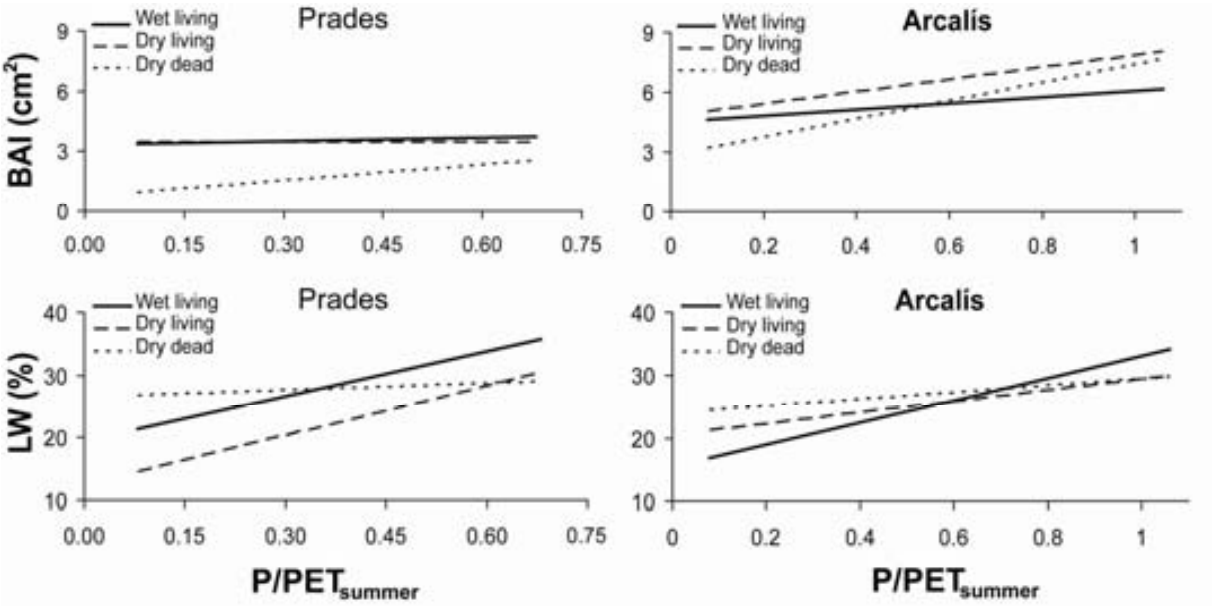

P/PET_{summer} had an overall positive effect on the percentage of latewood at both sites, albeit it was significant only for the living trees (Table 2.3 and Figure 2.4). Combined with the results of the BAI model, this outcome implies that the growth reduction at low P/PET_{summer} observed in the now-dead trees affected similarly the earlywood and the latewood. Temperature also tended to increase the proportion of latewood, its effect being significant for now-dead trees from both sites and for the living trees from the dry transect at Arcalís (Table 2.3 and Figure 2.5).

Table 2.3 – Summary of the mixed linear models with arcsine square root of LW% as a response variable. Bold values indicate significant relationships (P<0.05)

	Fixed effects	Estimate	SE	t-value	p-value
Prades	Intercept	**0.6087**	**0.1172**	**5.195**	**<0.001**
	Condition dryL	**-0.3648**	**0.0971**	**-3.756**	**<0.001**
	Condition dryD	**-0.4160**	**0.1073**	**-3.877**	**<0.001**
	P/PET_{summer}*Condition wetL	**0.2676**	**0.0482**	**5.557**	**<0.001**
	P/PET_{summer}*Condition dryL	**0.3225**	**0.0484**	**6.666**	**<0.001**
	P/PET_{summer}*Condition dryD	0.0414	0.0519	0.798	0.427
	T*Condition wetL	-0.0131	0.0096	-1.357	0.180
	T*Condition dryL	0.0113	0.0097	1.170	0.247
	T*Condition dryD	**0.0312**	**0.0104**	**3.004**	**0.004**
Arcalís	Intercept	**0.3017**	**0.1059**	**2.850**	**0.006**
	Condition dryL	-0.0605	0.0685	-0.883	0.377
	Condition dryD	-0.0518	0.0652	-0.794	0.427
	P/PET_{summer}*Condition wetL	**0.2026**	**0.0318**	**6.360**	**<0.001**
	P/PET_{summer}*Condition dryL	**0.1006**	**0.0321**	**3.139**	**0.002**
	P/PET_{summer}*Condition dryD	0.0610	0.0311	1.961	0.054
	T*Condition wetL	0.0115	0.0100	1.147	0.257
	T*Condition dryL	**0.0240**	**0.0101**	**2.386**	**0.021**
	T*Condition dryD	**0.0272**	**0.0099**	**2.739**	**0.009**

Figure 2.5 - Effect of temperature on Scots pine growth (Basal Area Increment, BAI, and percentage of latewood, LW%) at the two study sites (Prades and Arcalís) according to the mixed effects models reported in **Tables 2.2** and **2.3**.

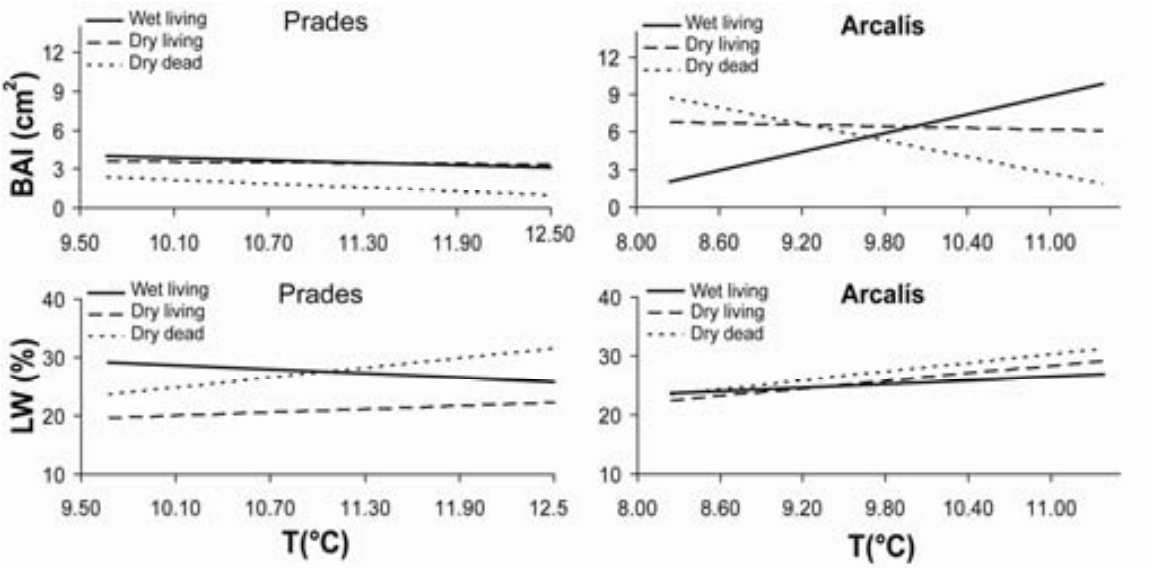

DISCUSSION

Scots pine mortality registered at our two study sites was associated with periods of severe drought conditions, characterized by low summer water availability (P/PET). Although the sample size was relatively low for dead trees, these results offer independent evidence supporting that recent mortality events at the two study sites were induced by drought, confirming previous observational accounts (Martínez-Vilalta and Piñol 2002; Galiano *et al.* 2010). These results also agree with previous reports of lagged tree mortality after drought (Guarín and Taylor 2005; Bigler *et al.* 2006; Bigler *et al.* 2007). Despite the claim that drought and heat-induced tree mortality events have become widespread (e.g., Allen *et al.* 2010), the direct link between water scarcity and tree death is often poorly documented (but see, for example, Villalba and Veblen 1998; Guarín and Taylor 2005; Bigler *et al.* 2007). In many instances, causation remains a challenge in the study of forest decline, in part due to the multiplicity of interacting factors that may contribute (Manion 1991; Pedersen 1998).

Consistent with our initial hypothesis, mortality affected preferentially trees that had lower radial growth rates (Pedersen 1998; Bigler and Bugmann 2003; Bigler *et al.*

2006). However, this difference in growth rate between surviving and now-dead trees was not present throughout the study period. It appeared around 1965 at Prades and around 1990 in Arcalís. This result implies a growth decline that started 15 – 40 years before the time of death (Figure 2.3*a, b*), in agreement with the figures reported in previous studies (Bigler and Bugmann 2003; Bigler *et al.* 2006). However, the growth decline we observed in now-dead trees appeared relatively continuous, without the abrupt reductions observed in other studies (Pedersen 1998; Das *et al.* 2007).

The fact that now-dead trees at the two sites were more sensitive to climate dryness (reduced P/PET_{summer} and increased temperatures) than surviving trees (Figures 2.4 and 2.5) suggests that growth decline and eventual mortality are related to different tree-level responses to water availability. This interpretation is consistent with the fact that rainfall declined and temperature and potential evapotranspiration increased over the period 1951 – 2008 at both sites (Figure 2.1). Summer water availability limits the duration of the growing season (Rigling *et al.* 2002; Weber *et al.* 2007; Eilmann *et al.* 2009) and, together with temperature, is the main abiotic factor influencing Scots pine growth in Mediterranean regions (Gutiérrez 1989; Martínez-Vilalta *et al.* 2008). A parallel study at one of the studied sites (Arcalís) shows that increased defoliation and mortality rates were associated with higher competition and with the level of drought stress experienced at the plot level (Galiano *et al.* 2010). In a study similar to ours, McDowell *et al.* (2010) also found greater growth sensitivity to climate in dead than in surviving *Pinus ponderosa* trees sampled across an elevation gradient in New Mexico (USA).

Drought effects on gas exchange and leaf area are obvious candidates for the mechanism behind the long-term decline in tree-condition observed in now-dead trees (cf. McDowell *et al.* 2008, 2010). In another recent study at the Arcalís site, Galiano *et al.* (2011) have related the immediate impact of drought on Scots pine radial growth with mid-term reductions in leaf area and stem carbon reserves, providing a link between tree physiology and long-term declines in tree growth induced by drought. The same study showed that low levels of stem carbon reserves resulted in increased mortality risk, in agreement with the carbon starvation hypothesis (McDowell *et al.* 2008). In our case, however, it is not possible to establish

whether the greater susceptibility to drought of now-dead trees is due to individual intrinsic factors (e.g., leaf-specific hydraulic conductivity, vulnerability to xylem embolism), or to edaphic or microclimatic effects.

Stand densification due to the abandonment of forest management (Poyatos *et al.* 2003; Linares *et al.* 2010) may have also contributed to the observed temporal trends. Vilà-Cabrera *et al.* (2011) have shown that forest structure interacts with water availability to determine mortality rates of Scots pine across Spain, suggesting that increased competition for water resources may reinforce the effects of reduced water availability. However, differences in forest management are very unlikely to explain the different behavior of living and now-dead trees within a site, because the studied forests have not been managed during the last decades and both tree types were sampled on the same transects.

In conclusion, our study provides strong evidence for drought-induced mortality at two Scots pine sites at the south-western limit of the distribution of the species. Additionally, a likely mechanism explaining the different susceptibility of coexisting trees is proposed which involves increased sensitivity to climate dryness over a long time period preceding death. If climate change predictions are fulfilled and the global increase in average and extreme temperatures (IPCC 2007) is accompanied by reductions in rainfall in many regions, including the Mediterranean Basin (Bates *et al.* 2008), forest decline events such as the ones reported in this study are likely to become widespread (cf. Allen *et al.* 2010). Populations at the dry limit of the species' range, such as Scots pine in the Mediterranean Basin are likely to be particularly vulnerable. Finally, the fact that growth patterns are different between surviving trees, and those that are going to die, as shown here and in previous studies (Pedersen 1998; Ogle *et al.* 2000; Suarez *et al.* 2004), offers a way to identify those trees prior to mortality events, which may aid the design of forest management plans to mitigate the effects of changing climate.

ACKNOWLEDGMENTS We would like to thank Miquel Ninyerola and the Servei Meteorològic de Catalunya (SMC) for providing the climatic datasets used in this

study. We are indebted to Dr. M. Mencuccini for field work and interesting discussions related to the study. Two anonymous referees are thanked for their thorough review and useful suggestions. Field and laboratory assistance of A. Vilà and M. Sabaté is very much appreciated. This study was supported by the Spanish Ministry of Science and Innovation via the competitive projects CGL2007-60120 and CSD2008-0040, and by the Spanish Ministry of Education via a FPU scholarship.

Supplementary Figure 2.1 - Temporal (1951-2008) ring widths (RW) of Scots pine trees from Prades. Error bars show standard errors.

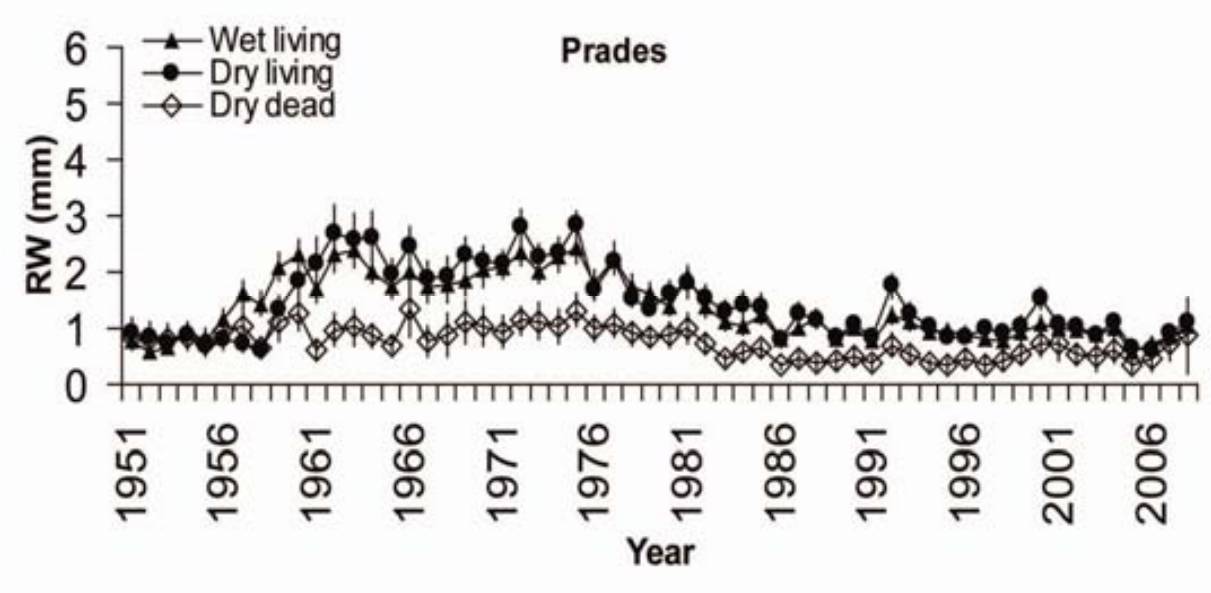

Supplementary Figure 2.2 - Temporal (1951-2008) ring widths (RW) of Scots pine trees from Arcalís. Error bars show standard errors.

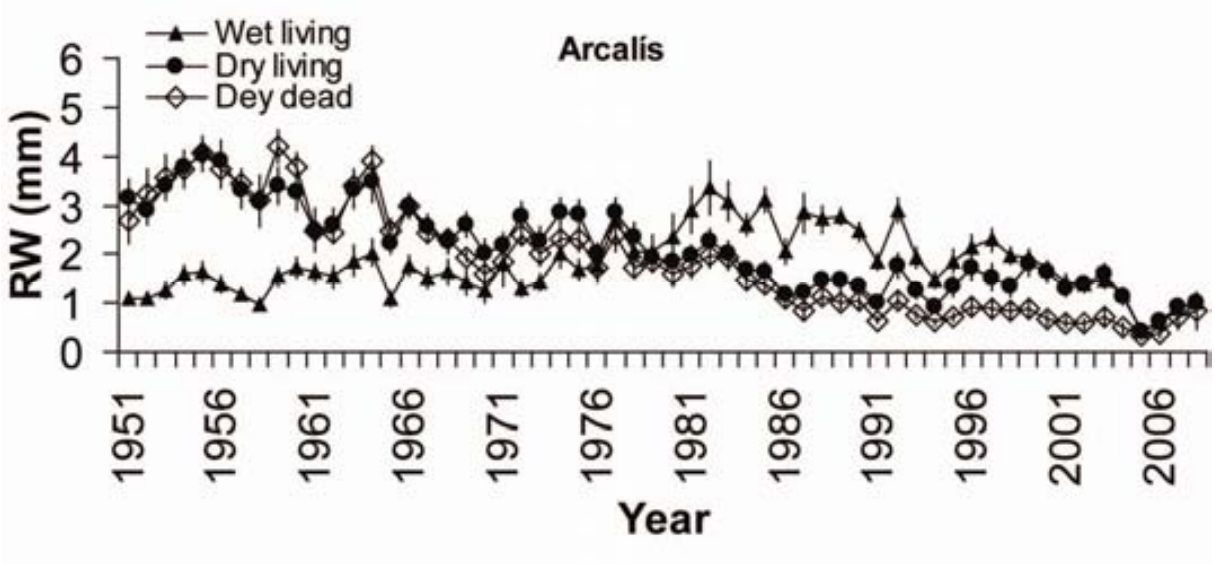

Supplementary Figure 2.3 - Correlation coefficients of growth indices with precipitation and temperature data corresponding to August (Year prior to growth) to December (Year of growth) period, for Prades (a) and Arcalís (b). Climate and growth data data are from the period 1952 to 2008. Asterisks indicate significant relationships (P<0.05).

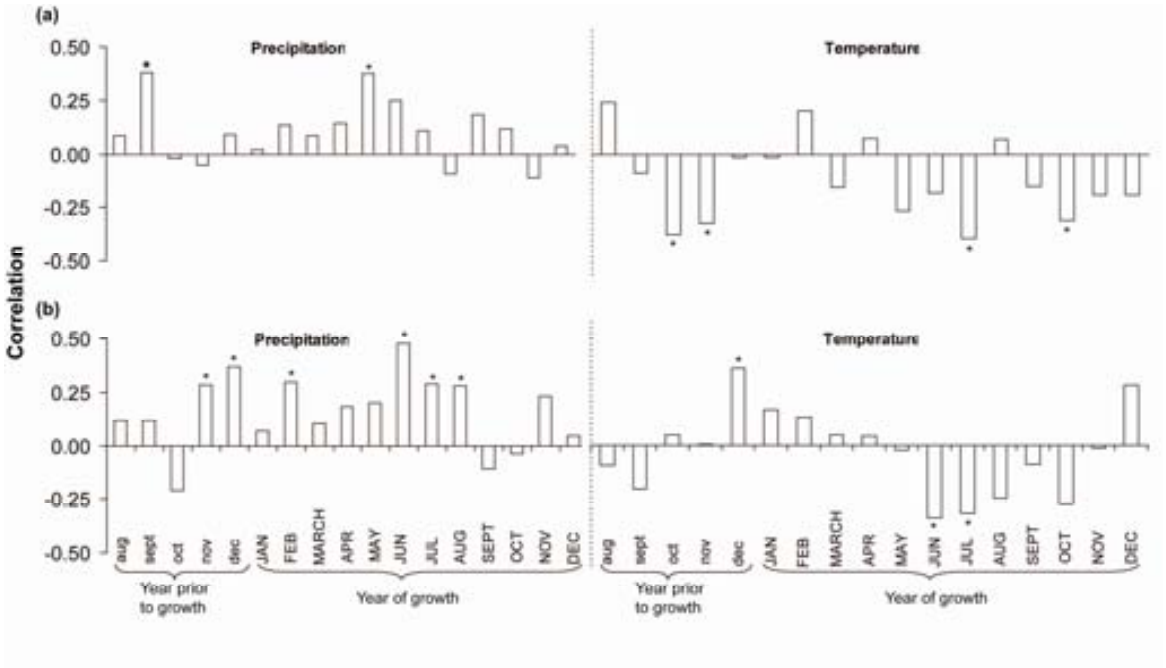

Chapter 3

DROUGHT-INDUCED MORTALITY SELECTIVELY AFFECTS *PINUS SYLVESTRIS* L. TREES THAT SHOW LIMITED INTRINSIC WATER-USE EFFICIENCY RESPONSIVENESS TO RAISING ATMOSPHERIC CO_2

A modified version of this chapter is accepted in *Functional Plant Biology*

Hereş AM, Voltas J, Claramunt López B, Martínez-Vilalta J, 2013

ABSTRACT

Widespread drought-induced tree mortality has been documented around the world and might increase in frequency and intensity under warmer and drier conditions. Nevertheless, ecophysiological differences between dying and surviving trees, which might underlie predispositions to mortality, are still poorly documented. Here we study Scots pines (*Pinus sylvestris* L.) from two sites located in north-eastern Iberian Peninsula where drought-associated mortality episodes were registered during the last decades. Time trends of discrimination against ^{13}C ($\Delta^{13}C$) and intrinsic water-use efficiency (WUE_i) in tree rings at annual resolution and for a 34 years period are used to compare co-occurring now-dead and surviving pines. Results indicate that both surviving and now-dead pines significantly increased their WUE_i over time, although this increase was significantly lower for now-dead individuals. These differential WUE_i trends corresponded to different scenarios describing how plant gas exchange responds to increasing atmospheric CO_2 (C_a): the estimated intercellular CO_2 concentration was nearly constant in surviving pines but tended to increase proportionally to C_a in now-dead trees. Concurrently, the WUE_i increase was not paralleled by a growth enhancement, regardless of tree state, suggesting that in water-limited areas like the Mediterranean, it cannot overcome the impact of an increasingly warmer and drier climate on tree growth.

INTRODUCTION

Drought-related episodes of tree mortality have been reported in many areas of the globe (Allen *et al.* 2010), and they are expected to become more frequent as climate gets warmer and drier (IPCC 2007**;** Williams *et al.* 2013). Western Mediterranean forests are ecosystems subjected to chronic water shortage. They are also likely to be especially vulnerable to an increase in the timing and severity of drought events (Bakkenes *et al.* 2002), since in this region temperature is estimated to raise about 3-4 ºC (Christensen *et al.* 2007) and precipitation might decrease up to 20% (Bates *et al.* 2008) during the 21st century. In particular, species reaching their southern distribution limit in the Mediterranean basin may be especially sensitive to the projected increases in drought frequency and intensity (Castro *et al.* 2004; Hampe and Petit 2005; Matías and Jump 2012).

The mechanisms that underlie drought-induced tree mortality are yet to be completely understood, although they are thought to be tightly linked to the tree water and carbon economy (Manion 1991; McDowell *et al.* 2008; Sala *et al.* 2010; McDowell 2011). Photosynthesis and metabolic sink activities can be substantially reduced or even ceased during severe drought, affecting the allocation of carbon to wood formation to varying degrees (McDowell *et al.* 2010). Thus, dying trees usually show characteristic growth patterns, including reduced growth (Pedersen 1998; Bigler *et al.* 2006; Hereş *et al.* 2012), high growth variability (Ogle *et al.* 2000) or greater growth sensitivity to climate (McDowell *et al.* 2010; Hereş *et al.* 2012).

Wood records climatic and physiological information traceable back in time (Fritts 2001; Vaganov *et al.* 2006) through features such as tree-ring width and carbon isotope composition ($\delta^{13}C$) (McCarroll and Loader 2004). In seasonally-dry climates, tree-ring $\delta^{13}C$ depends largely on tree water availability owing to the influence exerted by drought on the stomatal regulation of gas exchange (Warren *et al.* 2001; Ferrio *et al.* 2003). Thus, it reflects variation in intrinsic water-use efficiency (WUE_i; the ratio of assimilation to water loss through the stomata) (Farquhar *et al.* 1982). Under a warmer and drier climate with higher CO_2 concentrations (IPCC 2007), trees are expected to improve their WUE_i (Eamus 1991; Beerling 1997), as higher

temperatures and increased CO_2 concentrations stimulate photosynthesis (Long 1991; Sage *et al.* 1995) and stomata reduce water losses in response to drought. An enhancement of WUE_i in trees has already been observed for the 20th century, although it has not been paralleled by an expected stimulation of growth (Peñuelas *et al.* 2008; Peñuelas *et al.* 2011; Andreu-Hayles *et al.* 2011). However, the association between WUE_i and growth appears to be species-dependent in Mediterranean ecosystems (Peñuelas *et al.* 2008; Maseyk *et al.* 2011; Linares and Camarero 2012), which suggests that the impact of global change drivers on Mediterranean forests in the short-term and, hence, future vegetation shifts, will be strongly determined by the extent of acclimation responses of individuals (Pías *et al.* 2010).

Recent investigations reveal that dying hardwoods (Levanič *et al.* 2011) and declining conifer trees (Linares and Camarero 2012) also increase their WUE_i over time, although at different rates than surviving individuals. Other $\delta^{13}C$-related characteristics of dead trees include no apparent climatic sensitivity of their gas exchange traits and steeper negative relationships between gas exchange and growth (McDowell *et al.* 2010). However, retrospective analyses of tree-ring $\delta^{13}C$ on dead, dying or declining trees are still scarce. In this context, direct comparisons of living and dying trees growing together in a particular stand should provide insight into the physiological mechanisms underlying their differential responses to raising atmospheric CO_2 concentrations, including the observed decoupling between growth and WUE_i.

In this study, we focused on Scots pine (*Pinus sylvestris* L.), a widely distributed boreal tree species that reaches its southwestern (and dry) limit in the Iberian Peninsula (Barbéro *et al.* 1998; Matías and Jump 2012). During the last two decades, Scots pine has suffered important mortality episodes in the western part of the Mediterranean basin, following severe drought events (Martínez-Vilalta and Piñol 2002; Galiano *et al.* 2010; Hereş *et al.* 2012). This species presents a tight coupling between newly produced assimilates and wood formation for individuals undergoing severe drought conditions (Eilmann *et al.* 2010), which is consistent with a low

availability of reserve carbohydrates and its possible role in drought-induced mortality (Galiano *et al.* 2011).

Here, we examined, with an annual resolution and at the level of individual trees (i.e., without pooling samples, cf. Dorado Liñán *et al.* 2011), carbon isotope discrimination ($\Delta^{13}C$) and WUE_i derived from $\delta^{13}C$ records in tree rings of co-occurring living and now-dead Scots pines. These individuals were sampled at two sites where we recently found a direct association between tree mortality and severe drought episodes characterized by low summer water availability (Hereş *et al.* 2012). Our main objective was to investigate differences in ecophysiological performance between now-dead and surviving Scots pines so as to understand a possible long-term predisposition to mortality in a context of climate change. Also, we were interested in assessing the relationship between WUE_i and tree growth (in terms of basal area increment, BAI), as the growth of trees that died started to decline 15-40 years before death compared with that of surviving neighbours (Hereş *et al.* 2012). We hypothesized that now-dead trees would be intrinsically more vulnerable to drought and, therefore, would show a lower rate of WUE_i increase in response to rising atmospheric CO_2 concentrations, a more pronounced climatic sensitivity of WUE_i and a steeper negative relationship between WUE_i and growth (BAI), compared to their surviving neighbors.

MATERIALS AND METHODS

Study sites

Scots pine trees were sampled at two sites located in the North East of the Iberian Peninsula (Catalonia): Prades (Bosc de Poblet, Prades Mountains, 41°33'N, 1°01'E) and Arcalís (Soriguera, Central Pyrenees, 42°34'N, 1°09'E), where high mortality rates have been observed in the last two decades (Martínez-Vilalta and Piñol 2002; Galiano *et al.* 2010; Hereş *et al.* 2012). The climate in Prades is typically Mediterranean while in Arcalís it is characterized by cool-summer Mediterranean conditions (Köppen 1936). The mean annual temperature is higher in Prades (11.2°C) than in Arcalís (9.7°C), while the mean annual rainfall is slightly lower in Prades (611 mm) than in Arcalís (653 mm). July is the warmest month with an average of 21.3°C

for Prades and 19.9°C for Arcalís, while January is the coolest month with temperature averages of 3.1°C and 1.85°C in Prades and Arcalís, respectively (Climatic Digital Atlas of Catalonia, period 1951-2006) (Pons 1996; Ninyerola *et al.* 2000). Scots pine forests appear above 800 m a.s.l. in Prades, with an average density of about 350 trees ha^{-1} (Martínez-Vilalta *et al.* 2009), while at lower altitudes Scots pine is replaced by *Quercus ilex* (L.) and other typical Mediterranean species. At this site, the maximum tree age is ≈150 years (Hereş *et al.* 2012). In Arcalís, Scots pine grows between 600 and 1500 m a.s.l., with an average density of about 1070 trees ha^{-1}, while other species are dominant at lower (*Quercus humilis* Mill., *Quercus ilex* L.) or at higher altitudes (*Betula pendula* Roth) (Galiano *et al.* 2010). At Arcalís, the maximum tree age for Scots pine is ≈100 years (Hereş *et al.* 2012). Forest management has been minimal during the last decades at both study sites (Martínez-Vilalta *et al.* 2009; Galiano *et al.* 2010).

Sampling

The sampling campaigns were conducted in late autumn 2008 (Prades) and in early spring 2009 (Arcalís), and consisted in coring living and dead Scots pine trees along two transects per each site. The last complete annual ring for the living trees was 2008. The two transects were located on north-facing slopes and differed between them in altitude (800-1300 m a.s.l.) and humidity conditions (wet, dry) (Piñol *et al.* 1991; Galiano *et al.* 2010) (Table 3.1). Transects were linear and perpendicular to the slope. They started at random points and ended when all needed trees had been sampled, having thus a length that varied between 240 and 400 m. Trees were sampled within a 5 m distance from the line-track, taking care to keep a distance of at least 5 m between them (for more details see **Chapter 2**). At the wet transects, only living trees (wetL) were sampled, as mortality was very low, while at the dry transects, both living and dead individuals (dryL, dryD) were cored. Selected trees had similar diameter (around 30 cm) at breast height (DBH) (Table 3.1). Two wood cores per tree were extracted at breast height in a direction perpendicular to the slope, using 5 and 12 mm Pressler borers (Suunto©, Vantaa, Finland; Haglöf© AB, Långsele, Sweden). The 5 mm cores were used in **Chapter 2**, from where BAI data is available (Table 3.1) (Hereş *et al.* 2012). Thirty of the 12 mm wood cores (representing a total of 30 living and dead trees) were selected here to analyze tree-ring $\delta^{13}C$ (Table 3.1) with

annual resolution, after checking their cross-dating consistency with the previously published chronology (Hereş *et al.* 2012). One of the dead trees from Prades was removed from the final dataset as it gave very deviating isotopic values for some tree rings, most likely as a result of contamination during the α-cellulose extraction (see next section). The final dataset comprised 20 living (wetL and dryL) and nine dead trees (dryD) (Table 3.1).

Table 3.1 – Sites characteristics, BAI, $\delta^{13}C$ and WUE_i data. *BAI* values are calculated for the 1975-2008 period for the living trees and for the 1975-year of death interval for the npw-dead ones. Abbreviations: *DBH*, *DBH,* diameter at breast height; *s.d.*, standard deviation

	Altitude (m a.s.l.)	Number of trees	Mean DBH ± s.d. (mm)	Mean BAI ± s.d. (cm^2)	Mean $\delta^{13}C$ ± s.d. (‰)	Mean WUE_i ± s.d. (μmol mol^{-1})
Prades wet living (wetL)	800	5	28.64±3.14	6.92±4.39	-23.38±0.65	108.59±9.87
Prades dry living (dryL)	1000	5	31.18±3.19	10.25±5.85	-22.98±0.82	112.70±10.59
Prades dry dead (dryD)	1000	4	32.25±6.84	3.46±3.79	-23.37±0.84	107.93±9.05
Arcalis wet living (wetL)	1300	5	31.58±1.71	9.81±5.94	-23.55±0.85	106.83±10.95
Arcalis dry living (dryL)	1000	5	31.66±3.40	10.28±4.78	-23.82±0.64	104.13±8.90
Arcalis dry dead (dryD)	1000	5	33.76±6.36	9.39±6.61	-23.89±0.93	102.16±10.52

Carbon isotope analyses

To analyze $\delta^{13}C$ with annual resolution, the available wood cores were first separated with a scalpel into individual annual rings under a binocular microscope (Leica EZ4, Leica Microsystems, Germany) for a period that started at the outermost ring of each sample and went back to the year 1975. By doing this, at least the first 25 years of growth were excluded from the analyses, avoiding the juvenile imprinting of the carbon isotope signature (Loader *et al.* 2007). The total number of years for the living trees was 34, while for the dead trees it varied depending on the year of death of each individual, which ranged from 2001 to 2008. In order to optimize the recovery of climate signals, α-cellulose was extracted following a standard laboratory procedure (Modified Brendel and Water-Modified Brendel) (Brendel *et al.* 2000; Gaudinski *et al.* 2005). No treatment that could have altered the isotopic signal was applied to the sampled cores previous to the α-cellulose extractions. After α-cellulose was extracted from each whole annual ring, a homogenization with ultrasounds (Sonifier 250, Branson Ultrasonics, CT, USA) was applied in order to have a representative material of each annual ring (Laumer *et al.* 2009). $^{13}C/^{12}C$ ratios were determined by mass spectrometry analysis at the Stable Isotope Facility of the University of California, Davis (USA) and expressed relative to the international standard Vienna PeeDee Belemnite (VPDB). A total of 943 samples were processed and the accuracy of analyses (standard deviation of working standards) was 0.06‰.

The atmospheric decline in $\delta^{13}C$, caused by fossil fuel emissions (Keeling *et al.* 1989), was removed by calculating $\Delta^{13}C$ (Farquhar and Richards 1984) for the period 1975-2008:

$$\Delta^{13}C = \frac{\delta^{13}C_{air} - \delta^{13}C_{p}}{(1+\delta^{13}C_{p})} \qquad (1)$$

where $\delta^{13}C_{air}$ and $\delta^{13}C_{p}$ are the carbon isotope ratios of the air (derived from ice-core records) and tree rings, respectively. $\delta^{13}C_{air}$ values were obtained from published datasets (Ferrio *et al.* 2005*b*).

Using $\Delta^{13}C$ data, WUE_i and intercellular CO_2 concentration (C_i) values were estimated according to:

$$WUE_i = C_a \times \frac{(b - \Delta)}{[1.6 \times (b - a)]} \quad (2)$$

$$C_i = \frac{(\Delta - a) \times C_a}{(b - a)} \quad (3)$$

where C_a represents the atmospheric CO_2 concentration, a is the fractioning during diffusion through stomata (4.4‰; O'Leary 1981), and b is the fractioning during carboxylation by Rubisco and PEP carboxylase (27‰; Farquhar and Richards 1984). C_a values from 1975 to 2003 were taken from the literature (Robertson *et al.* 2001*a*; McCarroll and Loader 2004) while for the period 2004 - 2008 they were estimated by means of linear regressions, based on the above mentioned datasets.

Theoretical WUE_i values were also calculated according to the three scenarios proposed by Saurer *et al.* (2004). Those scenarios describe how the C_i might follow the C_a increase over time: (1) either not at all, when C_i is maintained constant (referred to also as "ct" throughout the text); (2) in a proportional way, when C_i/C_a is maintained constant; or (3) at the same rate, when C_a-C_i is maintained constant. Initial C_i values were obtained for each individual tree by applying equation (3) to the average $\Delta^{13}C$ and C_a values of the first five years of the study period (1975-1979). We used these three scenarios to calculate theoretical WUE_i values that were compared to the WUE_i data obtained from measured $\delta^{13}C$.

Climatic data

Monthly temperature (T, ºC) and precipitation (P, mm) values (until 2006) were modelled at a spatial resolution of 180 m from discrete climatic data provided by the Spanish Weather-Monitoring System (www.aemet.es) (Ninyerola *et al.* 2007*a*, *b*). Data for 2007 and 2008 were estimated by means of linear regression models using a second climatic dataset that was available from the Catalan Meteorological Service (SMC) (www.meteo.cat).

From the available climatic datasets, we calculated the average *T*, the accumulated *P* and the accumulated *P* over potential evapotranspiration (P/PET, used as a drought index), corresponding to annual (12 months from January to December of the same year) and to a 13-month period (from October previous to growth year to October current year of growth). The 12-month time period was chosen to represent the time trends (from 1975 to 2008) for the climatic variables. The 13-month time interval was used for statistical modelling to take into account that pines may use reserve carbohydrates assimilated during the previous year for earlywood formation (Saurer *et al.* 1995; Weber *et al.* 2007; Planells *et al.* 2009), and was selected based on the extent of simple correlations between WUE_i and monthly *T* and *P* data (see Supplementary Figure 3.1). In all cases, PET was estimated using the Hargreaves method (Hargreaves and Samani 1982).

Data analysis

All variables were first checked for normality (Kolmogorov-Smirnov test) and logarithm-transformed whenever necessary (BAI). Pearson correlation coefficients were used as a measure of association between WUE_i and monthly *T* and *P*, while linear regressions were conducted to assess temporal trends of annual climatic variables (*T*, *P* and P/PET). In order to check for differences in the relative strength of the common $\Delta^{13}C$ variance signal for different within- and between-sites series combinations, we used the concept of fractional common variance (hereafter referred to as a_{fcv} throughout the text) as defined for dendroclimatology (e.g., Wigley *et al.* 1984):

$$a_{fcv} = \frac{\hat{\sigma}_y^2}{\hat{\sigma}_y^2 + \hat{\sigma}_e^2} \qquad (4)$$

where $\hat{\sigma}_y^2$ and $\hat{\sigma}_e^2$ represent the population between-year (or within-series) and the population error estimates of variance component, respectively, that appear in a two-way mixed model analysis of variance in which the tree identity effect is considered as fixed factor and the year effect as random factor. The term a_{fcv} is directly related to the average inter-series correlation, which indicates how closely the various time series are related (Wigley *et al.* 1984). Closely related series are therefore expected

to have a high a_{fcv} and a strong common signal. Being a_{fcv} a function of variance components, its standard error was approximated from the variance and covariance of between-year and error variance as reported elsewhere (Fischer *et al.* 2004). The expressed population signal statistic (EPS) was estimated as follows (Wigley *et al.* 1984):

$$EPS = \frac{Na}{1+(N-1)a} \quad (5)$$

where N is the number of $\Delta^{13}C$ tree-ring series. The number of trees (t) needed to achieve EPS=0.85 (the consensus acceptable threshold for signal strength; Wigley *et al.* 1984) was also calculated.

The similarity of $\Delta^{13}C$-based WUE_i data with the three theoretical scenarios was quantified by means of linear regressions and root mean square error (RMSError) statistics. In order to analyze the time trends of $\Delta^{13}C$ and WUE_i, the influence of the climatic variables on WUE_i and the relationships between WUE_i and growth (logBAI), three different sets of mixed linear models testing the assumption of constant responses among tree groups to selected covariates (i.e., heterogeneity of slopes ANOVA) were fitted to the data. The first model explained $\Delta^{13}C$ or WUE_i as a function of: Condition, Site (Prades, Arcalís), the interaction Condition × Site, the covariate Year (from 1975 to 2008), and the interactions Condition × Year, Site × Year, and Condition × Site × Year, which tested for heterogeneity of responses over time due to differences between conditions, sites or their interaction. Condition was defined as a categorical variable with three levels (wetL, dryL, dryD) coding for transect humidity (wet or dry) and tree state (Living or Dead). The second model was fitted to test for the joint impact of atmospheric CO_2 rise and climate on WUE_i. To this end, WUE_i was modelled by sequentially introducing the following terms: Condition, Site, the interaction Condition × Site, the covariate C_a and its interactions Condition × C_a, Site × C_a, and Condition × Site × C_a, and the covariate P/PET and its interactions Condition × P/PET, Site × P/PET, Condition × Site × P/PET. The covariate P/PET was introduced after correcting for the effect of C_a as it seemed sensible to test for the

potential effect of climate warming on WUE_i once the impact of rising atmospheric CO_2 had been removed from the data. Other climatic variables, such as *T* or *P*, were also tested but not included in the final models because they were highly correlated with each other and with P/PET and C_a over the study period (r >0.4 in all cases). P/PET was preferred over *T* or *P* because it can be interpreted as an integrative measure of the severity of the annual dry season in Mediterranean-like bioclimates (UNESCO 1979; Le Houerou 2004). In the third mixed linear model, logBAI was fitted according to the following model: Condition, Site, the interaction Condition × Site, the covariate WUE_i, and the interactions Condition × WUE_i, Site × WUE_i, and Condition × Site × WUE_i. Explanatory variables were introduced into the models following the ordering stated above for each of them (i.e., using type I sum of squares). In all three models, tree identity was introduced as subject (random effect), while Year was introduced as repeated effect at the tree level with a first-order autoregressive covariance structure to account for temporal autocorrelation. Significant differences in the response (slopes) of tree groups to the selected covariates were further examined by means of the following set of orthogonal contrasts comparing: a) dead (dryD) versus living (wetL and dryL) trees, and b) living trees between them (wetL versus dryL). If second order interactions were significant, independent contrasts for every site were considered. Model parameters were estimated using restricted maximum likelihood methods (REML). Relationships were considered significant at P<0.05. Statistical analyses were carried out with SAS (version 9.3, SAS Inc., Cary, NC) and SPSS (version 19.0, SPSS Inc., Chicago, IL).

RESULTS

Time trends

Mean annual temperature increased significantly both in Prades (R^2=0.39, P<0.001) and Arcalís (R^2=0.54, P<0.001) from 1975 to 2008 (Figure 3.1), at a similar rate of ≈0.05°C year^{-1}. For the same time period, mean annual precipitation decreased significantly in Arcalís (R^2=0.16, P<0.05) with an average rate of -5.87 mm year^{-1}, while in Prades it showed no significant trend (R^2=0.005, P=0.696) (Figure 3.1). P/PET also showed a significant decrease in Arcalís, at a rate of -0.007 year^{-1} (R^2=0.22, P<0.01) and no time trend in Prades (R^2=0.001, P=0.884) (Figure 3.1).

Figure 3.1 - Temporal trends (1975-2008) of *T*, *P*, P/PET and $\Delta^{13}C$ for Prades and Arcalís. The $\Delta^{13}C$ trend for the dryD trees ends in 2006, as this was the last year with a sample size > 2. Error bars indicate standard error. Regression lines are represented only if significant.

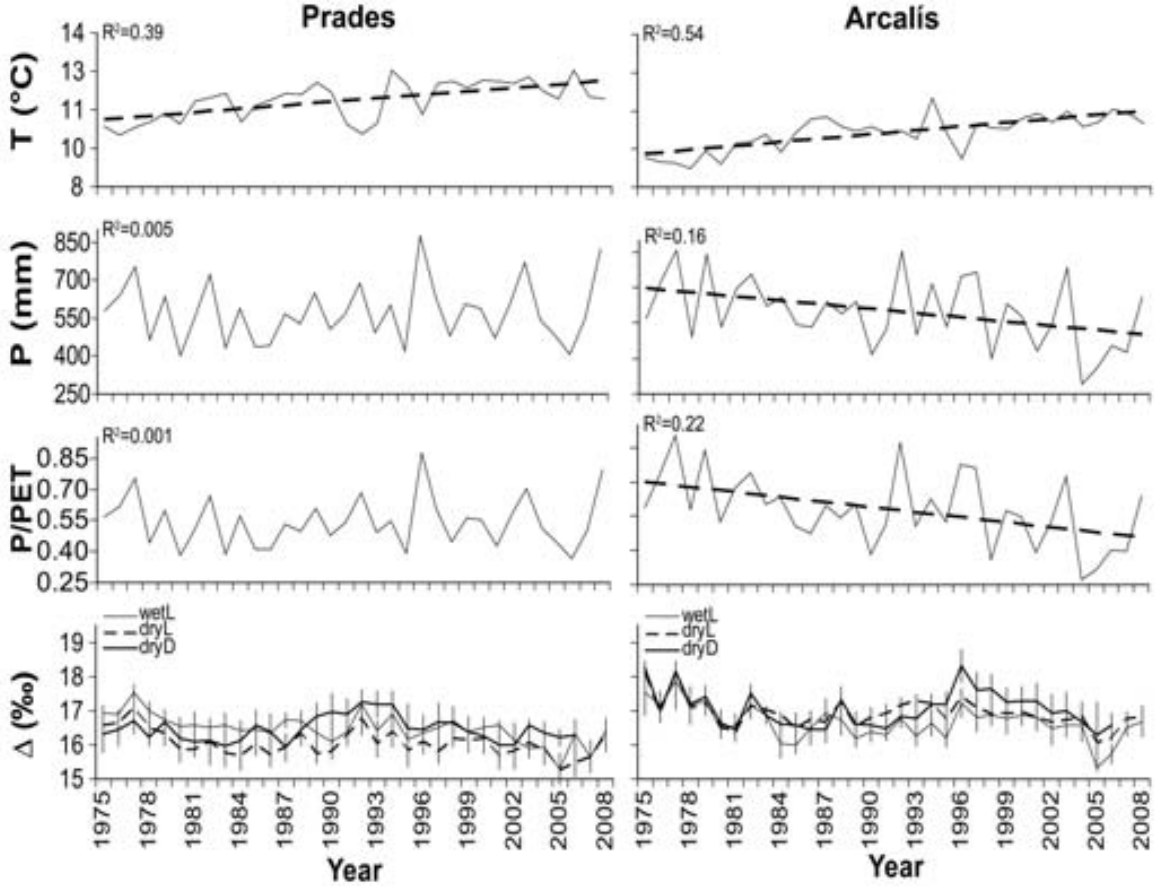

Overall, $\Delta^{13}C$ showed a negative tendency for the 34-year period of this study (Figure 3.1). The comparison of slope responses suggested that changes in $\Delta^{13}C$ over time were probably not homogeneous among tree conditions (*P*=0.056 for the term Condition × Year, Table 3.2*a*). In fact, the contrast between dryD and living (wetL and dryL) trees was found to be significant irrespective of site (the slope was 0.017‰ year^{-1} higher (less negative) in dryD trees than in living trees, *P*<0.05). On the other hand, no statistical difference was found between the wetL and dryL groups (*P*=0.345). Although $\Delta^{13}C$ values were higher at Arcalís than at Prades, there were no significant changes in $\Delta^{13}C$ over time due to either site or site by condition interaction (Table 3.2*a*).

Table 3.2*a* – Results of mixed linear models (ANOVA table) with $\Delta^{13}C$ as a function of Condition, Site and Year. Significant relationships (P<0.05) are marked in bold. Abbreviations: *DF*, degrees of freedom

Fixed effects	DF (numerator)	DF (denominator)	*F* value	*P* value
Condition	2	905	0.61	0.546
Site	**1**	**905**	**5.78**	**0.016**
Condition × Site	2	905	0.78	0.460
Year	**1**	**905**	**33.02**	**<0.001**
Condition × Year	2	905	2.89	0.056
Site × Year	1	905	0.17	0.682
Condition × Site × Year	2	905	0.17	0.841

Overall, WUE_i registered a positive tendency between 1975 and 2008 for all Scots pine groups from both sites (Figure 3.2). The comparison of slope responses indicated that changes in WUE_i over time differed among tree conditions, regardless of site (P<0.05 for the term Condition × Year, Table 3.2*b*). The contrast between dryD and living (wetL and dryL) trees was statistically significant (the slope was 0.172 μmol mol^{-1} $year^{-1}$ smaller (less positive) in dryD than in living trees, P<0.05), whereas the slope comparison between living individuals (wetL versus dryL) showed no statistical significance (P=0.374). As for $\Delta^{13}C$, there were no significant changes in WUE_i over time due to either site or site by condition interaction (Table 3.2*b*).

Table 3.2*b* – Results of mixed linear models (ANOVA table) with WUE_i as a function of Condition, Site and Year. Significant relationships (P<0.05) are marked in bold. Abbreviations: *DF*, degrees of freedom

Fixed effects	DF (numerator)	DF (denominator)	*F* value	*P* value
Condition	2	905	0.89	0.411
Site	**1**	**905**	**5.94**	**0.015**
Condition × Site	2	905	0.79	0.453
Year	**1**	**905**	**414.30**	**<0.001**
Condition × Year	**2**	**905**	**3.12**	**0.045**
Site × Year	1	905	0.00	0.981
Condition × Site × Year	2	905	0.08	0.924

Signal strength of $\Delta^{13}C$ series

The strength of the common $\Delta^{13}C$ signal for different series combinations is summarised in Table 3.3. At the within-site level, the six tree groups were initially considered as separate (wetL, dryL and dryD for the two sites). For this primary grouping, the mean inter-series correlation (a_{fcv}) took values around 0.5 or less, and no obvious differences in signal strength were evident when comparing these six groups (as indicated also by the magnitudes of SE (a_{fcv})). EPS did not reach the 0.85 threshold value, although in most cases it was close to it (0.84). Therefore, the estimated number of trees required to achieve EPS=0.85 exceeded the amount of sampled trees for each group (t>5 in most cases).

Table 3.3 – Strenght of the common $\Delta^{13}C$ signal. Abbreviations: *n*, number of trees combined; a_{fcv}, fractional common variance; *SE* (a_{fcv}), standard error associated to the mean inter-correlation a_{fcv}; *EPS*, expressed population signal; *t*, number of trees needed to achive an EPS=0.85

Site	Condition	*n*	a_{fcv}	SE (a_{fcv})	EPS	*t*
Prades	wetL	5	0.51	0.134	0.84	6
	dryL	5	0.34	0.151	0.72	11
	dryD	4	0.57	0.301	0.84	5
	wetL + dryL + dryD	14	0.36	0.135	0.89	10
	wetL + dryL	10	0.41	0.122	0.88	8
Arcalís	wetL	5	0.38	0.146	0.76	9
	dryL	5	0.51	0.101	0.84	6
	dryD	5	0.52	0.122	0.84	6
	wetL + dryL + dryD	15	0.45	0.095	0.92	7
	wetL + dryL	10	0.43	0.105	0.88	8
Prades and	wetL + dryL + dryD	29	0.36	0.101	0.94	10
Arcalís	wetL + dryL	20	0.41	0.112	0.93	8
	dryD	9	0.32	0.210	0.81	12

When combining series of living trees (wetL and dryL) at either site, a_{fcv} values did not depart substantially from the averaged a_{fcv}'s of the original tree groups, indicating that there was not a transect-specific chronology signal for the surviving individuals. EPS values were now >0.85, as this parameter is strongly dependent on the number of series. In Prades, when now-dead individuals were also added, a decrease of a_{fcv} coupled with an increase of *t* was registered, indicating that those trees did not have a good synchronicity with their surviving neighbours. This wasn't the case for Arcalís, where a_{fcv} value slightly increased and *t* value slightly decreased when now-dead trees were considered together with the surviving ones. EPS values remained higher than 0.85 at both sites.

When living trees from Prades and Arcalís were pooled together, the quality of the signal strength remained unaffected (i.e., a_{fcv} and *t* exhibited similar values to those observed for either site separately). In contrast, now-dead trees from Prades and Arcalís behaved quite differently, as a_{fcv} and EPS decreased when they were pooled together (yielding the lowest a_{fcv} value of all possible combinations), and *t* increased, as compared with the values of both sites separately. When all trees of both sites were combined to provide an estimate of signal strength at a broad geographical scale, the a_{fcv} and *t* estimates were similar to those of Prades alone.

WUE_i scenarios and climate influence on WUE_i

The results obtained comparing the time trends of $\Delta^{13}C$-based WUE_i records against the three theoretical scenarios of WUE_i change (C_i=ct, C_i/C_a=ct, C_a-C_i=ct) indicated that the surviving trees from Prades and Arcalís (wetL and dryL) had a behaviour similar to the C_i=ct scenario. By contrast, the behaviour of now-dead trees from Prades and Arcalís was closer to the C_i/C_a=ct scenario, particularly at the former site (see Supplementary Table 3.1, Figure 3.2). These results remained qualitatively similar if year 1996, which showed unusually low values for all trees at the Arcalís site (Figure 3.2), was not included in the analyses (data not shown).

Figure 3.2 - Time trends of $\Delta^{13}C$-based WUE_i data in relation to three theoretical scenarios (described in Materials and methods) for living and now-dead Scots pines from Prades and Arcalís. The $\Delta^{13}C$-based WUE_i trend for the dryD trees ends in 2006, as this was the last year with a sample size > 2. Abbreviation: ct, constant.

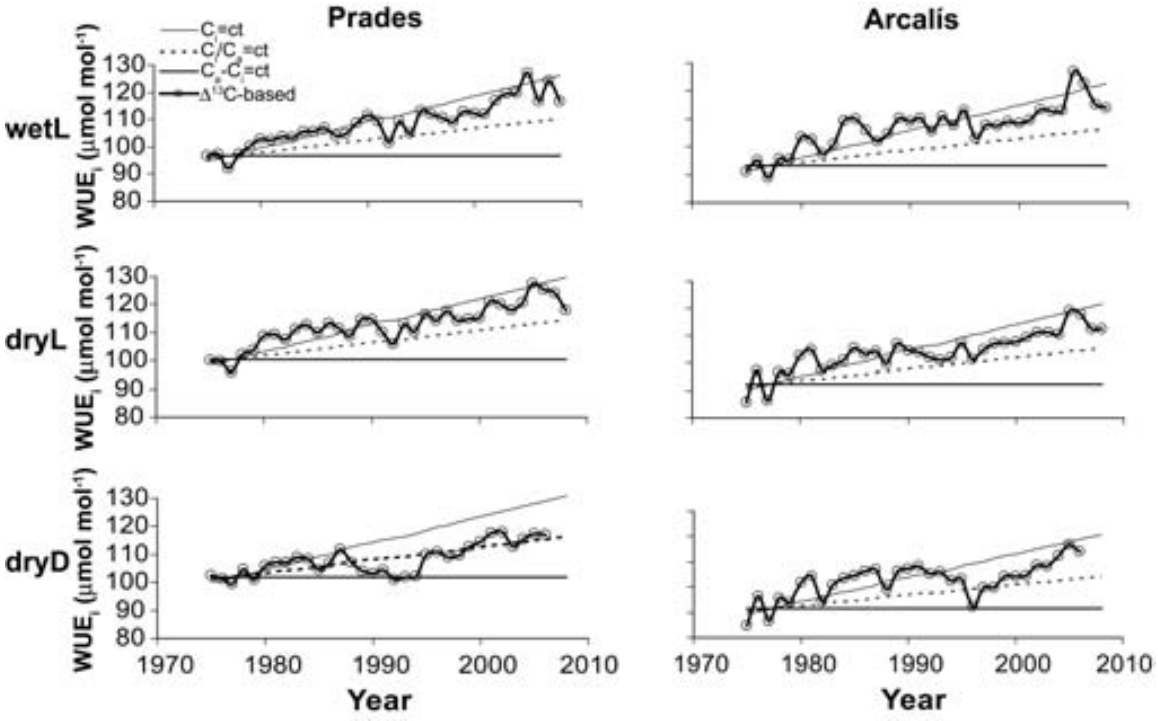

Both C_a and P/PET significantly influenced WUE_i at the two study sites (Table 3.4). C_a had an overall positive effect, while P/PET determined an overall negative influence on WUE_i during the 34 years considered here (Figure 3.3). The comparison of slope responses indicated that changes in WUE_i due to raising atmospheric CO_2 were heterogeneous among tree conditions, regardless of site (P<0.05 for the term Condition × C_a, Table 3.4). The contrast between dryD and living (wetL and dryL) trees was statistically significant (the slope was 0.125 µmol mol^{-1} ppm^{-1} smaller (less positive) in dryD than in living trees, P<0.01), whereas the slope comparison between living individuals (wetL versus dryL) showed no statistical significance (P=0.369). There were no significant changes in the response of WUE_i to raising atmospheric CO_2 due to either site or site by condition interaction. On the other hand, changes in WUE_i driven by P/PET fluctuations did not depend on condition, site or condition by site interaction (Table 3.4).

Table 3.4 – Results of mixed linear models (ANOVA table) with WUE_i as a function of Condition, Site, C_a and P/PET. Significant relationships (P<0.05) are marked in bold. Abbreviations: *DF*, degrees of freedom

Fixed effects	DF (numerator)	DF (denominator)	*F* value	*P* value
Condition	2	899	0.91	0.415
Site	**1**	**899**	**6.09**	**0.022**
Condition × Site	2	899	0.80	0.463
C_a	**1**	**899**	**456.89**	**<0.001**
Condition × C_a	**2**	**899**	**3.55**	**0.031**
Site × C_a	1	899	0.00	0.954
Condition × Site × C_a	2	899	0.08	0.926
P/PET	**1**	**899**	**159.70**	**<0.001**
Condition × P/PET	2	899	0.08	0.927
Site × P/PET	1	899	1.61	0.206
Condition × Site × P/PET	2	899	2.09	0.125

Figure 3.3 - The effects of C_a and P/PET on WUE_i as a function of Condition and Site. Different letters indicate significant differences between slopes of wetL, dryL and dryD trees according to a Least Significant Difference test (α=0.05).

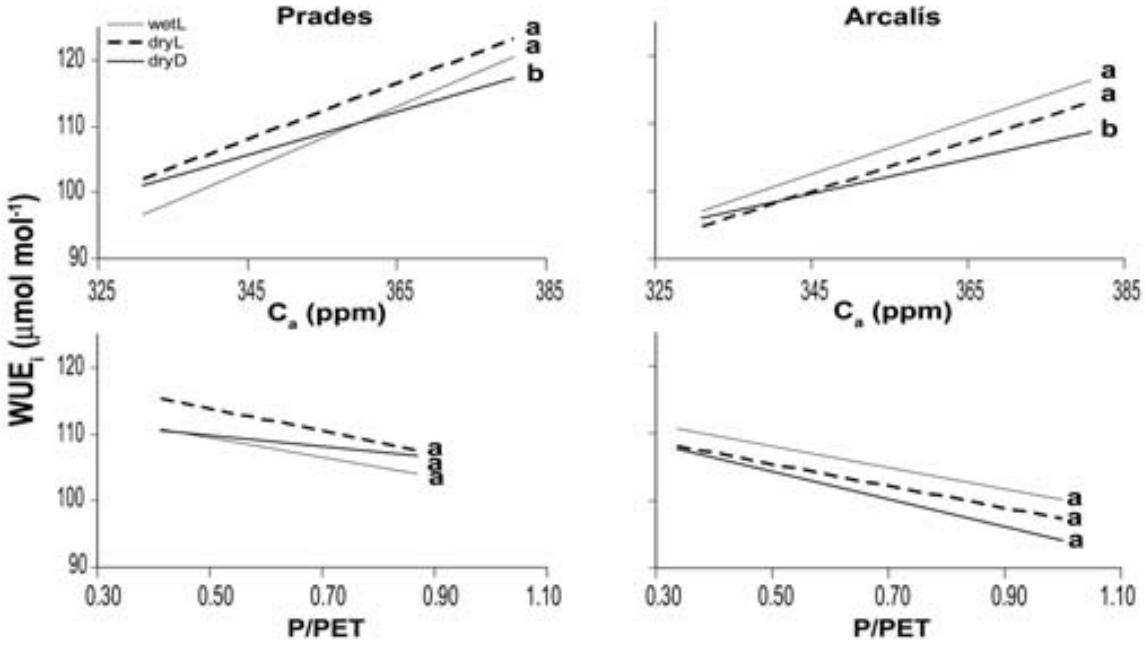

Relationships between WUE_i and BAI

The positive trend that WUE_i showed over the 34 years study period did not translate into an enhancement of BAI. In fact, a negative relationship was found between these two variables, indicating that while Scots pines experienced an increase in WUE_i, their BAI decreased (Figure 3.4). The comparison of slopes indicated that the response of BAI to WUE_i depended simultaneously on condition and site (Table 3.5). In Prades the contrast between dryD and living (wetL and dryL) trees was statistically significant (the slope was 0.009 cm^2 mol μmol^{-1} smaller (more negative) for surviving trees, $P<0.05$). In Arcalís, however, the contrast was statistically significant between dryL and wetL individuals (the slope was 0.008 cm^2 mol μmol^{-1} smaller (more negative) for living trees from the dry transect, $P<0.01$), but not between now-dead and surviving individuals.

Figure 3.4 - Relationships between WUE_i and BAI as a function of Condition and Site. Different letters indicate significant differences between slopes of wetL, dryL and dryD trees according to a Least Significant Difference test (α=0.05).

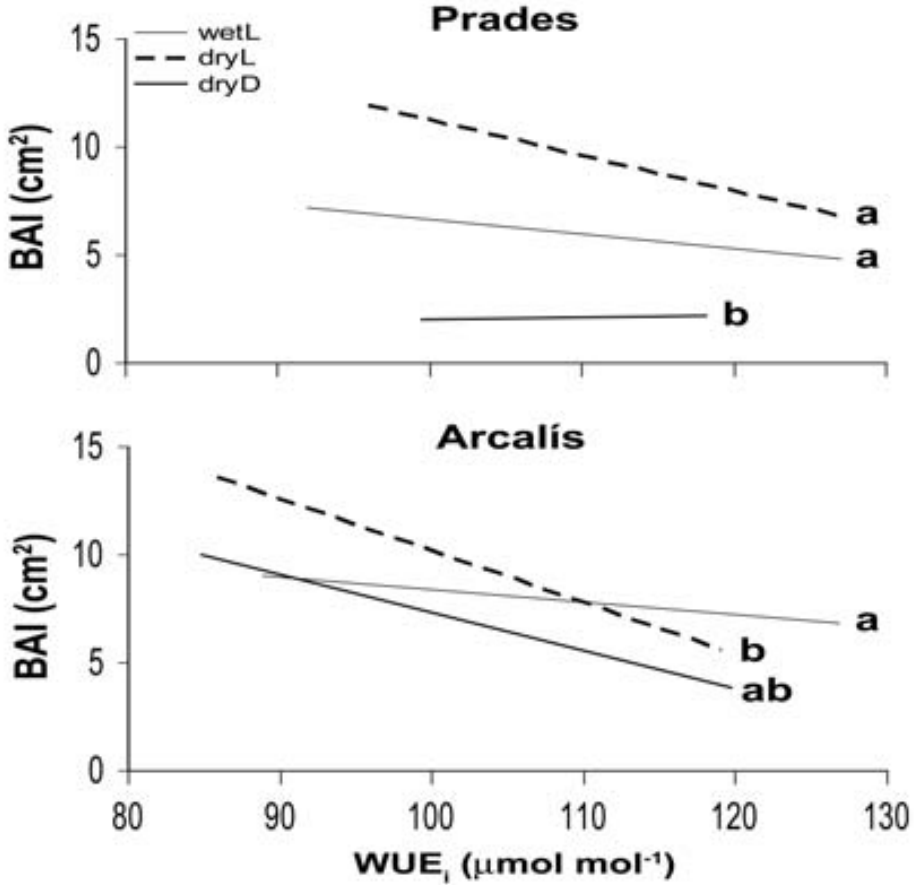

Table 3.5 - Results of mixed linear models (ANOVA table) with logBAI as a function of Condition, Site, and WUE_i. Significant relationships ($P<0.05$) are marked in bold. Abbreviations: *DF*, degrees of freedom

Fixed effects	DF (numerator)	DF (denominator)	*F* value	*P* value
Condition	**2**	**905**	**5.28**	**0.005**
Site	**1**	**905**	**4.65**	**0.031**
Condition × Site	**2**	**905**	**3.24**	**0.040**
WUE_i	**1**	**905**	**49.71**	**<0.001**
Condition × WUE_i	2	905	2.91	0.055
Site × WUE_i	**1**	**905**	**4.18**	**0.041**
Condition × Site × WUE_i	**2**	**905**	**4.59**	**0.010**

DISCUSSION

Structure of the $\Delta^{13}C$ signal in now-dead and living trees

Overall, mean inter-series correlations (a_{fcv}) for $\Delta^{13}C$ at the within-site level were in the lower range of values reported in the literature, e.g., 0.62-0.80 for *Pinus sylvestris* (L.) in Finland (McCarroll and Pawellek 1998) or 0.57 for *Pinus edulis* (Engelm.) in Arizona (Leavitt 2010). Accordingly, EPS values below the consensus threshold value of 0.85 (Wigley *et al.* 1984) were observed at the group level, regardless of site, transect and tree condition. This threshold value is considered particularly relevant for paleoclimatic reconstructions (McCarroll and Pawellek 1998), while in dendroecological studies it is just an indicator of signal strength useful to compare different series combinations. Our EPS values, however, were similar to those reported in mountain dry environments for ^{13}C chronologies made up of 4-6 trees, either for conifers (0.80-0.90; Gagen *et al.* 2004) or hardwoods (0.84; Aguilera *et al.* 2011), which suggests that under such conditions it may be advisable to increase the number of sampled trees to at least 7-8 individuals in order to strengthen the combined chronology ^{13}C signal.

At the within-site level, our results suggest that now-dead trees were slightly more synchronous than their surviving neighbours. However, it must be stressed that the

associated SE's were high enough as to prevent strong conclusions on this point. The clear reduction in synchronicity observed after pooling series of now-dead and living individuals from Prades (the most xeric of the two sites) points to the presence of a differential physiological reaction in dying and surviving Scots pine trees to the climatic fluctuations of the last decades under very limiting conditions. Indeed, such an outcome is related to the differential response to factors underlying WUE_i variation at the tree groups level (see below), and may be associated to differences in their ability to cope with different local factors (e.g., drought, microecological conditions) (Andreu *et al.* 2008). On the other hand, the realisation that living trees from a particular site were about equally correlated between them regardless of ecological condition (dry or wet transect) might indicate that microenvironmental heterogeneity (e.g., edaphic, age or competition effects) tends to blur larger-scale ecological constraints of tree performance (e.g., water availability) registered in tree rings, at least in this Mediterranean system.

At a larger geographical scale, the relatively high a_{fcv} (unrelated to sample size) and EPS (highly dependent on sample size) values found when living individuals from Prades and Arcalís were combined, suggests that climate could be the principal cause underlying synchronicity among trees. Prades and Arcalís are >100 km away from each other and no other factors besides the climatic ones are likely to act at such a wide spatial scale (Hughes *et al.* 1982; Andreu *et al.* 2007). Previous studies have shown that $\delta^{13}C$ series are less sensitive to local factors than growth patterns and therefore they reflect better the climatic signal at larger scales (Gagen *et al.* 2004; Andreu *et al.* 2008).

Temporal dynamics of WUE_i

Now-dead and living Scots pines from Prades and Arcalís significantly increased their WUE_i over the 34 years considered for this study, consistent with recent findings for temperate and boreal forests of the Northern Hemisphere (Keenan *et al.* 2013). Nevertheless, the rate of increase of WUE_i was lower in now-dead individuals, implying that, compared to surviving individuals, those pines were not able to take full advantage (e.g., controlling water losses while maintaining photosynthetic rates) of the increasing C_a over time (Waterhouse *et al.* 2004). Contrary to our hypothesis that

now-dead trees would show a more pronounced climatic sensitivity of WUE_i (i.e., a steeper response to P/PET), no such differences were found with surviving individuals. In contrast, McDowell *et al.* (2010) found that *Pinus ponderosa* (Doug.) trees that died showed no climatic sensitivity of their gas exchange traits, although this sensitivity was strong in surviving individuals. The lower rates of WUE_i increase shown by the now-dead Scots pine trees from Prades and Arcalís were the result of a behaviour that was consistent with the constant C_i/C_a scenario over time (Prades) or in between the C_i/C_a=ct and C_i=ct scenarios (Arcalís), in contrast to the constant C_i behaviour observed for the surviving trees at both sites. These results are in agreement with those reported by Linares and Camarero (2012) showing that declining *Abies alba* (Mill.) individuals also behaved closer to the constant C_i/C_a scenario. Nevertheless, this behaviour seems not to be limited to trees affected by drought-induced decline, as it has also been reported for *Pinus* and *Larix* species growing at high northern latitudes in Eurasia, where it has been attributed to a regulative response to the rising CO_2 concentrations in which C_i/C_a is used as a set point for the gas exchange (Saurer *et al.* 2004).

The constant C_i/C_a scenario implies a progressive increase of the WUE_i due to the proportional regulation of stomatal conductance and photosynthesis (Wong *et al.* 1979; Saurer *et al.* 2004). Water stress conditions are known to reduce stomatal conductance and photosynthesis, although stomatal conductance is normally more affected (Farquhar *et al.* 1989). A possible explanation of the result that trees suffering drought-induced decline are not able to react to changes in C_a over time as efficiently (i.e., maintaining a constant C_i) as their living counterparts, is the presence of non-stomatal limitations to photosynthesis. Under drought conditions, these limitations might involve decreases in mesophyll conductance to CO_2, as has been reported in experimental (e.g., Galmés *et al.* 2007) and modelling studies (Keenan *et al.* 2010) for Mediterranean species. Differences in whole plant structure and tolerance to hydraulic failure, either environmentally- or genetically-induced, have been reported to determine different rates of recovery of mesophyll conductance after recurrent drought events (Flexas *et al.* 2012), which may have conditioned the capacity to survive drought in declining trees by hindering photosynthetic activity and WUE_i in the long-term.

Since respiration rate increases with temperature, an alternative explanation of the shallower response of WUE_i to C_a in now-dead trees could be the higher sensitivity of respiration to rising temperature in these trees. Both higher non-stomatal limitations to photosynthesis and increased respiration affect negatively the tree carbon balance and, in combination with drought-induced defoliation, may lead to depleted reserves and carbon starvation, as has been observed at the study sites (Galiano *et al.* 2011; Poyatos *et al.* 2013). In any case, the partial decoupling between rising CO_2 concentrations and WUE_i in now-dead trees suggests that a critical point in raising WUE_i under increasing CO_2 concentrations may have been reached, and that drought can counterbalance the stimulating effect of increasing CO_2 concentrations on the plant carbon budget (Duquesnay *et al.* 1998; Saurer *et al.* 2004; Waterhouse *et al.* 2004; Linares *et al.* 2009; Linares and Camarero 2012).

Relationship between WUE_i and radial growth

Overall, Scots pine trees from Prades and Arcalís showed a negative relationship between WUE_i and BAI, indicating that increasing WUE_i over time may not translate into growth enhancements, particularly in drought-prone areas (Peñuelas *et al.* 2008; Peñuelas *et al.* 2011; Andreu-Hayles *et al.* 2011). Contrary to McDowell *et al.* (2010) in *Pinus ponderosa* (Doug.) or Voltas *et al.* (2013) in *Pinus sylvestris* (L.) affected by a winter-drought induced die-back, we did not observe a steeper negative relationship between WUE_i and BAI in now-dead trees. This might be due, at least in part, to the fact that measured BAI values were low and showed less variability over the study period considered in this study (Hereş *et al.* 2012). In addition, it remains unclear how changes in volumetric growth would translate into biomass growth rates, as wood density might have also changed. Although we did not measure wood density, our own wood anatomy data for these same trees shows that most of the radial growth difference between now-dead and surviving trees was explained by differences in tracheid cell production per year (and not by tracheid dimensions) (Hereş *et al.* unpublished data) which suggests that wood density changes did not play a major role in this case.

Our results show that increasing WUE_i might not be sufficient to overcome the impacts of a warmer and drier climate on growth, as those conditions might actually

overcome the stimulating effect of rising CO_2 in water-limited areas such as the Mediterranean (Peñuelas *et al.* 2008; Linares *et al.* 2009). This indicates that water availability, when limiting, tips the balance towards low growth rates due either to low carbon gain per se (Linares *et al.* 2009), either to the direct effect of drought on cell formation and development (Hsiao 1973), or to a combination of both factors.

A direct effect of drought on growth, not necessarily mediated by lowered photosynthesis, is supported by the notion that growth is normally more sensitive to moderate drought than assimilation (Sala *et al.* 2012 and references therein). Previous studies show that now-dead pines from the same sites studied here started to reduce their growth (compared to surviving neighbours) decades before death (Hereş *et al.* 2012) and that decaying pines have low leaf area and extremely low levels of carbohydrate reserves (Galiano *et al.* 2011). As it is unclear whether under extreme drought the growth of decaying trees relies increasingly on stored carbon pools (cf. Eilmann *et al.* 2010), an alternative (or complementary) hypothesis would be that stored carbon is preferentially allocated to other metabolic uses (e.g., defence, rooting).

CONCLUSIONS

Our study shows that now-dead Scots pine trees had a distinct time trend of WUE_i, with lower rates of increase in response to rising C_a than surviving individuals. This result adds to previous studies at the same sites showing that tree mortality is the last stage of a long declining process marked by characteristic growth patterns (Hereş *et al.* 2012) and ecophysiology (Galiano *et al.* 2011), and suggests fundamental differences in photosynthetic limitations and, perhaps, carbon allocation or respiration costs between dying and surviving trees. Considering that all studied trees at each site were growing in the same valley and thus exposed to reasonably similar environmental conditions, our results also suggest that Scots pine trees from Prades and Arcalís may be living close to an abrupt survival threshold that, once exceeded, leads to tree mortality (Peñuelas *et al.* 2008; Linares *et al.* 2009; Linares and Camarero 2012; Williams *et al.* 2013). If the projections of increased drought in the studied region are correct (IPCC 2007), episodes of Scots pine die-off are likely to

continue, leading eventually to a shift in the dominant vegetation (Galiano *et al.* 2010; Matías and Jump 2012).

ACKNOWLEDGMENTS The authors would like to thank JP Ferrio, M Aguilera, P Sopeña and M Lucà for laboratory assistance and interesting discussions related to the study. We are indebted to M Mencuccini for field work and valuable discussion on the research topic. The authors also thank M Ninyerola and the Catalan Meteorological Service (SMC) for providing the two climatic datasets used in this study. Two anonymous referees contributed to the improvement of the original version of the article. This research was funded by the Spanish Ministry of Science and Innovation via competitive projects ("CGL2007-60120", "CSD2008-0040", "CGL2010-16373"), a FPU PhD scholarship and a short study stay at the University of Lleida, Department of Crop and Forest Sciences.

Supplementary Table 3.1 – Results of linear regressions between $\Delta^{13}C$-based and theoretical WUE_i values according to the three scenarios proposed by Saurer *et al.* (2004). RMSError values are also given. Abbreviations: β_0, intercept; β_1, slope; β_1', slope when the intercept is set to 0; *RMSError*, root mean square error; *ct*, constant

Site	Condition	Scenario	β_0	Confidence interval (95%) for β_0	β_1	Confidence interval (95%) for β_1	β_1'	Confidence interval (95%) for β_1'	RMSError
Prades	wetL	C_i=ct	22.831	9.21 – 36.45	0.777	0.65 - 0.90	0.982	0.97 - 0.99	4.22
	wetL	C_i/C_a=ct	-64.031	(-)91.38 – (-)36.68	1.675	1.41 – 1.94	1.054	1.04 – 1.07	6.98
	wetL	C_a-C_i=ct	-	-	-	-	-	-	14.25
	dryL	C_i=ct	34.178	19.60 – 48.75	0.689	0.56 – 0.82	0.987	0.97 – 1.00	4.56
	dryL	C_i/C_a=ct	-40.445	(-)68.81 - (-)12.09	1.432	1.17 – 1.70	1.054	1.04 – 1.07	6.89
	dryL	C_a-C_i=ct	-	-	-	-	-	-	14.22
	dryD	C_i=ct	53.853	36.73 – 70.98	0.474	0.33 – 0.62	0.941	0.92 – 0.96	8.63
	dryD	C_i/C_a=ct	3.245	(-)29.78 – 36.27	0.970	0.67 – 1.28	1.000	0.99 – 1.01	3.49
	dryD	C_a-C_i=ct	-	-	-	-	-	-	8.24
Arcalis	wetL	C_i=ct	29.471	11.58 – 47.36	0.724	0.56 – 0.89	0.998	0.98 – 1.01	5.01
	wetL	C_i/C_a=ct	-54.084	(-)91.19 - (-)16.98	1.619	1.25 – 1.99	1.076	1.06 – 1.09	8.98
	wetL	C_a-C_i=ct	-	-	-	-	-	-	15.70
	dryL	C_i=ct	34.221	19.04 – 49.40	0.660	0.52 – 0.80	0.980	0.96 – 1.00	5.19
	dryL	C_i/C_a=ct	-42.541	(-)74.28 - (-)10.80	1.490	1.17 – 1.81	1.059	1.04 – 1.07	7.09
	dryL	C_a-C_i=ct	-	-	-	-	-	-	13.73
	dryD	C_i=ct	44.982	22.28 – 67.68	0.553	0.34 – 0.77	0.982	0.96 – 1.00	6.61
	dryD	C_i/C_a=ct	-19.880	(-)68.03 – 28.27	1.262	0.77 – 1.76	1.057	1.04 – 1.08	7.57
	dryD	C_a-C_i=ct	-	-	-	-	-	-	13.09

Supplementary Figure 3.1 - Pearson correlations between WUE_i and monthly climatic variables (*T* and *P*). Time interval covers months from previous to growth year (jul to dec) and from current year of growth (JAN to DEC). Significant correlations are indicated with * (*P*<0.05) and ** (*P*<0.01).

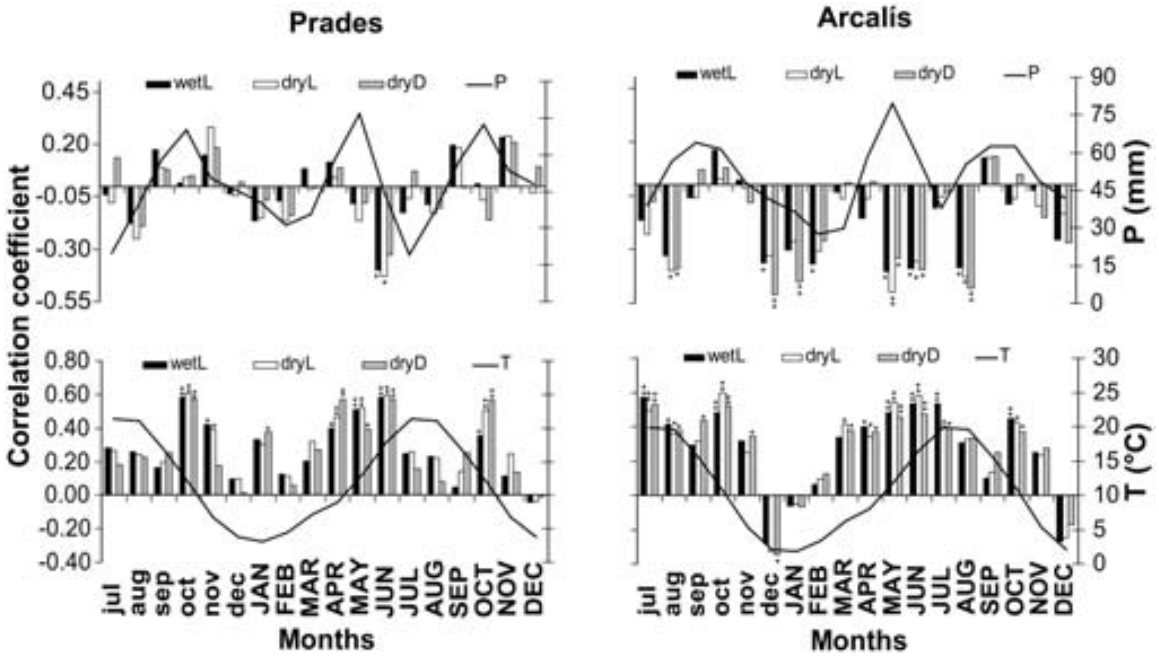

Chapter 4

DECLINING HYDRAULIC PERFORMENCES AND LOW CARBON INVESTMENTS PREDATE SCOTS PINE DROUGHT-ASSOCIATED MORTALITY AT ITS SOUTH-WESTERN DISTRIBUTION LIMIT

This chapter is *in prep.*

Hereş AM, Camarero JJ, Claramunt López B, Martínez-Vilalta J

ABSTRACT

Widespread episodes of drought-associated tree mortality are predicted to increase in intensity and frequency as climate becomes warmer and drier. Nevertheless, mechanisms related to tree mortality are still poorly understood. Wood anatomical features carry on valuable information that can be extracted at high temporal resolution and used in retrospective analyses of tree death. We studied two Scots pine (*Pinus sylvestris* L.) sites, located in North Eastern Iberian Peninsula, where drought-induced mortality events have been registered over the last decades. Co-occurring now-dead and living trees were sampled and their wood anatomical features were measured and compared at annual resolution. Our objectives were to investigate differences in anatomical features between the two vitality classes and to infer past physiological performances that might have determined their death or survival. Now-dead trees showed lower tracheid and resin duct production, and smaller radial lumen sizes than living trees. These anatomical differences were observed throughout the 34-year study period in one site (Prades), but appeared more recently, i.e. when mortality rates peaked, at the other site (Arcalís). This indicates that dead trees' hydraulic conductance was severely affected and that carbon investment in xylem formation, including resin duct production, was constrained, probably due to limited and/or unavailable carbon reserves. Interestingly, no differences were found in terms of vulnerability to xylem embolism in the stem (inferred from tracheid anatomy) between now-dead and surviving individuals. Altogether, our findings show that both hydraulic deterioration and low allocation of carbon into the xylem were associated to drought-induced mortality at the studied Scots pine sites, although the temporal dynamics of these processes differed markedly between populations.

INTRODUCTION

Episodes of drought-associated tree mortality have been reported in all major forest biomes of the Earth (Allen *et al.* 2010), and are likely to become more frequent under a progressively warmer and drier climate (IPCC 2007). Consequently, understanding the mechanisms that underlie tree mortality has become a research priority. In Mediterranean regions like the Iberian Peninsula, water availability is the main limiting factor for tree growth (Cherubini *et al.* 2003; Martínez-Vilalta *et al.* 2008 and references therein). In these regions, temperature and evapotranspiration have increased during the last decades, in concert with the frequency and intensity of severe droughts (Piñol *et al.* 1998; IPCC 2007). Mediterranean forests are thus considered to be especially vulnerable to the increase in the occurrence of severe droughts predicted by climate change models (Giorgi and Lionello 2008; Martínez-Vilalta *et al.* 2012; Matías and Jump 2012).

The mechanisms that underlie drought-induced tree mortality are still poorly understood and highly debated (McDowell *et al.* 2008, 2011; Sala *et al.* 2010; McDowell and Sevanto 2010; McDowell 2011). The efficiency and safety of the water transport through the xylem is critical for tree performance, especially under stressful climatic conditions such as those imposed by droughts (e.g. Choat *et al.* 2012). Trees growing in dry areas must maintain a functional water transport system by keeping the xylem water potentials above cavitation thresholds when facing drought events (Bréda *et al.* 2006; Brodribb and Cochard 2009). In the case of conifers, building tracheids with narrow lumens and thick walls might be advantageous under these circumstances, as the risk of cavitation generally decreases with smaller lumen diameter and thicker cell walls reduce the risk of collapse (Hacke *et al.* 2001; Cochard *et al.* 2004). Conduit lumen size is expected to be reduced when trees face water stress, as radial enlargement is particularly sensitive to water deficit (Hsiao and Acevedo 1974; von Wilpert 1991). At the same time, tracheids that have a reduced lumen diameter are less efficient for water transport, as the hydraulic conductivity increases with the fourth power of lumen diameter according to the Hagen-Poiseuille law (Tyree and Zimmermann 2002). In addition, prolonged water deficit can affect tracheid division to such degree that later on precipitations might not be able to

compensate for past cumulative stress. As a consequence, narrow rings formed by tracheids with reduced lumen size are built, which translates into reduced water supply to the crown (Zweifel *et al.* 2006).

Wood anatomy studies on dead/dying trees *vs.* living ones are still scarce (but see Levanič *et al.* 2011), yet they can bring valuable information about mortality processes because xylem represents a reliable and long-term proxy of hydraulic performance. A retrospective analysis of the potential hydraulic performance of trees is feasible through wood-anatomical analyses, which constitute a powerful tool for investigating tree responses to past stress conditions (Vaganov *et al.* 2006). Further, this tool has the advantage of a higher temporal resolution than tree rings (Fritts 2001). The environmental conditions acting during wood formation determine cells' features, leaving permanent imprints at the conduit level (Denne and Dodd 1981; Wimmer 2002; Fonti *et al.* 2010). The long-term theoretical hydraulic performance of a tree can be thus reconstructed through the analyses of anatomical characteristics of transversal wood cross sections.

In Europe, especially in areas characterized by dry climatic conditions, several episodes of drought-induced mortality of Scots pine (*Pinus sylvestris* L.) have been reported (Martínez-Vilalta and Piñol 2002; Bigler *et al.* 2006; Eilmann *et al.* 2006; Galiano *et al.* 2010; Hereş *et al.* 2012; Vilà-Cabrera *et al.* 2013; Rigling *et al.* 2013). Scots pine is a boreal tree species, widespread in the Northern Hemisphere and considered the most widely distributed conifer in the world (Nikolov and Helmisaari 1992). It reaches its south-western (and dry) distribution limit in the Iberian Peninsula (Barbéro *et al.* 1998), where about half of its range is represented by natural populations (Catalan Bachiller *et al.* 1991; Martín *et al.* 2010). Scots pine is a "drought-avoiding" species, with a relatively high vulnerability to xylem embolism (Cochard 1992) and a fast stomatal response to reduce evaporative water loss under drought conditions (Irvine *et al.* 1998; Poyatos *et al.* 2013).

In this study, we compare the wood anatomy of co-occurring now-dead and living Scots pine trees sampled at two sites located in North Eastern Iberian Peninsula. The analyses are made at an annual resolution for a period of 34 years (1975 to 2008).

Previous studies on the same individuals showed that tree mortality was associated with severe drought periods and that now-dead individuals started to grow less than their surviving neighbours 15 to 40 years before death occurred, depending on the site (Hereş *et al.* 2012). Our main objective here was to compare the stem xylem structure of now-dead trees and their surviving neighbours during the period previous to death. We retrospectively describe wood anatomy variability in terms of hydraulic conductivity and carbon investment in xylem structure (e.g. number of tracheids, cell-wall thickness) and defence (production of resin ducts). More specifically, we aimed at establishing whether now-dead trees were structurally more vulnerable to xylem embolism than living ones, had an impaired hydraulic system due to the production of very narrow tracheids or reduced their carbon investment in the xylem, which could reflect low carbon availability.

MATERIALS AND METHODS

Study sites

Two Scots pine sites located in the North East of the Iberian Peninsula were selected: Prades (Prades Mountains, 41°33'N, 1°01'E) and Arcalís (Soriguera, Central Pyrenees, 42°34'N, 1°09'E). At these two sites, high mortality rates following particularly dry years have been observed starting in the 1990s (Martínez-Vilalta and Piñol 2002; Galiano *et al.* 2010; Poyatos *et al.* 2013). In addition, a direct association between tree mortality and severe drought periods characterized by low water availability in summer has been reported (Hereş *et al.* 2012). The climate in Prades is typically Mediterranean while in Arcalís it is characterized by cool-summer Mediterranean conditions (Köppen 1936). Mean annual temperature in Prades is around 11.2°C, and the mean annual rainfall is 611 mm. In Arcalís, the mean annual temperature is lower (9.7°C), and the mean annual rainfall is slightly higher (653 mm) than in Prades (Climatic Digital Atlas of Catalonia, period 1951-2006) (Pons 1996; Ninyerola *et al.* 2000). The vegetation type at the two sites follows an altitudinal gradient, with Mediterranean species at low altitudes and Scots pine appearing above 800 m in Prades and between 600 and 1500 m in Arcalís. The soils in Prades are xerochrepts with a clay-loam texture (Hereter and Sánchez 1999), and in Arcalís they

are calcareous with a clay-loam texture and have a low water retention capacity (Galiano *et al.* 2010).

Sampling

Scots pine trees used in this study were sampled in late autumn 2008 (Prades) and early spring 2009 (Arcalís) along constant altitude transects (1000 m a.s.l for both sites) located on north facing slopes. Sampling consisted in coring at breast height (1.3 m) and orthogonal to the slope co-occurring living (L) and dead (D) individuals using increment borers. Here we use 20 trees (10 per site, i.e. 5 L and 5 D trees) that were cross-dated in a previous study (see **Chapter 2**), from where basal area increment (BAI, cm^2) and tree-ring width (mm) data are available (Hereş *et al.* 2012). L and D trees did not differ significantly in terms of diameter at breast height (DBH) neither in Prades (P=0.793) nor in Arcalís (P=0.533). The age of the L and D individuals was also similar between L and D trees both in Prades (P=0.144) and Arcalís (P=0.411). Sampled trees were separated from each other or from other adult Scots pines, by a distance of at least 5 m. For more details on sampling see **Chapter 2** (Hereş *et al.* 2012).

Wood anatomy measurements

The segments of the cores that included the 1975-2008 period were separated into small blocks (≈ 1cm long) that were further cut transversally with a sliding microtome (Leica SM 2010R; Leica Microsystems, Germany) to obtain fine wood sections (12-18 µm thick). These sections were stained with a mixture of safranin (0.5%) and astrablue (1%) to get a better contrast between tracheid lumen and walls, dehydrated repeatedly in an alcohol concentration gradient (50% an 96%), and mounted using a synthetic resin (Eukitt; Merck, Darmstadt, Germany) onto permanent glass microscope slides. Images of the sections were taken at magnifications of ×40 using a camera (Leica DFC290; Leica Microsystems, Germany) attached to a transmitted light microscope (Olympus BH2; Olympus, Hamburg, Germany). When tree rings were too wide to fit in one image, several adjacent pictures were taken and then merged using Adobe Photoshop CS4 (Adobe Systems; San Jose, USA). The images were later on used to analyze a total of 646 annual rings, using new Matlab®-based

software (DACiA, Dendrochronological Analysis on Conifer Wood Anatomy) developed in this study (see next section on Software Description and **Chapter 5**).

Tracheids were measured along three to five complete radial rows per ring. Measured variables, analyzed at the whole ring level (RW) and separately for the earlywood (EW) and latewood (LW), included: number of tracheids (NoCells), radial lumen diameter (LD) and cell-wall thickness (CWT). The visual identification of LW, based on the abrupt shifts in colour and tracheid size was preferred over the delineation based on the Mork index (Denne 1988), which proved to largely overestimate LW in our case. Radial dimensions were chosen because they vary along time, while the tangential dimensions are considered to be practically constant (Vysotskaya and Vaganov 1989). Using the measured anatomical features listed above, we calculated the theoretical hydraulic conductance (K_h) according to the Hagen-Poiseuille law (Tyree and Zimmermann 2002), the $(CWT/LD)^2$ ratio (Hacke *et al.* 2001), here used as a surrogate of the xylem vulnerability to embolism, and the cell carbon cost investments (C_{cost}). C_{cost} was estimated by multiplying NoCells by CWT for each tree ring. In order to estimate the carbon allocation to defence (Kane and Kolb 2010), the number of resin ducts produced per annual ring (RD_{RW}) was counted.

A selection of the measured anatomical features was used in further analyses, their subscript indicating if they refer to RW, EW or LW portion of the ring: $NoCells_{RW}$, LD_{RW}, LD_{EW}, CWT_{RW}, CWT_{LW}, K_{hRW}, K_{hEW}, $(CWT/LD)^2_{EW}$, C_{costRW} and RD_{RW} (Table 4.1). This selection was mainly based on the concept that EW has predominantly a water conductive function, while LW has mainly a mechanical one (Eilmann *et al.* 2006; Vaganov *et al.* 2006).

Software description: DACiA

To obtain the anatomical features across transversal wood sections, we developed a new semi-automatic Matlab®-based software (**DACiA**), which is available upon request. Based on state-of-the-art thresholding techniques, the software automatically identifies the tracheid features of the radial rows initially marked along the tree rings, using segmented flexible lines. Further on, a manual procedure corrects pixel by pixel possible measurement errors through an interactive graphic interface that helps to

precisely delimitate tracheid lumens and walls. Finally, the software exports the measured anatomical features directly into their corresponding units of measurements to an Excel© or plain text file.

Climatic and environmental data

Monthly temperature (*T*, ºC) and precipitation (*P*, mm) values (period 1975- 2006) were modelled at a spatial resolution of 180 m from discrete climatic data provided by the Spanish Weather-Monitoring System (www.aemet.es) (Ninyerola *et al.* 2007*a*, *b*). Missing data for the 2007 and 2008 years were estimated by means of regression models using a second climatic dataset that was available from the Catalan Weather Service (www.meteo.cat). Based on the available climatic data, the ratio between precipitation (P) and evapotranspiration (PET) was calculated (P/PET) and used as a drought index. PET was estimated using the Hargreaves method (Hargreaves and Samani 1982).

Preliminary correlation analyses had shown that RW, EW and LW anatomical features responded to climatic variables averaged over different time periods. On the basis of these results and xylogenesis studies on Scots pine (Camarero *et al.* 1998, 2010), three different sets of P/PET measures were used, covering the following time intervals: 1) from previous August to October of the year of tree-ring formation (named current year) for RW (P/PET_{RW}); 2) from previous August to current June for EW (P/PET_{EW}), and 3) from current May to October for LW (P/PET_{LW}). P/PET_{RW}, P/PET_{EW} or P/PET_{LW} values were used in further analyses depending if the analyzed wood anatomical feature represented RW, EW or LW, respectively (see Table 4.1).

Additionally, the 12-month scale standardized precipitation evapotranspiration index (SPEI) (Vicente-Serrano *et al.* 2010*a, b*), was used to explore the correlations between drought and the measured wood anatomical features. SPEI is a multi-scalar drought index that accounts for both the effects of temperature and precipitation on drought severity across different time scales. The lower the SPEI value is, the drier the conditions are (Vicente-Serrano *et al.* 2010*a*, *b*). Based on the best correlation results (Supplementary Figures 4.2*a*, *b*) different SPEI time intervals were selected

(see Supplementary Table 4.1) specifically for each of the selected wood anatomical features (see Table 4.1) and used in further analyses.

Values for the CO_2 atmospheric concentration (C_a) for the 1975 to 2003 period, which were also used to account for their potential effects on anatomical features, were taken from the literature (Robertson *et al.* 2001*a*; McCarroll and Loader 2004). Missing values for the 2004 to 2008 time interval were estimated by means of linear regressions, based on the above mentioned datasets.

Table 4.1 - Statistical parameters of the wood anatomical features measured in living (L) and dead (D) trees. Abbreviations: *NoCells*, number of tracheids; *LD*, radial lumen diameter; *CWT*, cell-wall thickness; K_h, hydraulic conductance; $(CWT/LD)^2_{EW}$, ratio estimating the xylem vulnerability to embolism according to Hacke *et al.* (2001); C_{cost}, carbon cost investment; *RD*, number of resin ducts; *SD*, standard deviation; *CV*, coefficient of variance. For all anatomical features, subindices indicate if they were calculated for the whole ring (RW), for earlywood (EW) or latewood (LW), respectively

Variable (unit)	Statistics	Prades						Arcalis					
		RW		EW		LW		RW		EW		LW	
		L	D	L	D	L	D	L	D	L	D	L	D
$NoCells_{RW}$	Mean	40	13	-	-	-	-	40	34	-	-	-	-
	SD	22.35	11.75	-	-	-	-	20.23	17.68	-	-	-	-
	CV	0.38	0.66	-	-	-	-	0.34	0.48	-	-	-	-
LD_{RW} and LD_{EW} (µm)	Mean	20.81	16.87	26.85	21.97	-	-	19.82	19.25	26.26	25.52	-	-
	SD	3.31	3.34	3.70	3.87	-	-	3.08	2.70	3.53	3.58	-	-
	CV	0.14	0.17	0.13	0.16	-	-	0.13	0.13	0.11	0.12	-	-
CWT_{RW} and CWT_{LW} (µm)	Mean	11.16	9.29	-	-	11.73	8.91	10.28	10.73	-	-	11.21	12.38
	SD	1.40	1.48	-	-	2.17	1.83	1.68	1.50	-	-	2.55	2.28
	CV	0.12	0.14	-	-	0.16	0.18	0.14	0.14	-	-	0.17	0.15
K_{hRW} and K_{hEW} ($kgmMPa^{-1}s^{-1}$)	Mean	3.E-06	5.E-07	3.E-06	5.E-07	-	-	2.E-06	2.E-06	2.E-06	2.E-06	-	-
	SD	2.E-06	6.E-07	2.E-06	6.E-07	-	-	2.E-06	1.E-06	2.E-06	1.E-06	-	-
	CV	0.68	0.96	0.68	0.95	-	-	0.59	0.64	0.59	0.63	-	-
$(CWT/LD)^2_{EW}$	Mean	-	-	0.27	0.27	-	-	-	-	0.20	0.24	-	-
	SD	-	-	0.13	0.13	-	-	-	-	0.08	0.13	-	-
	CV	-	-	0.41	0.42	-	-	-	-	0.34	0.40	-	-
C_{costRW} (µm)	Mean	464	133	-	-	-	-	422	383	-	-	-	-
	SD	296	140	-	-	-	-	243	236	-	-	-	-
	CV	0.44	0.77	-	-	-	-	0.37	0.59	-	-	-	-
RD_{RW} (no $year^{-1}$)	Mean	1.75	0.85	-	-	-	-	1.67	1.38	-	-	-	-
	SD	1.23	1.00	-	-	-	-	1.18	1.13	-	-	-	-
	CV	0.72	1.09	-	-	-	-	0.69	0.84	-	-	-	-

Data analyses

All variables were first checked for normality (Kolmogorov-Smirnov test) and logarithm transformed when necessary ($NoCells_{RW}$, K_{hRW}, K_{hEW}, $(CWT/LD)^2_{EW}$, C_{costRW}, BAI). In the case of RD_{RW} (a count response variable) no transformation was applied, but a Poisson generalized mixed model was used (see below). The $NoCells_{RW}$ variable was not normalized to a common number for all trees (Vaganov 1990), as raw data clearly showed large differences for this variable between D and L Scots pine trees.

Independent samples t-tests were used to analyze differences in DBH and age between L and D Scots pines from Prades and Arcalís. Pearson and Spearman's rank correlation coefficients (the Spearman coefficient was used only in the case of RD_{RW}) were used to quantify the associations between wood anatomical features and climatic variables (*T*, *P* and SPEI), while linear regressions were conducted to assess temporal trends of annual climatic variables (*T*, *P* and P/PET) (see Supplementary Figure 4.1). To evaluate the time-related variability of each of the selected wood anatomical features, the coefficient of variation (CV) was calculated by dividing the standard deviation of each variable by its mean.

In order to analyze the time trends of the wood anatomy features ($NoCells_{RW}$, LD_{EW}, CWT_{LW}, K_{hEW}, $(CWT/LD)^2_{EW}$ and C_{costRW}), the influence of the environmental variables (C_a and P/PET or SPEI) on them and the relationship between BAI and wood anatomical features ($NoCells_{RW}$, LD_{RW}, CWT_{RW}, K_{hRW} and C_{costRW}), linear mixed-effects models were fitted to the data. A first set of models was fitted for each of the studied anatomical variables ($NoCells_{RW}$, LD_{EW}, CWT_{LW}, K_{hEW}, $(CWT/LD)^2_{EW}$ and C_{costRW}). In each case, the fixed part of the model included the effects of tree Condition (L, D), Site (Prades, Arcalís), the interaction Condition × Site, the covariate Year (from 1975 to 2008), and the interactions Condition × Year, Site × Year, and Condition × Site × Year.

Secondly, a more complex set of models was fitted in which the wood anatomy features ($NoCells_{RW}$, LD_{EW}, CWT_{LW}, K_{hEW}, $(CWT/LD)^2_{EW}$ and C_{costRW}) were analyzed as a function of Condition, Site, the interaction Condition × Site, the covariate C_a and

its interactions Condition × C_a, Site × C_a, and Condition × Site × C_a, and the covariate P/PET (or SPEI) and its interactions Condition × P/PET (or SPEI), Site × P/PET (or SPEI), and Condition × Site × P/PET (or SPEI).

A third set of models was used to study the response of BAI to different wood anatomical features ($NoCells_{RW}$, LD_{RW}, CWT_{RW}, K_{hRW} or C_{costRW}). In each case, the fixed part of the models included the effect of Condition, Site, the interaction Condition × Site, the corresponding wood anatomical feature and its interactions with Condition, Site, and Condition × Site.

In all models, tree identity was introduced as subject (random effect) and a first-order autoregressive covariance structure was used to account for temporal autocorrelation. In order to characterize differences between L and D groups, the estimated marginal means were analyzed, applying a Bonferroni correction to compare the main effects. If second order interactions were significant, separate relationships for every site were considered.

In the case of the RD_{RW}, three Poisson generalized mixed models were used. The first model accounted for RD_{RW} time trends, and the second model evaluated the influence of the environmental variables (e.g. C_a and P/PET (or SPEI)) on RD_{RW}. These two models had the same structures as described above for the other selected wood anatomical features. The third model accounted for the relationship between RD_{RW} and ring width, including the (fixed) effects of Condition, Site, the interaction Condition × Site, the covariate ring width, and the interactions Condition × ring width, Site × ring width, and Condition × Site × ring width. As before, tree identity was introduced as subject (random effect) while a first-order autoregressive covariance structure accounted for temporal autocorrelation.

For all models, coefficients were estimated using restricted maximum likelihood methods (REML), and relationships were considered significant or marginally significant when $P<0.05$ and $0.05<P<0.1$, respectively. Statistical analyses were carried out with SPSS (version 15.0, SPSS Inc., Chicago, IL) or R v.3.0 packages (The R Foundation for Statistical Computing 2012).

RESULTS

Patterns and trends of wood anatomical features in L and D trees

In Prades, the temporal variability of the wood anatomical features, evaluated through the CV values, was always higher for the D trees as compared with their L counterparts (Table 4.1). In Arcalís, although this pattern was also observed for most anatomical features, there were cases where the CV values were either similar between L and D individuals (LD_{RW} and CWT_{RW}), or slightly lower for the D trees (CWT_{LW}) (Table 4.1).

The majority of wood anatomical features considered in this study presented a significant negative time trend, the values of the D trees being usually lower than those of the L ones, particularly in Prades (Table 4.2, Figure 4.1). Nevertheless, there were some wood anatomical features like the LD_{EW} of the L trees from both Prades and Arcalís that showed no time trend; or the $(CWT/LD)^2_{EW}$ of the D trees from both Prades and Arcalís that presented a significant positive time trend, whereas no trend (Arcalís) was observed for this feature in L trees (Table 4.2, Figure 4.1). Overall, statistically significant differences were found between the L and D Scots pines from Prades and Arcalís in most of the studied anatomical features ($NoCells_{RW}$, LD_{EW}, CWT_{LW}, K_{hEW}, C_{costRW} and RD_{RW}) (Table 4.2, Figure 4.1). For all the aforementioned features, the predicted values (estimated marginal means) were always lower for the D than for the L trees (data not shown). No statistically significant differences were found between L and D trees in the case of the $(CWT/LD)^2_{EW}$ feature (P=0.454).

Table 4.2 - Results of linear mixed-effects models (estimate ± SE) in which anatomical variables varied as a function of Condition (living, L; dead, D), Site (Prades, Arcalís) and Year (from 1975 to 2008). Significant relationships at 0.1, 0.05, 0.01 and 0.001 probability levels are marked with $^{+}$, *, ** and ***, respectively

Variables	$logNoCells_{RW}$	LD_{EW}	CWT_{LW}	$logK_{hEW}$	$log(CWT/LD)^2_{EW}$	$logC_{costRW}$	RD_{RW}
Intercept	1.676±0.08***	26.600±1.13***	13.826±0.61***	-5.727±0.13***	-0.731±0.05***	2.722±0.10***	0.559±0.15***
L	0.099±0.11	-0.377±1.58	-1.999±0.86*	0.052±0.18	0.005±0.01	0.071±0.13	0.321±0.20
Prades	-0.435±0.11**	-2.387±1.59	-4.255±0.87***	-0.480±0.19*	0.082±0.07	-0.489±0.13**	-0.531±0.22*
L*Prades	0.418±0.16*	2.420±2.24	4.923±1.22***	0.658±0.26*	0.108±0.10	0.520±0.19*	0.521±0.29^{+}
Year	-0.014±0.00***	-0.075±0.04*	-0.101±0.02***	-0.015±0.00**	0.003±0.00^{+}	-0.016±0.00***	-0.020±0.01**
L*Year	0.000±0.00	0.083±0.05^{+}	0.066±0.03*	0.004±0.01	-0.004±0.00	0.001±0.00	-0.005±0.01
Prades*Year	-0.001±0.00	-0.083±0.05	0.056±0.03^{+}	-0.013±0.01*	-0.000±0.00	-0.002±0.00	0.005±0.01
L*Prades*Year	0.003±0.00	0.107±0.07	-0.066±0.04^{+}	0.012±0.01	-0.004±0.00	0.003±0.01	-0.001±0.01

Figure 4.1 - Time trends of anatomical features (means ± SE) for living (L) and dead (D) trees in Prades and Arcalís study sites. Regression lines represent estimated slopes from the corresponding general (generalized in the case of RD_{RW}) linear mixed-effects models and they are represented only if significant. Asterisks (*) indicate significant differences between slopes of L and D trees. Data for D trees end in 2006, as this was the last year with a sample size >2. See **Table 4.1** for the meaning of variables' abbreviations.

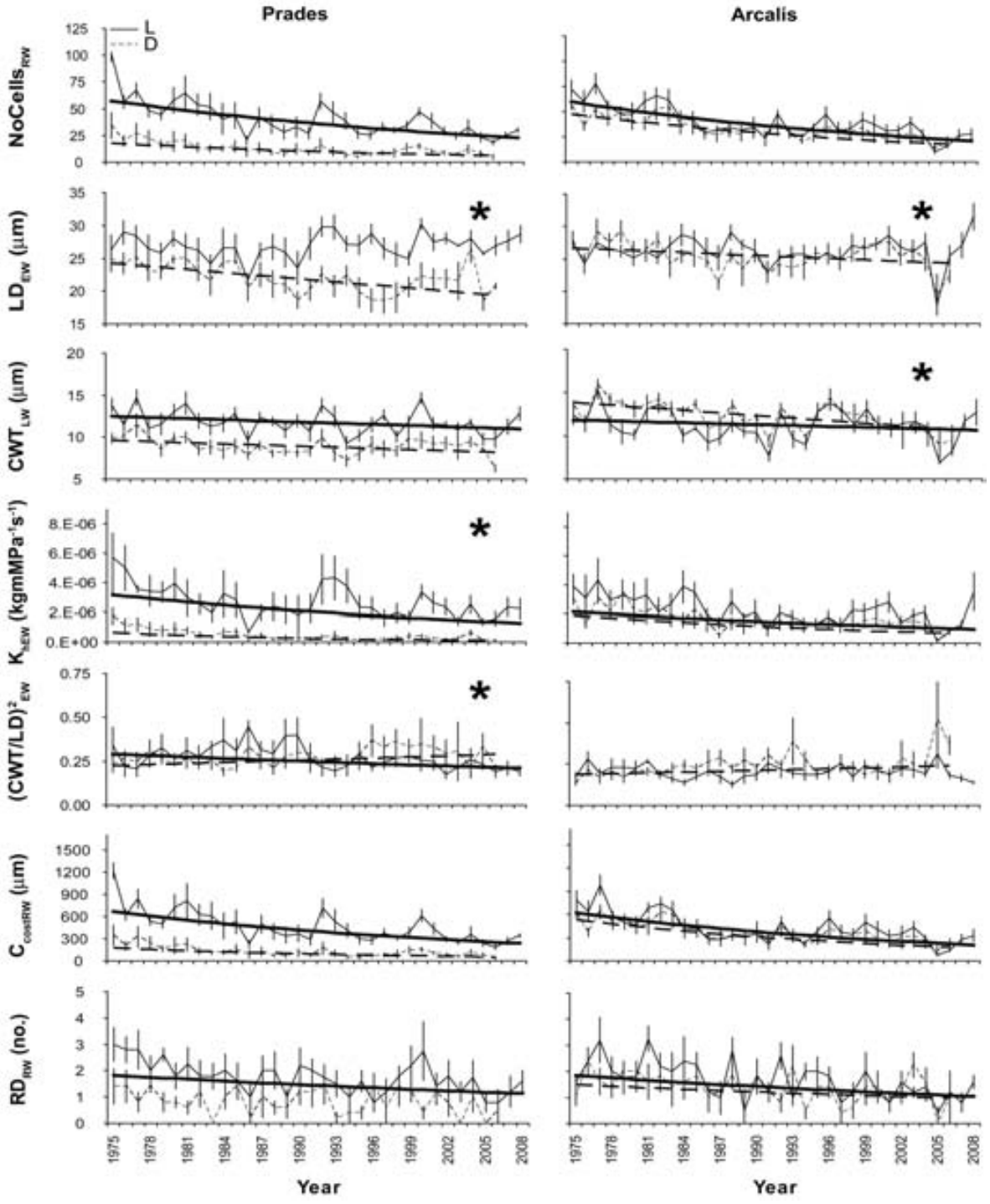

Resin duct production (RD_{RW}) was positively associated with the tree-ring width (Supplementary Table 4.2). The slope of this relationship was similar for L and D trees in Arcalís, whereas in Prades it was significantly steeper in D trees (Figure 4.2).

Figure 4.2 - Relationship between the number of resin ducts (RD_{RW}) and ring width for living (L) and dead (D) trees at the Prades and Arcalís sites. Regression lines represent slopes estimates from the corresponding Poisson generalized mixed models and they are represented only if significant. Asterisks (*) indicate significant differences between slopes of L and D trees.

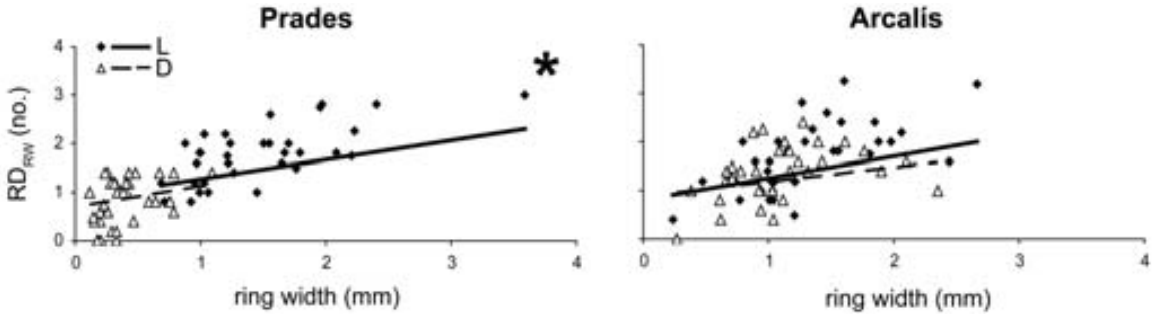

Environmental influences on anatomical features

Both C_a and P/PET significantly influenced most of the wood anatomical features. C_a had a predominantly negative effect, and P/PET presented a predominantly positive one (Table 4.3). The significant effects of C_a did not depend on Condition, Site or the Condition by Site interaction for most anatomical features (e.g. $NoCells_{RW}$, C_{costRW}, RD_{RW}) (Table 4.3). In the case CWT_{LW}, the significant influence of C_a depended on the Condition and on the Condition by Site interaction (Table 4.3). For this anatomical feature, the two sites differed significantly between them ($P<0.05$), with Prades presenting a significant positive difference between L and D trees ($P<0.01$), while in Arcalís this difference between the two groups of trees was not significant ($P=0.283$). The effect of C_a on K_{hEW} depended on Site, but not on tree Condition (Table 4.3).

Table 4.3 - Results of linear mixed-effects models (estimate ± SE) in which anatomical variables varied as a function of Condition (living, L; dead, D), Site (Prades, Arcalís), C_a (CO_2 atmospheric concentration) and P/PET (ratio between precipitation (P) and evapotranspiration (PET)). Significant relationships at 0.1, 0.05, 0.01 and 0.001 probability levels are marked with $^{+}$, *, ** and ***, respectively

Variables	$logNoCells_{RW}$	LD_{EW}	CWT_{LW}	$logK_{hEW}$	$log(CWT/LD)^2_{EW}$	$logC_{costRW}$	RD_{RW}
Intercept	1.388±0.10***	20.977±1.58***	12.662±0.81***	-6.111±0.21***	-0.556±0.08***	2.338±0.12***	0.249±0.39
L	-0.062±0.15	-0.056±2.22	-3.315±1.14**	-0.043±0.29	0.007±0.11	-0.128±0.17	-0.291±0.53
Prades	-0.405±0.14**	1.607±2.16	-3.985±1.13**	-0.382±0.28	0.004±0.11	-0.379±0.17*	-0.836±0.59
L*Prades	0.654±0.20**	1.222±3.02	5.291±1.58**	0.792±0.40*	0.125±0.15	0.756±0.24**	1.272±0.75
C_a	-0.008±0.00***	-0.012±0.03	-0.059±0.01***	-0.007±0.00*	0.001±0.00	-0.008±0.00***	-0.011±0.00*
L*C_a	0.001±0.00	0.055±0.03	0.051±0.02**	0.004±0.00	-0.002±0.00	0.002±0.00	0.001±0.01
Prades*C_a	-0.002±0.00	-0.092±0.04*	0.030±0.02	-0.011±0.00*	0.001±0.00	-0.003±0.00	0.001±0.01
L*Prades*C_a	0.001±0.003	0.072±0.05	-0.052±0.03*	0.007±0.01	-0.003±0.00	0.000±0.00	-0.004±0.01
P/PET	0.436±0.10***	7.154±1.42***	2.071±0.96*	0.488±0.21*	-0.222±0.08**	0.578±0.12***	0.458±0.54
L*P/PET	0.241±0.14^{+}	-0.455±1.99	2.444±1.35^{+}	0.114±0.29	-0.000±0.11	0.296±0.17^{+}	0.885±0.71
Prades*P/PET	0.057±0.15	-4.586±2.07*	0.122±1.59	-0.039±0.30	0.069±0.12	-0.057±0.18	0.707±0.94
L*Prades*P/PET	-0.372±0.21^{+}	1.871±2.88	-0.009±2.18	-0.169±0.42	-0.032±0.16	-0.358±0.25	-1.157±1.16

The effect of P/PET on $NoCells_{RW}$ was significantly influenced by Condition and the Condition by Site interaction. Thus, the two sites differed significantly between them (P<0.05), with Prades presenting a significant positive difference between L and D Scots pines (P<0.01) that was not observed in Arcalís (P=0.288) (Table 4.3, Figure 4.3). The significant effect of P/PET on LD_{EW} depended on Site, while its effect on CWT_{LW} and C_{costRW} depended on Condition, with significant positive differences between L and D trees in both cases (CWT_{LW}, P<0.1; C_{costRW}, P<0.001) (Table 4.3, Figure 4.3). Finally, the effect of P/PET on K_{hEW} and $(CWT/LD)^2_{EW}$ did not depend on Condition, Site or the Condition by Site interaction (Table 4.3).

Figure 4.3 - Relationships between wood anatomical features and the ratio between precipitation and evapotranspiration (P/PET) as a function of tree Condition (living, L; dead, D) and study Site (Prades, Arcalís). Asterisks (*) indicate significant differences between slopes of L and D trees. P/PET intervals differ within the same site as different P/PET intervals were used depending if the anatomical features represented RW, EW or LW (see Materials and methods). See **Table 4.1** for the meaning of variables' abbreviations.

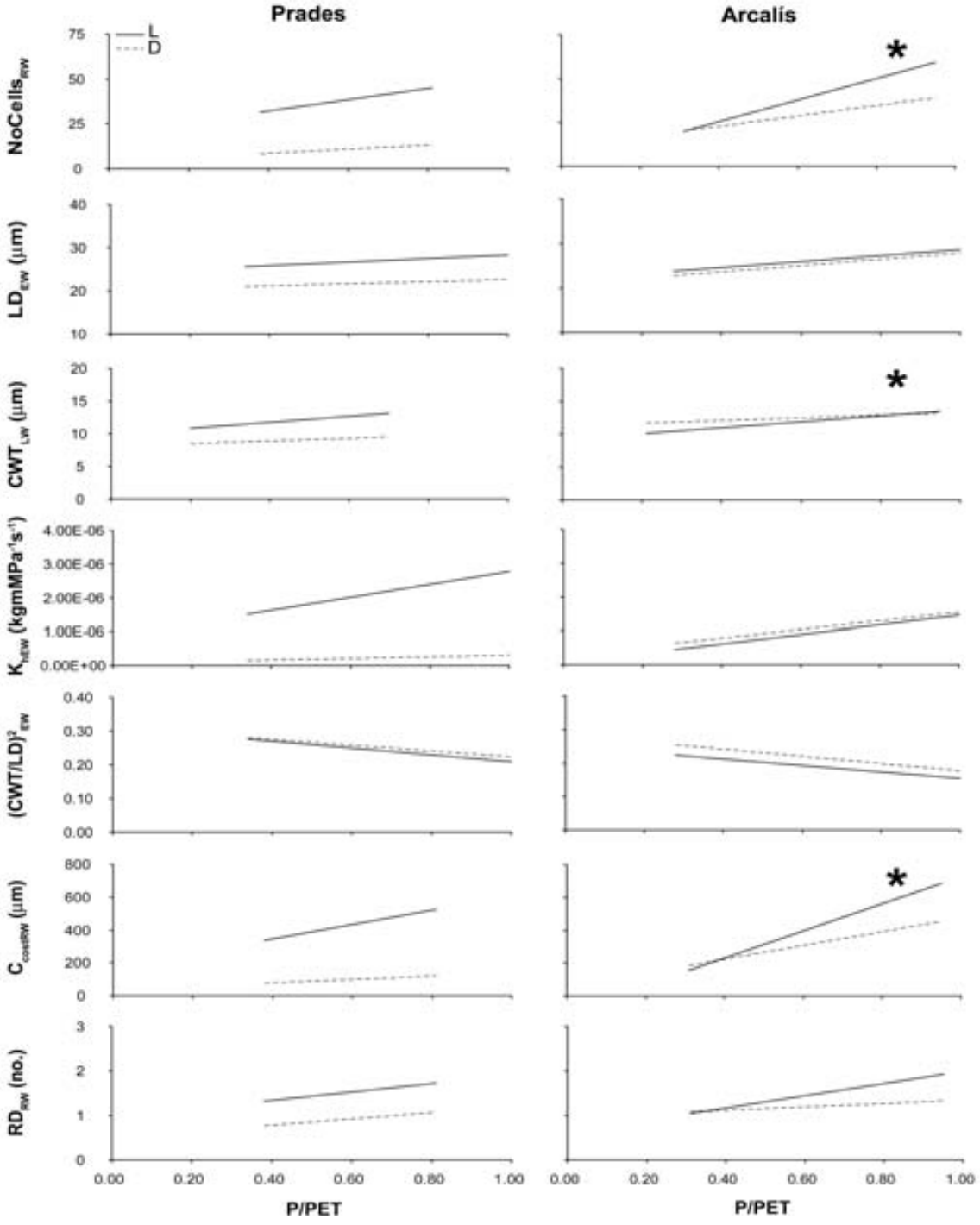

The overall response of the wood anatomical features to the SPEI drought index was positive, except in the case of $(CWT/LD)^2_{EW}$ (Supplementary Table 4.3, Supplementary Figures 4.2*a*, *b*). In general, the strongest relationships between wood anatomical features and SPEI were observed in spring (May) and summer (June, July, and August) and, as expected, earlier responses were observed for EW than for LW features (Supplementary Figures 4.2*a*, *b*). At the same time, D trees tended to respond over longer time scales than L trees for most anatomical features (Supplementary Table 4.1, Supplementary Figures 4.2*a*, *b*). Concerning the mixed models of anatomical features including SPEI as an explanatory variable instead of P/PET, the results were qualitatively similar to those of the P/PET models (Supplementary Table 4.3).

BAI association with wood anatomical features

BAI was significantly and positively related to several wood anatomical features (Supplementary Table 4.4), and this association was particularly strong with $NoCells_{RW}$ (Figure 4.4). For all the relationships of BAI with the wood anatomical features ($NoCells_{RW}$, LD_{RW}, CWT_{RW}, K_{hRW} and C_{costRW}), the estimated marginal means were always lower for the D trees than for the L ones (data not shown). Statistically significant differences between the L and D trees were found for LD_{RW}, CWT_{RW} and K_{hRW} (P<0.1) (Supplementary Table 4.4, Figure 4.4).

Figure 4.4 - Relationships between basal area increment (BAI) and wood anatomical features ($NoCells_{RW}$, LD_{RW}, CWT_{RW}, K_{hRW} and C_{costRW}). Regression lines represent slope estimates from the corresponding linear mixed-effects models and they are represented only if significant. Asterisks (*) indicate significant differences between slopes of living (L) and dead (D) trees. See **Table 4.1** for the meaning of variables' abbreviations.

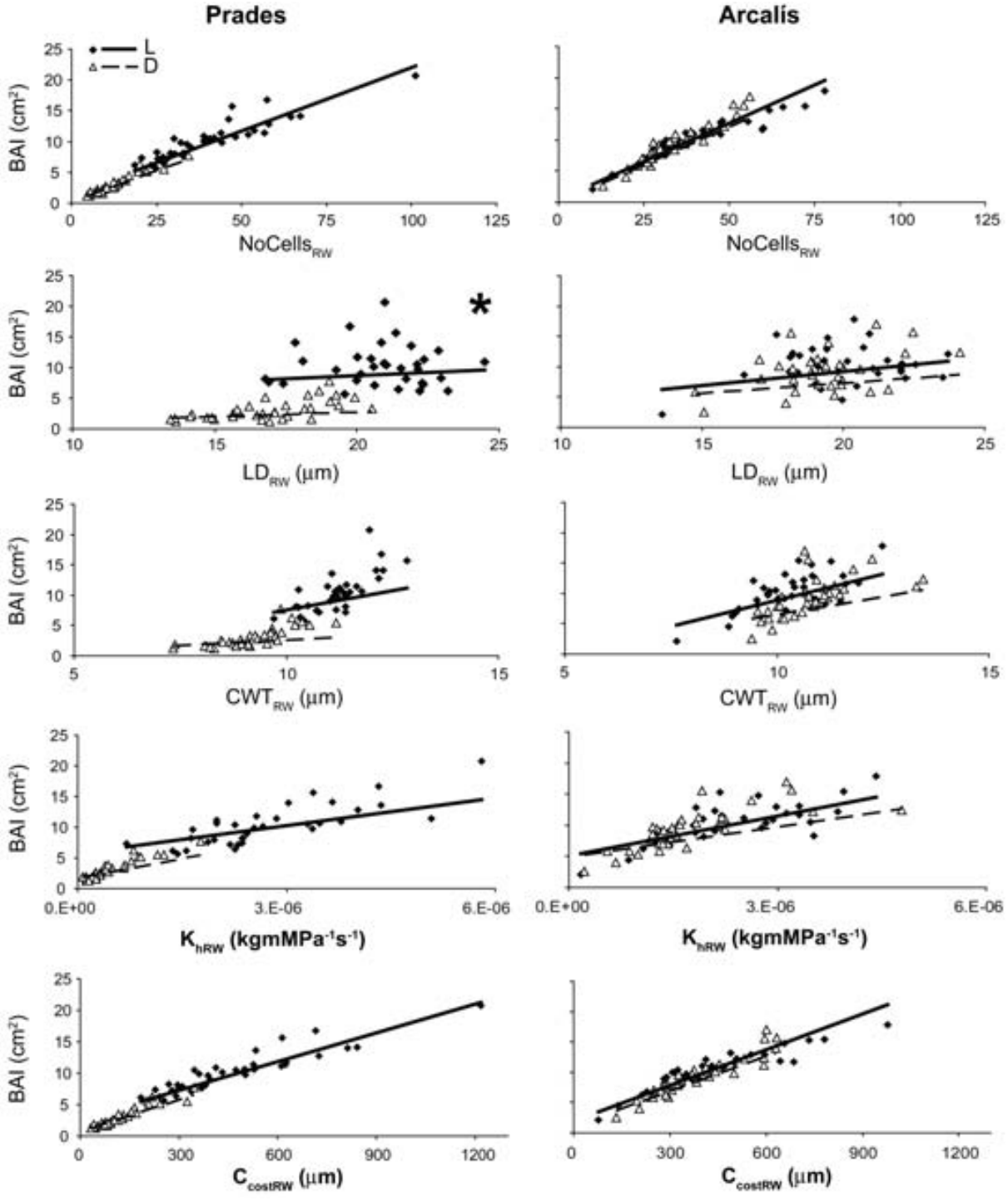

DISCUSSION

Surviving and now-dead Scots pine trees from Prades and Arcalís showed significant differences in their wood anatomical features' responses to drought (Supplementary Figure 4.1). Now-dead individuals usually presented smaller tracheids and lower tracheid production than living trees, indicating that lower hydraulic capacity and reduced investment of carbon into growth and defence characterized these mortality processes. Nevertheless, the two study sites seemed to have two different stories, since living and dead trees showed a long-term divergent hydraulic performance in Prades, whereas this divergence was less accentuated and more recent in Arcalís.

High growth variability has been associated to increased mortality risks (e.g., Ogle *et al.* 2000). Our results show that lower and more variable growth in now-dead compared to surviving individuals at the studied sites (Hereş *et al.* 2012) is associated to a higher variability in wood anatomical traits in now dead trees. This is consistent with Levanič *et al.* (2011), who also found a greater variability for the anatomical features of dying pedunculate oak trees in comparison with surviving individuals of the same species. Nevertheless, and in contrast to our findings, dying pedunculate oak trees presented higher hydraulic diameter and hydraulic conductivity of vessels than the surviving ones until the last 5 years prior to mortality, at which point the two groups of trees converged into similar values.

The response of the now-dead and surviving Scots pines from Prades and Arcalís to SPEI also marked interesting differences between the two groups of trees. The fact that now-dead trees tended to respond to drought (as measured by the SPEI index) over longer time scales than surviving individuals is consistent with a general physiological slowdown previous to death. This suggests a carryover effect on growth and hydraulic performance which constrains the responses of trees prone to die. The mechanisms underlying this pattern are not clear, but it is likely that the long-distance transport systems of the plant are involved (Anderegg *et al.* 2012) and could implicate drought 'legacy' effects on the plant hydraulic system as recently reported for sudden aspen decline (Anderegg *et al.* 2013*b*).

In agreement with the previous considerations, our results show lower hydraulic conductance in the stem xylem of now-dead trees, reflecting a lower water transport capacity over the whole period studied, particularly at the most xeric Prades site. This lower hydraulic capacity at the growth ring level does not necessarily translate into lower capacity to supply leaves with water, as concurrent changes in sapwood and leaf area need to be taken into account. However, the reduction in K_{hEW} in Prades was even greater than the average defoliation levels currently observed in trees that are suffering drought-induced mortality at this site (Poyatos *et al.* 2013). This appears not to be compensated by an increase in functional sapwood (R Poyatos, unpublished), and implies a reduction in the capacity to support canopy water demands.

We did not observe any difference between now-dead and surviving pines in terms of vulnerability to xylem embolism in the stem (estimated from the ratio between cell-wall thickness and radial lumen diameter, Hacke *et al.* 2001). This was due to the fact than in Prades tracheid lumens and cell-wall thickness co-varied, and both variables presented lower values in now-dead individuals than in living trees (Figure 4.1). This result is consistent with previous reports showing limited plasticity of the vulnerability to embolism in Scots pine (Martínez-Vilalta and Piñol 2002; Martínez-Vilalta *et al.* 2009) and with our own measurements at the Prades site showing no difference in vulnerability to xylem embolism (in stems) between healthy and heavily defoliated pines (Poyatos *et al.* 2013; M Gómez, unpublished data).

Reduced hydraulic conductance is linked to the formation of narrow rings in now-dead trees. But, at the same time, declining growth is also considered to be an indicator of low carbon availability. Under drought, whole-tree carbon assimilation tends to be impaired due to defoliation and stomatal closure (McDowell *et al.* 2008; Galiano *et al.* 2011). In addition, trees subjected to drought may allocate assimilates preferentially to other organs (e.g. buds, needles, roots) than to wood formation (Waring 1987; Eilmann *et al.* 2009). In our case, the low carbon investment (C_{cost} and RD_{RW}) was especially evident for the now-dead individuals from Prades. The lower production of resin ducts in now-dead trees is consistent with previous results (Kane and Kolb 2010; Gaylord *et al.* 2013), although in our case insect attacks do not seem to be

involved in the mortality process (authors' personal observation). Depleted carbohydrate reserves have been reported in dying trees at both study sites (Galiano *et al.* 2011; Poyatos *et al.* 2013), suggesting that lower growth and resin duct production in dying trees might be associated to nearly exhausted (or unavailable) carbon reserves (Galiano *et al.* 2011; Sala *et al.* 2012; Poyatos *et al.* 2013).

Overall, the growth reductions previously observed for the now-dead trees (Hereş *et al.* 2012) were more related to lower tracheid production than to a reduction in tracheid size (see also Camarero *et al.* 1998; Martin Benito *et al.* 2013), minimizing the impact of reduced growth on hydraulic conductivity without increasing the carbon investment. However, the positive relationship between BAI and lumen diameter found for both now-dead and surviving individuals indicates that Scots pines from Prades and Arcalís reduce radial growth also at the expense of reductions in conduit size and proportionally higher decreases in K_{hRW}. It is also worth noting that the relationship between BAI and cell-wall thickness was tighter than the relationship between BAI and lumen size. This result suggests that overall carbon availability may be constraining the thickness of tracheid cell walls in the studied trees.

To conclude, differences in wood-anatomical features between surviving and now-dead individuals are much more apparent at one of the sites (Prades) than the other (Arcalís). This pattern is consistent with the different forest decline dynamics observed at the two sites. At Prades, there is a long-term decline process, with declining trees starting to grow less on average 40 years before the time of death, and mortality episodes have been observed periodically since the early 1990s (Martínez-Vilalta and Piñol 2002; Hereş *et al.* 2012). At Arcalís, instead, tree mortality peaked more recently and growth declines started around 15 years before the time of death (Galiano *et al.* 2010; Hereş *et al.* 2012). Carbohydrate depletion in Prades appears to be connected with long-term lowered hydraulic capacity at the tree level (Poyatos *et al.* 2013, this study), whereas the pattern is not so clear in Arcalís, and the mechanism by which some trees become defoliated, deplete their carbohydrates and later die at this site (Galiano *et al.* 2011) remains to be explored.

ACKNOWLEDGEMENTS The authors would like to thank HA Chaparro Mendivelso, AQ Alla, E Pasho and MC Sancho Molina for laboratory assistance. We are indebted to M Mencuccini for field work and valuable discussion on the research topic. The authors are also thankful to M Ninyerola and the Catalan Meteorological Service (SMC) for providing the two climatic datasets used in this study. This research was funded by the Spanish Ministry of Science and Innovation (projects "CGL2007-60120", "CSD2008-0040", "CGL2010-16373"), a FPU PhD scholarship and a short study stay at the Instituto Pirenaico de Ecología (CSIC, Zaragoza, Spain).

Supplementary Table 4.1 - SPEI (standardized precipitation evapotranspiration index) time scale (in number of months) and month showing the highest correlations between SPEI and the studied wood anatomical features. See **Table 4.1** for the meaning of variables' abbreviations

Variable		Prades		Arcalís	
		L	D	L	D
$NoCells_{RW}$	SPEI time scale	3	5	7	7
	Month	August	July	August	August
LD_{EW} (μm)	SPEI time scale	2	6	3	7
	Month	May	July	June	June
CWT_{LW} (μm)	SPEI time scale	3	6	5	5
	Month	July	August	August	August
K_{hEW} ($kgmMPa^{-1}s^{-1}$)	SPEI time scale	5	5	4	2
	Month	July	July	June	June
$(CWT/LD)^2_{EW}$	SPEI time scale	5	10	2	7
	Month	March	June	May	June
C_{costRW} (μm)	SPEI time scale	2	5	4	7
	Month	July	July	August	August
RD_{RW} ($no\ year^{-1}$)	SPEI time scale	5	8	2	6
	Month	July	July	June	July

Supplementary Table 4.2 - Results of Poisson generalized mixed models (estimate ± SE) with RD_{RW} as a function of Condition (living, L; dead, D), Site (Prades, Arcalís) and ring width. Significant relationships at 0.1, 0.05, 0.01 and 0.001 probability levels are marked with $^{+}$, *, ** and ***, respectively

Variables	RD_{RW}
Intercept	-0.123±0.13
L	0.005±0.18
Prades	-0.353±0.18^{+}
L*Prades	0.489±0.25^{+}
ring width	0.345±0.07***
L*ring width	0.096±0.09
Prades*ring width	0.294±0.15^{+}
L*Prades*ring width	-0.386±0.17*

Supplementary Table 4.3 - Results of linear mixed-effects models (estimate ± SE) with anatomical variables varying as a function of Condition (living, L; dead, D), Site (Prades, Arcalís), C_a (CO_2 atmospheric concentration) and SPEI (standardized precipitation evapotranspiration index). Significant relationships at 0.1, 0.05, 0.01 and 0.001 probability levels are marked with $^{+}$, *, ** and ***, respectively

Variables	$logNoCells_{RW}$	LD_{EW}	CWT_{LW}	$logK_{hEW}$	$log(CWT/LD)^2_{EW}$	$logC_{costRW}$	RD_{RW}
Intercept	1.652±0.08***	26.280±1.11***	13.429±0.61***	-5.745±0.13***	-0.722±0.05***	2.691±0.09***	0.521±0.15***
L	0.100±0.11	-0.516±1.56	-2.058±0.85*	0.035±0.18	0.005±0.07	0.078±0.13	0.283±0.20
Prades	-0.455±0.11***	-2.631±1.57	-4.243±0.86***	-0.556±0.19**	0.076±0.07	-0.509±0.13**	-0.604±0.23*
L*Prades	0.422±0.16*	2.874±2.21	4.812±1.21***	0.737±0.26**	0.103±0.09	0.520±0.19*	0.597±0.30^{+}
C_a	-0.008±0.00***	-0.027±0.02	-0.045±0.01**	-0.009±0.00**	0.002±0.00	-0.009±0.00***	-0.011±0.00*
L*C_a	0.000±0.00	0.054±0.03*	0.046±0.02**	0.004±0.00	-0.002±0.00	0.000±0.00	-0.002±0.01
Prades*C_a	0.000±0.00	-0.043±0.04	0.038±0.02^{+}	-0.004±0.00	-0.000±0.00	0.000±0.00	0.008±0.01
L*Prades*C_a	0.002±0.00	0.048±0.05	-0.036±0.03	0.003±0.01	-0.002±0.00	0.002±0.00	-0.005±0.01
SPEI	0.047±0.01***	0.874±0.22***	0.799±0.16***	0.041±0.04	-0.023±0.01*	0.060±0.02***	0.095±0.08
L*SPEI	0.006±0.02	0.201±0.31	0.251±0.22	0.047±0.05	-0.002±0.02	-0.000±0.02	0.072±0.10
Prades*SPEI	0.034±0.02^{+}	0.148±0.37	-0.140±0.25	0.132±0.06*	-0.015±0.02	0.034±0.02	0.124±0.12
L*Prades*SPEI	-0.014±0.03	-0.457±0.49	0.290±0.34	-0.147±0.08^{+}	0.043±0.03	0.012±0.03	-0.165±0.15

Supplementary Table 4.4 - Results of linear mixed-effects models (estimate ± SE) with BAI as a function of Condition (living, L; dead, D), Site (Prades, Arcalís) and wood anatomical features ($NoCells_{RW}$, LD_{RW}, CWT_{RW}, K_{hRW} and C_{costRW}). Each model uses a different wood anatomical feature, as indicated in the corresponding column heather. Significant relationships at 0.1, 0.05, 0.01 and 0.001 probability levels are marked with $^{+}$, *, ** and ***, respectively

Variables	logBAI by $logNoCells_{RW}$	logBAI by LD_{RW}	logBAI by CWT_{RW}	logBAI by $logK_{hRW}$	logBAI by $logC_{costRW}$
Intercept	-0.651±0.09***	0.439±0.13**	0.172±0.15	3.102±0.23***	-1.339±0.12***
L	0.125±0.12	0.082±0.18	-0.051±0.20	0.416±0.30	0.234±0.15
Prades	0.034±0.11	-0.603±0.18**	-0.420±0.20*	-0.104±0.30	0.093±0.14
L*Prades	0.096±0.15	0.820±0.25**	0.573±0.28*	-0.086±0.42	0.017±0.20
Wood anatomical feature	1.019±0.05***	0.021±0.00***	0.064±0.01***	0.383±0.04***	0.877±0.04***
L* Wood anatomical feature	-0.059±0.06	0.001±0.01	0.018±0.01	0.062±0.05	-0.069±0.05
Prades* Wood anatomical feature	-0.070±0.06	0.009±0.01	0.001±0.02	0.020±0.05	-0.072±0.05
L*Prades* Wood anatomical feature	-0.026±0.08	-0.021±0.01*	-0.022±0.02	-0.047±0.07	0.011±0.07

Supplementary Figure 4.1 - Temporal trends (period 1975-2008) of annual climatic variables: mean temperature (*T*, ºC), total precipitation (*P*, mm) and the ratio between precipitation P and evapotranspiration PET (P/PET) in Prades and Arcalís. Regression lines are represented only if significant.

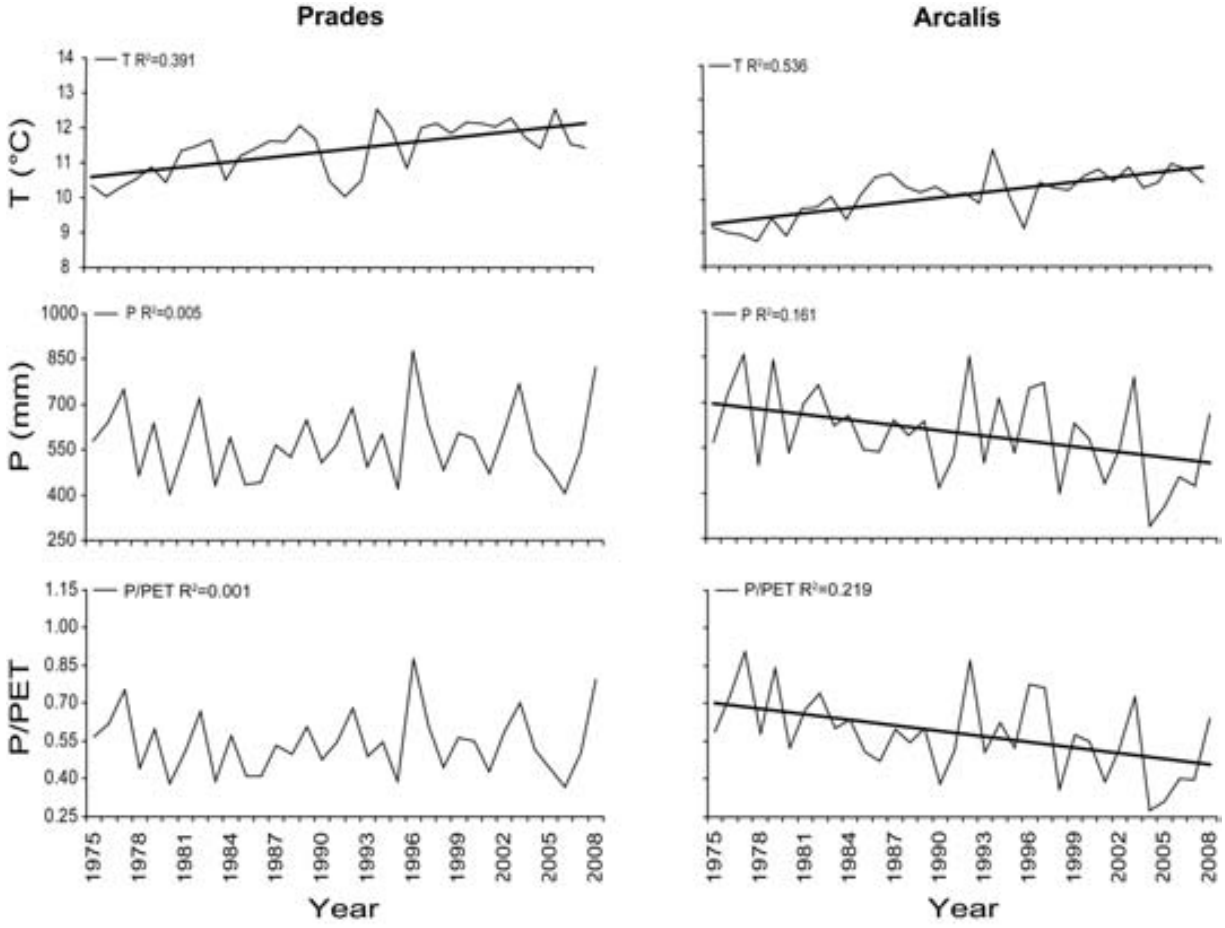

Supplementary Figure 4.2*a* - Correlations obtained between wood anatomical features and SPEI (standardized precipitation evapotranspiration index) for different months and time scales considering living (L) and dead (D) trees from Prades site. See **Table 4.1** for the meaning of variables' abbreviations.

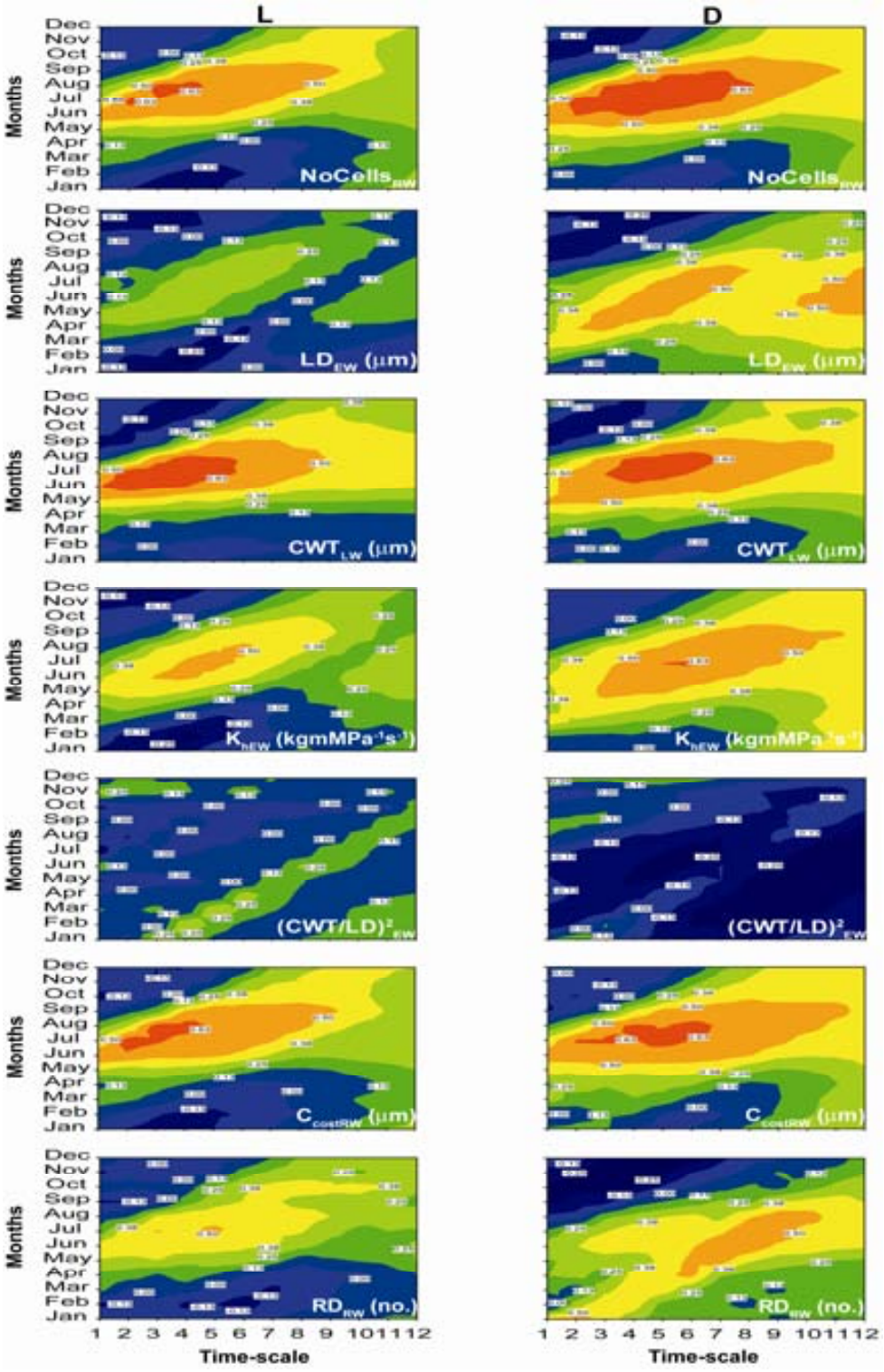

Supplementary Figure 4.2*b* - Correlations obtained between wood anatomical features and SPEI (standardized precipitation evapotranspiration index) for different months and time scales considering living (L) and dead (D) trees from Arcalís site. See **Table 4.1** for the meaning of variables' abbreviations.

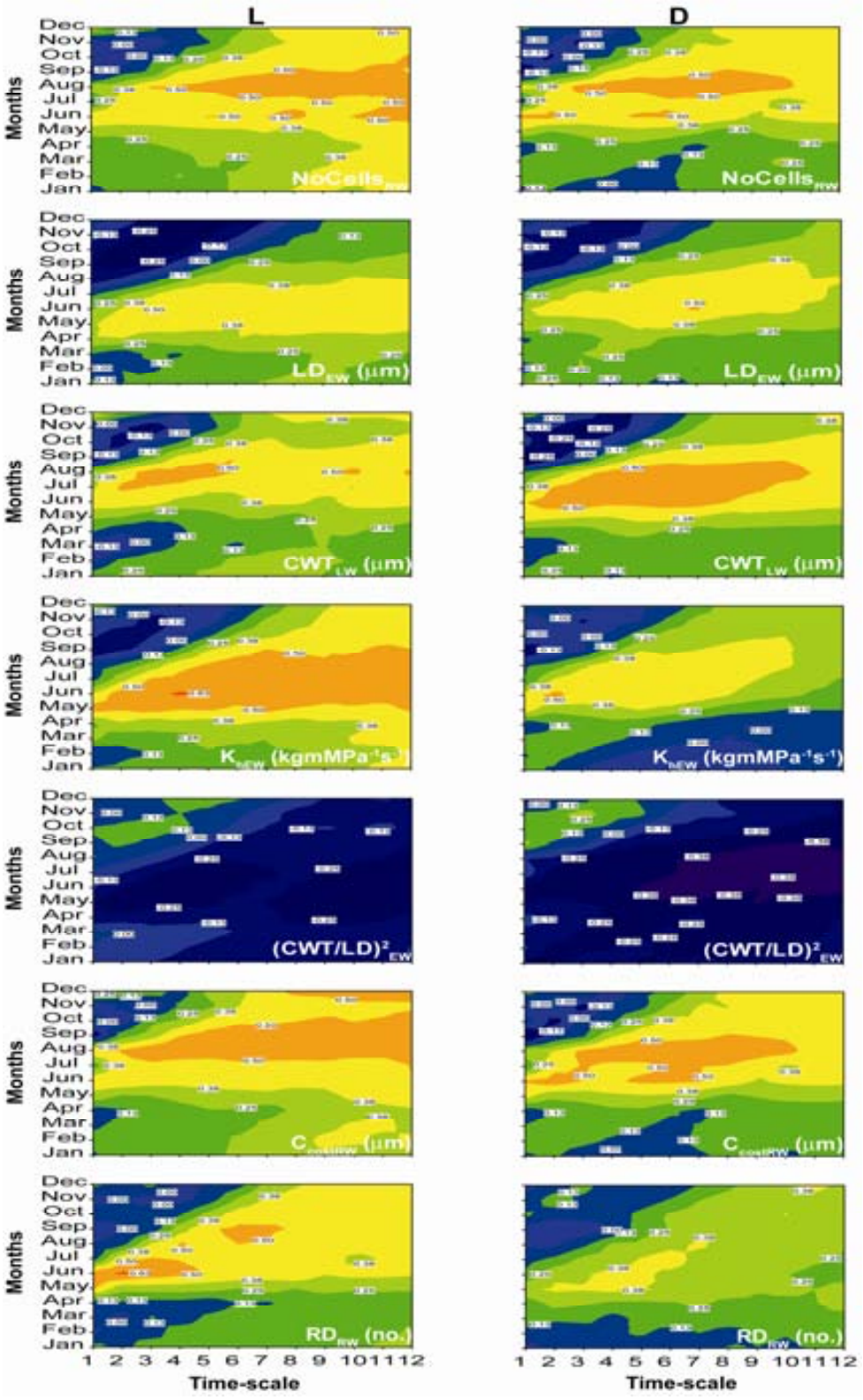

CHAPTER 5

MEASUREMENTS OF WOOD ANATOMICAL FEATURES IN CONIFER SPECIES

IMAGE ANALYSES WITH DACIA

TECHNICAL REPORT

This chapter is *in prep.*

Hereş AM, Gil D, Camarero JJ, Claramunt López B, Martínez-Vilalta J

1. WHAT IS DACiA?

DACiA (Dendrochronological Analysis on Conifer Wood Anatomy**)** is a free, Matlab based, image processing and analysis software to measure wood anatomical features of conifer species. **DACiA**, available from the authors upon request, runs as a standing alone application. The software is currently available for Windows XP and 7 versions, with the possibility to develop versions for other operating systems. The wood anatomical features that **DACiA** measures are: number of tracheids, cross-sectional lumen diameter (LD), cell wall thickness (CWT), total tracheid diameter (TD) and total lumen area (LA). The values are returned directly in their units of measurement, so no further transformations are necessary. **DACiA** gives the possibility of measuring wood anatomical features at the whole ring level (RW) or separately for the earlywood (EW) and latewood (LW) segments.

2. A BRIEF REVIEW OF WOOD ANATOMY MEASUREMENTS

Wood anatomy analyses are a powerful tool for investigating tree responses to past environmental events having the advantage of a higher temporal resolution than tree rings (Fritts 2001; Vaganov 2006). The idea of using wood anatomy analyses with this purpose goes back to the years 1960s and 1970s (Knigge and Schulz 1961; Eckstein *et al.* 1974), when this type of measurements were done visually on wood sections mounted on microscope slides. It has been only during the last two decades that the use and reliability of wood anatomy analyses has increased thanks to the technological improvements in the field of the digital image analyses (Fonti *et al.* 2010). Nowadays, cells can be measured directly from the wood surface (if big enough), or through image captures of fine cut wood sections (Fonti *et al.* 2010 and references therein). Continuous development and progress of laboratory equipment for cutting wood sections (microtones), capturing high resolution images (scanners, digital cameras) and sophisticated software to analyze wood sections has resulted in faster and higher quality measurements. As a result, it is currently possible to measure very detailed wood anatomical structures and achieve unprecedented sample sizes (Fonti *et al.* 2010 and references therein).

3. AVAILABLE SOFTWARE FOR WOOD ANATOMY ANALYSIS

Several software packages have been used to conduct wood anatomy analyses, including WinCELL, ROXAS and ImageJ, which are briefly described in the following paragraphs.

WinCELL (Régent Instruments Inc Quebec Canada 2013) is a commercially available image analysis system specifically designed for wood cells analysis, which can quantify the changes in wood structure over annual rings. WinCELL measures wood cell morphology on thin wood slices cut with a microtome or, for larger cells like earlywood vessels of deciduous species, directly on wood surfaces. Wood cells morphological data can be measured per annual ring in one or more images per ring with the aid of XLCell (Régent Instruments Inc Quebec Canada 2013), a companion program for data post-processing and visualization (see http://www.regentinstruments.com/assets/wincell_about.html for additional information). It is one of the most widely used software in dendroecology and example applications include the study of drought-induced adaptation as reflected in the xylem anatomy of Scots pine and pubescent oak (Eilmann *et al.* 2009) or the study of cellular phenology during annual ring formation of *Abies balsamea* (L.) Mill. (Deslauriers *et al.* 2003).

ROXAS (von Arx and Dietz 2005) is a tool for the quantitative analysis of xylem anatomy in cross-sections and cores of trees (angiosperms and conifers), shrubs and herbaceous plants. ROXAS allows building chronologies of vessel size in a fast and efficient manner and is able to handle a wide range of suboptimal images (http://www.wsl.ch/dienstleistungen/produkte/software/roxas/index_EN). ROXAS has been used to study annual root rings in perennial forbs (von Arx 2006), to build ring-porous earlywood vessel chronologies (Fonti *et al.* 2009) and to study the long-term functional plasticity in xylem hydraulic characteristics (von Arx *et al.* 2012). ROXAS was designed originally for analyzing angiosperm wood, but it has recently been upgraded to handle also conifer wood (von Arx and Carrer in review), although this new version is still not freely available. In addition, ROXAS itself is freely available in the web above, but it requires Image-Pro Plus (Media Cybernetics) v6.1-7, which is a commercially available, general purpose image analysis software.

ImageJ (Ferreira and Rasband 2010, 2012, http://rsbweb.nih.gov/ij/) is a public domain, Java-based image processing program developed at the National Institutes of Health (USA). It is nowadays probably among the most widely used image processing and analysis software to extract quantitative anatomical measurements of wood (e.g., DeSoto *et al.* 2011; Martín Benito *et al.* 2013; Gaylord *et al.* 2013). Nevertheless, this software has not been developed specifically for this purpose, and thus suffers from important limitations and shortcomings. It is in many ways the software most comparable to the one we have developed and, hence, we will describe it with more detail. Some of its features will be illustrated with the same Scots pine (*Pinus sylvestris* L.) samples used in the analyses conducted for this thesis and also the same ones used to illustrate the functioning of the newly developed **DACiA** software in the next sections.

Similar to other pieces of software, ImageJ allows quantifying changes in gray levels along a line (e.g., horizontal, segmented) that crosses a row of tracheids within a tree ring (Figure 5.1). Tracheids are identified along the marked line by thresholding the image gray profile extracted from the line considering the changes in gray levels of lumen and walls. Since the software does not allow marking several lines in parallel, rows of tracheids must be individually marked, processed and analyzed. This can be a time consuming process if there are many images to analyze.

Figure 5.1 – Example of ImageJ processing of a conifer tree ring: segmented line crossing a row of tracheids within a tree ring. The sample corresponds to Scots pine wood.

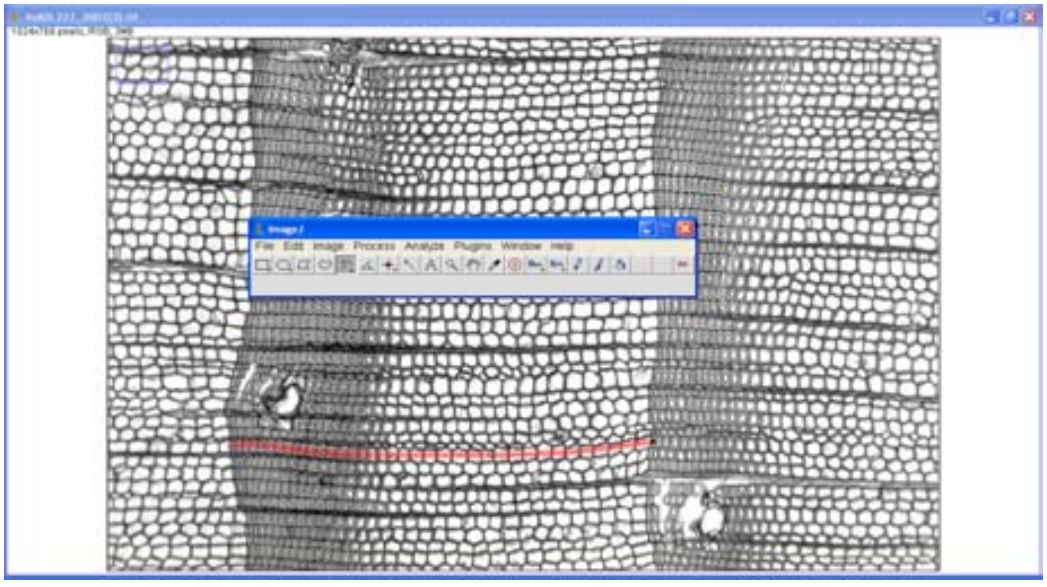

In ImageJ, the gray threshold value that discriminates between the tracheid lumen and walls is constant along the marked line, and must be visually established by the user based on the gray profile (Figure 5.2). As illustrated in Figure 5.2 (red line), a constant thresholding value for a given marked line and/or image can be problematic due to variations in section width or illumination conditions across the image, which can introduce variable gray colour patterns along the marked lines. In order to apply a common threshold for all cells, ImageJ requires the contrast and brightness along the line to be manually adjusted. This is a tedious task that may also introduce errors in final tracheid measurements. Further on, processing does not allow for corrections to be made on the identification and delimitation between individual tracheid lumens and their corresponding cell walls. Finally, ImageJ only exports the image intensity profile together with the positions of tracheids. These data have to be further processed to extract the final measures of tracheids' dimensions using other software, such as the R (The R Foundation for Statistical Computing) package "tgram" (DeSoto *et al.* 2011) or EXCEL.

Figure 5.2 – Image processing and thresholding with ImageJ. The straight red line indicates the constant along the line thresholding gray value that must be established by the user. The curved blue line marks approximately the shape and the variable grey scale values that should have been followed in order to correctly identify all tracheids in the row. The graph corresponds to the same line marked in Figure 5.1 on a Scots pine wood sample.

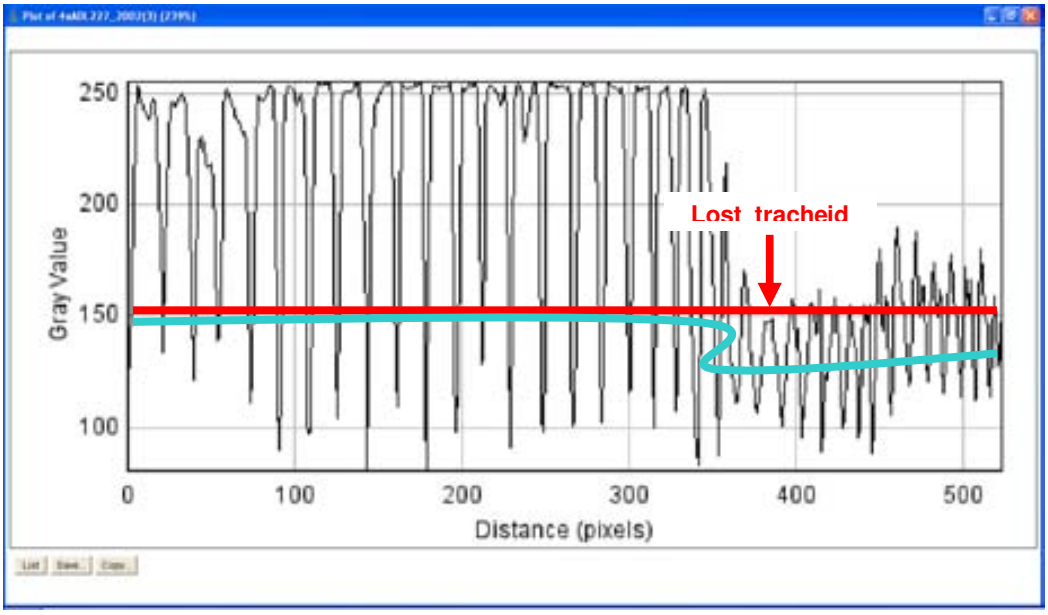

4. A NEW SOFTWARE FOR WOOD ANATOMY ANALYSIS: DACiA

The fact that none of the available software fulfilled the requirements for our wood anatomy analyses lead us to develop a new piece of software. **DACiA** software has been specifically created to measure wood anatomical features on conifer species. Thus, it solves or improves several of the above mentioned shortcomings. It is freely available and does not require any pre-installed image analysis software to run. Compared to ImageJ the main improvements are:

a. An automatic contrast adjustment of the processed image together with an automatic identification of the main ring structures: tracheids' lumens and walls. Any trend in gray value along the marked line is automatically corrected and centred at zero, so that this zero value becomes the threshold for all analyzed images regardless of the tree species or specimen characteristics. This adjustment is done automatically and corrects for the effects of different image acquisition conditions or section widths across the image.
b. The possibility to mark several polygonal lines (e.g., as many as the user needs) on the same ring, providing, at the same time, a high capacity of manipulation and correction of the marked lines by using intermediate points.
c. An interactive graphic interface that allows correcting pixel by pixel the processed tracheids marked along the tree ring. Thus, the user has complete control on the limits that define tracheids' lumens and walls.
d. Final wood anatomical measures are retrieved at different scales (pixel, tracheids, lines, and tree rings) and exported directly into their units of measurements based on the magnification of the processed images, so no further processing with other software is necessary.

4a. Automatic contrast adjustment and tracheid segmentation

The image intensity profile is approximately periodic, as tracheids repeat along the line. In an ideal situation, this tracheid repetition would produce a perfect wavy pattern with no trend along the line. However, variations in the wood structure, the quality of the samples and/or acquisition conditions may distort the pattern and introduce secondary non-stationary signals along the tree ring (Figure 5.3, left panel). Such

secondary signal introduces errors in a segmentation based on a constant threshold and should be corrected.

In order to remove the secondary non-stationary signals, **DACiA** applies Fourier analysis to decouple the image intensity profile into high and low frequency components. High frequencies are associated to the tracheid profile, while low ones correspond to variations in acquisition conditions and section quality. The low frequency range was adjusted over a representative set of images and rings and was set to ensure that the high frequency signal always contained the sinusoidal wavy profile associated to the tracheid-wall transitions. An example result of Fourier decoupling is shown in Figure 5.3 (right panel). After removal of the non-stationary signal, the profile of the tracheid-wall transitions is a stationary wave centered at zero (Figure 5.3, right panel). Therefore, tracheids are segmented by using a constant zero threshold.

Figure 5.3 - Adjustments along the tree ring: original (left panel) and corrected profiles (right panel). The sample corresponds to Scots pine wood.

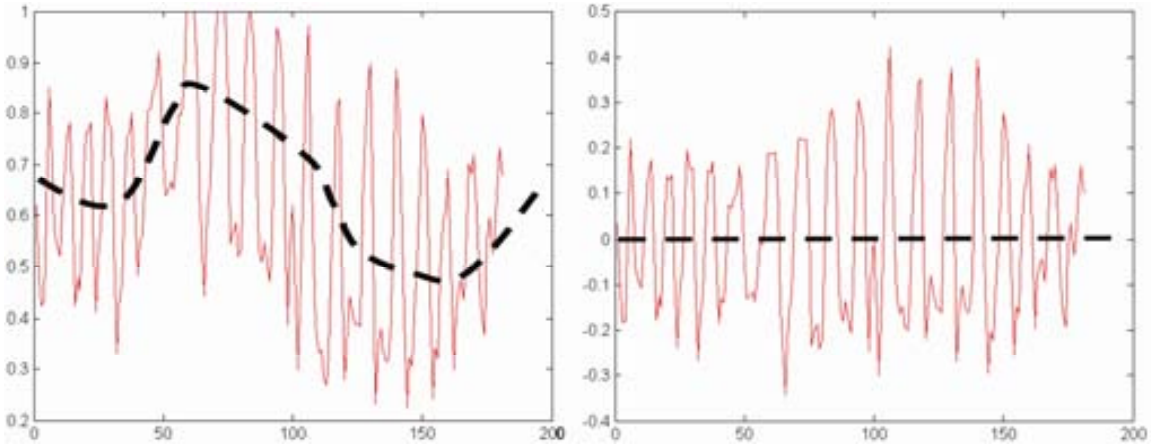

4b. Multiple tracing of several polygonal lines for each ring

The software allows tracing several polygonal lines for each ring for its joint processing. This allows the extraction of measurements on several rows of tracheids marked across the ring for further statistical analysis. Each polygonal line is defined by a finite number of points, (X_i,Y_i), i=1,...,N, that are interactively selected by the user. Points should be placed from EW to LW. Each segment of the polygonal line is given by the formula:

$$(X_i + t(X_{i+1} - X_i), Y_i + t(Y_{i+1} - Y_i)),$$

for t a sampling of the interval [0,1]. The image gray intensity is interpolated along these points and this constitutes the input for the contrast adjustment and tracheid segmentation. Details about the interactive tracing of multiple lines are given in **Section 5**.

4c. Interactive interface allowing fine corrections

The automatic contrast and threshold adjustment described above are improvements over ImageJ. Nevertheless, they do not provide a perfect identification of all the tracheids marked within the tree ring. In order to ensure that the limits between tracheid lumens and walls are perfectly delimited, **DACiA** allows a fine correction process. This is done manually through an interactive graphical interface that illustrates the lumen diameter of the automatically identified tracheids within a line (Figure 5.8, but see **Section 5** for a detailed explanation). Possible errors are easily visualized and marked directly by clicking on the graph. A sequence of very detailed (zoomed in) images of the marked tracheids are returned by the software, and the user is able to add or delete individual pixels, having perfect control on the limits between the tracheid lumens and walls (Figure 5.9*a, b*, but see **Section 5** for a detailed explanation).

4d. Exporting final wood anatomical measurements

The results are stored at three levels of aggregation: (1) individual pixels with their corresponding (corrected) grey level profile and the positions of tracheids (x and y coordinates); also, it is indicated if the grey level corresponds to a tracheid lumen (code numbers ≥1 that also indicate the number of the tracheid within each marked row of tracheids) or wall (code 0); (2) measurements on individual tracheids, including number of tracheids per line, lumen diameter (LD), half tracheid wall thickness (CWT-1, half of the wall shared with the previous tracheid; and CWT+1, half of the wall shared with the following tracheid) of the contact between the target tracheid and the neighbouring ones, total tracheid wall thickness (CWT) calculated from the half cell

wall thickness values, total tracheid diameter (TD) and its lumen area (LA); also a last column indicates for each tracheid if it belongs to the EW (0 code) or LW (1 code); and (3) measures aggregated at the tree-ring level (averages and standard deviations of LD, CWT, TD and LA); these values are given for the whole tree ring (-1 code) and separately for EW (0 code) and LW (1 code) if the user separates the tree ring into these two segments. All these values are directly exported in their units of measurement. Two export format files are available: Excel© and plain text.

5. HOW DOES DACiA WORK? A BRIEF USER MANUAL

DACiA is easy and intuitive. It has a simple Menu - File (Figure 5.4) through which images can be loaded. In order to avoid overcharging the computers' memory, temporary files can be periodically deleted, but only after the corresponding measurements have been exported and saved, otherwise the information is lost. The Menu also includes a Help button where information about the software and how to use it is provided in a step by step fashion. "Zoom in", "Zoom out" and "Pan" buttons that will be needed to manipulate and process the images are also available (Figure 5.4).

Figure 5.4 – Menu presentation.

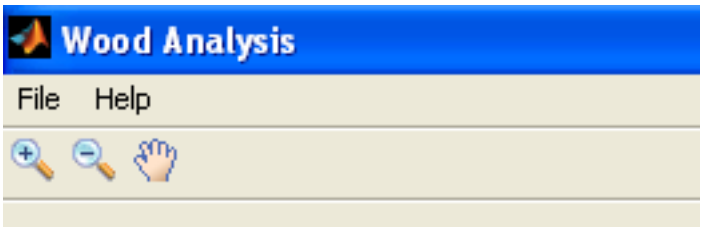

DACiA is able to read and work with images of different size and format (TIFF, JPG, GIF, BMP). Each image must be analyzed individually. Once the image is loaded, a window appears asking for basic information about the image: "Image Identifier, "Tree Identifier" and "Resolution (microns per pixel)" (Figure 5.5). This information will be used by the software to distinguish between measurements and to name and organize the output files.

Figure 5.5 – Image loading and identification. The sample corresponds to Scots pine wood.

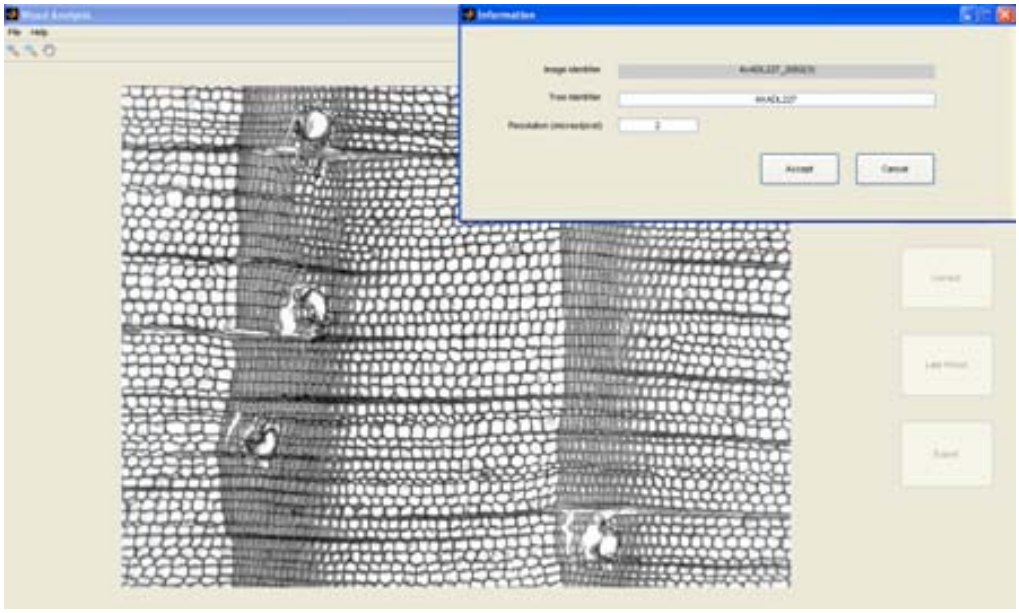

Analysis of the wood anatomical features at the tree ring level are further on conducted through a series of four buttons available on the right-hand side of the window ("New Ring", "Correct", "Late Wood", "Export") that become active as the process advances (Figure 5.6).

Figure 5.6 – Image showing an annual ring to be analyzed. The sample corresponds to Scots pine wood.

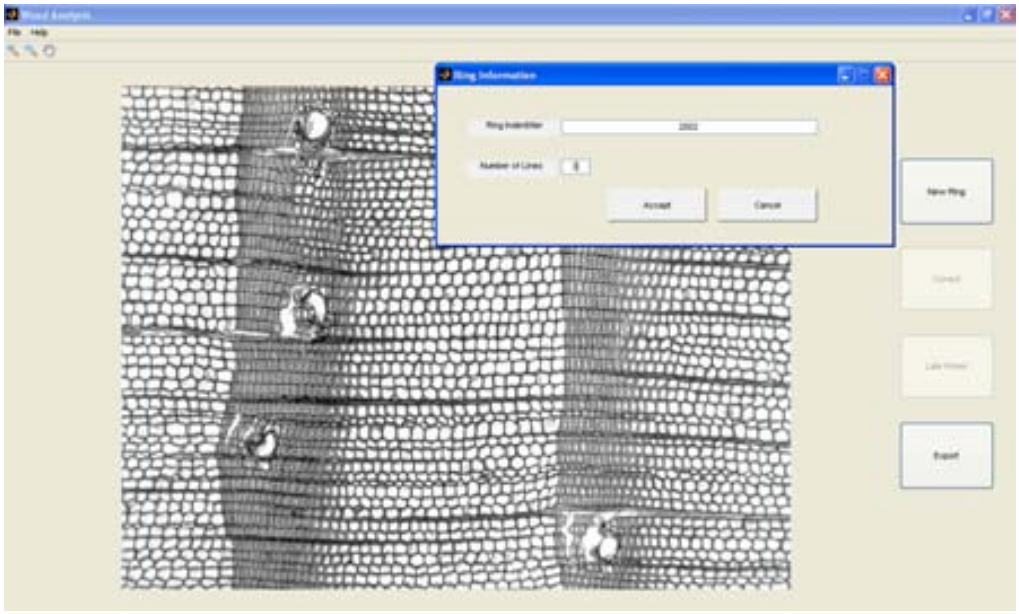

The images to be analyzed can contain one or several tree rings. To start the analysis of a ring, the user must click on the “New Ring” button, and the software will ask for the identification of that particular annual ring (for example, the corresponding calendar year) and the number of lines to be analysed per ring (Figure 5.6). Further on, the different lines can be marked using a segmented flexible (polygonal) line that will allow the user to pass exactly through the middle of the tracheids in a row and to follow the exact shape of the tracheids’ row along the tree ring. The user has a complete control guiding the line while marking the rows of tracheids and so no tracheid is missed if the row does not describe a perfect straight line. A double-click indicates the end of the line. At this point, the user can use the intermediate points (by simply clicking and dragging them) of the polygonal line to correct its track, if necessary. Another double-click on the end point of the marked line allows the user to continue and mark the next line. A short message will appear on the screen giving the number of the line that will be marked next. Rows of tracheids must always be marked from EW to LW (Figure 5.7). By marking the rows of tracheids, the software automatically identifies and establishes the limits between tracheid lumens and walls, and measures the anatomical features mentioned before (LD, CWT, TD and LA).

Figure 5.7 – An example with three rows of tracheids marked from earlywood (EW) to latewood (LW) using the segmented flexible line along a conifer tree ring. The sample corresponds to Scots pine wood.

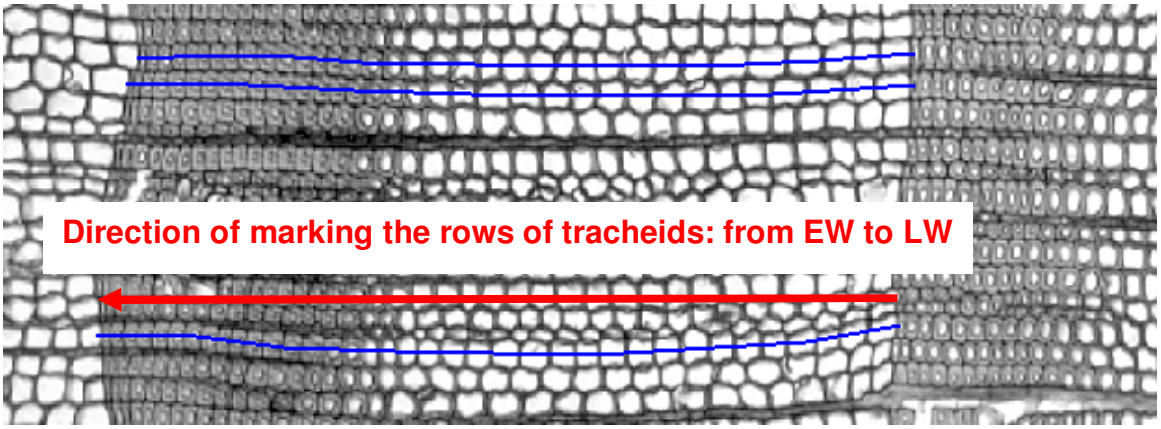

In order to ensure the accuracy of the tracheid identification and of the measurements, a pixel by pixel correction process, accessible through the “Correct” button, is further on available. The marked lines of tracheids will be opened one by

one, following the order on which they have been marked. Once opened, interactive graphs are produced for each line (Figure 5.8). These graphs illustrate the lumen diameters of the identified tracheids (vertical black lines ended with a pink circle), the user being now able to visualize if there are errors based on, for example, inconsistent lumen diameter changes among neighbouring cells (Figure 5.8). The identified tracheids with possible errors can be marked by simply clicking the corresponding pink circle, which will be marked with an "X" once all the tracheids to correct have been marked along the line. Instructions on how to mark the tracheids and finish the marking process of one particular line (by pressing the "Enter" button on the keyboard) appear also on the screen, in the upper part of the interactive graph (Figure 5.8).

Figure 5.8 – Interactive graph and selection of the tracheids with possible measurement errors. Instructions are given on the upper part of the interactive graph. The sample corresponds to Scots pine wood.

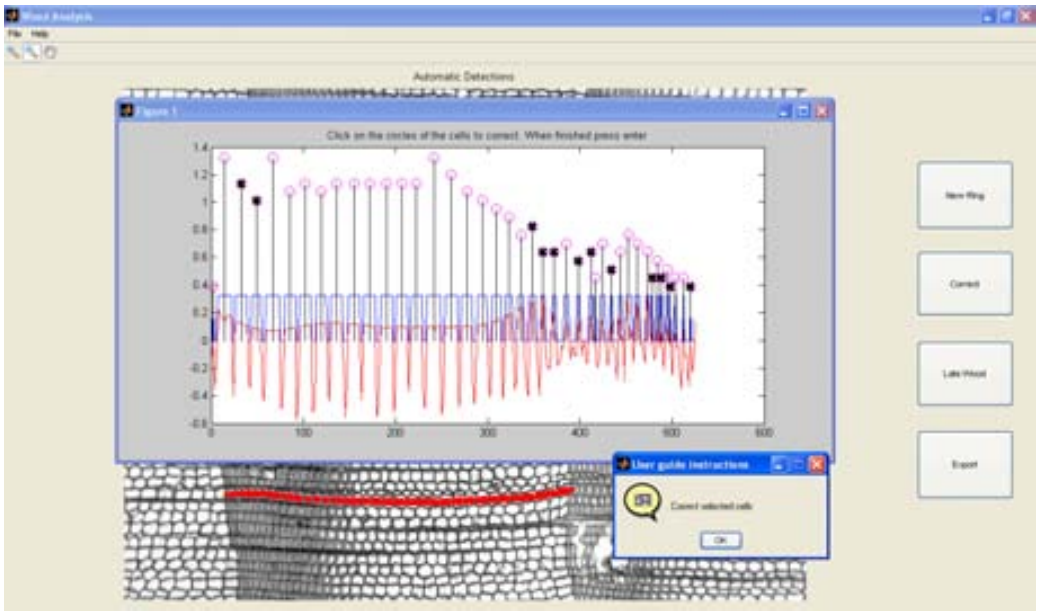

Further on, an additional window opens showing a zoom into the previously marked tracheids with possible errors, one by one. The user can now easily add or delete individual pixels, perfectly establishing the limits between tracheid lumens and walls (Figure 5.9*a*, *b*). Instructions on how to do this appear in the upper part of the window. The "a" and "d" letters from the keyboard will be used to add and delete pixels,

respectively, to a tracheid. In order to pass to the next marked tracheid the “Esc” button on the keyboard must be pressed. Once all the marked tracheids on a line have been corrected the same “Esc” button allows moving forward to the next line of tracheids marked on the tree ring.

Figure 5.9 – Zoom in of one of the selected tracheids containing a possible error of lumen identification (***a***) and correction of the error by adding the missing pixels (***b***). Note that the portions of the lines with red symbols indicate tracheid lumens, while the ones with blue symbols indicate tracheid walls. The sample corresponds to Scots pine wood.

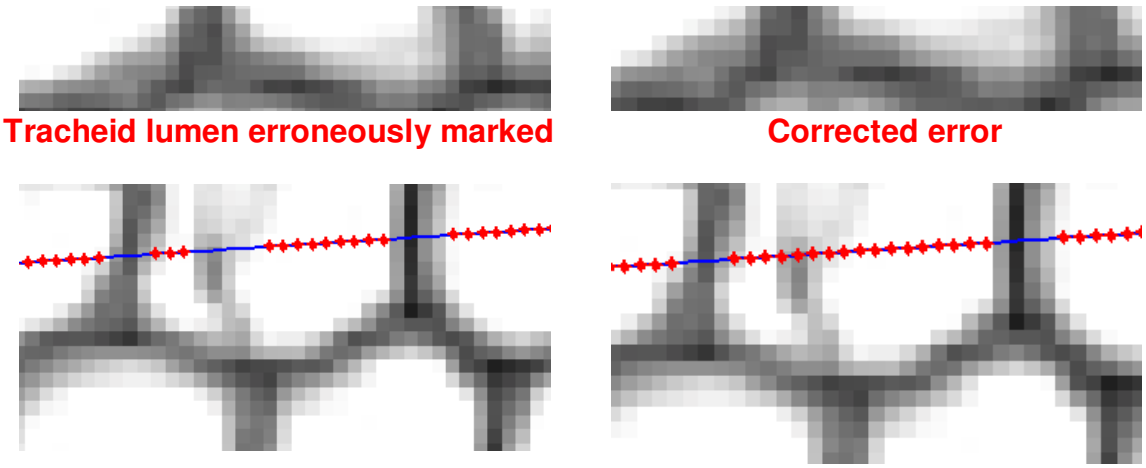

Once corrections for all marked lines of tracheids are finished, the user can separate the rows of tracheids into EW and LW by clicking on the “Late Wood” button. This step can be skipped if the user is not interested in having separate measurements for EW and LW. The LW marking must be done manually by the user, based on the abrupt shifts in colour and tracheid size (Figure 5.10). This visual identification of LW was preferred over the Mork index (Denne 1988), as this latter one, tested on an initial version of the **DACiA** software, proved to largely overestimate LW in our case (tests made for Scots pine wood). In order to separate the EW from the LW, the first LW tracheid must be carefully identified by the user and marked by clicking on it. Since the rows of tracheids have been marked from EW to LW, the first LW tracheid corresponds to the one next to the last EW tracheid on the row (see Figure 5.10). Once the first LW tracheid is marked, the software automatically marks (black lumen, Figure 5.10) the rest of the tracheids (until the end of the row of tracheids) as being

LW. The EW cells are further on left in red. The advantage of the visual identification of the limit between EW and LW is represented by the fact that it avoids errors caused by the appearance of the latewood-like tracheids (small size EW tracheids) in EW and vice versa, which might appear if LW identification is based on Mork index (i.e., cell lumen is smaller than twice the cell wall, Denne 1988).

Figure 5.10 – Latewood (black lumens) and earlywood (red lumens) separation of the tracheids in an annual tree ring. The sample corresponds to Scots pine wood.

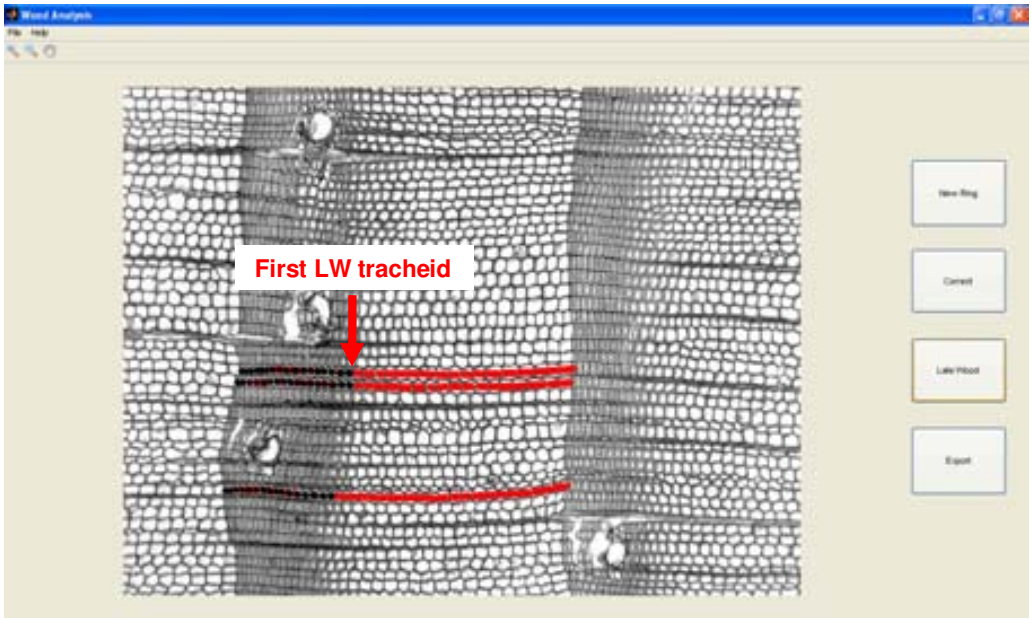

At the end of the process, the software exports and saves the measurements by clicking on the "Export" button. A total of three files (Excel© or plain text formats) are exported: "*RawData*", "*RawMeasures*" and "*FinalMeasures*". Measurements are given at the whole ring level (RW) and separately for EW and LW, if LW has been distinguished. A detailed description of the export files, including the names of the columns within the files, is given below.

"RawData" file:

1. Image name
2. Line number
3. x line coordinate
4. y line coordinate
5. Cell index

6. Greyscale
7. Lumen (tracheid no; code numbers ≥1) or wall (0)

"RawMeasures" file:

1. Image name
2. Line number
3. Tracheid number (within each line)
4. LD (μm)
5. CWT-1 (half of the one shared with the previous tracheid, μm)
6. CWT+1 (half of the one shared with the following tracheid, μm)
7. CWT (total CWT, μm)
8. TD (μm)
9. Area (LA, μm^2)
10. LW (1) (indicates if the tracheids belong to the EW (0 codes) or LW (1 code).

"FinalMeasures" file:

1. Image name
2. Ring identifier
3. Ring segment (LW, EW, RW)
4. AvLD (the average LD values of all tracheids within a tree ring or segment, μm)
5. StdLD (the standard deviation for the LD values of all tracheids within a tree ring or segment, μm)
6. AvCWT (the average CWT values of all tracheids within a tree ring or segment, μm)
7. StdCWT (the standard deviation for the CWT values of all tracheids within a tree ring or segment, μm)
8. AvTD (the average TD values of all tracheids within a tree ring or segment, μm)
9. StdTD (the standard deviation for the TD values of all tracheids within a tree ring or segment, μm)

10. AvArea (the average LA values of all tracheids within a tree ring or segment, μm^2)
11. StdArea (the standard deviation for the LA values of all tracheids within a tree ring or segment, μm^2)

ACKNOWLEDGMENTS The development of the software was possible thanks to Agnés Borràs from the Computer Vision Center (CVC), Univ. Autònoma Barcelona, Spain. Funding was obtained from the Spanish Ministry of Education and Sciences via the competitive grant DRIM (CGL2010-16373).

Chapter 6

GENERAL DISCUSSION AND CONCLUSIONS

This thesis documents several Scots pine mortality episodes following severe drought events at two sites located in the NE of the Iberian Peninsula, where this species approaches its south-western (and dry) distribution limit. The results presented here contribute to the active debate on the mechanisms that underlie drought-induced tree mortality, by retrospectively analyzing and comparing different tree-ring patterns between co-occurring now-dead and living Scots pines. More specifically the contributions of this thesis can be discussed following Diagram 1.1 presented in **Chapter 1** (General Introduction), and slightly modified here (Diagram 2.1).

Diagram 2.1 – Structure of the General Discussion, based on the initial hypotheses presented in the General Introduction (**Chapter 1**). Each red arrow corresponds to a direct association as implied by our results and to a different section of the Discussion.

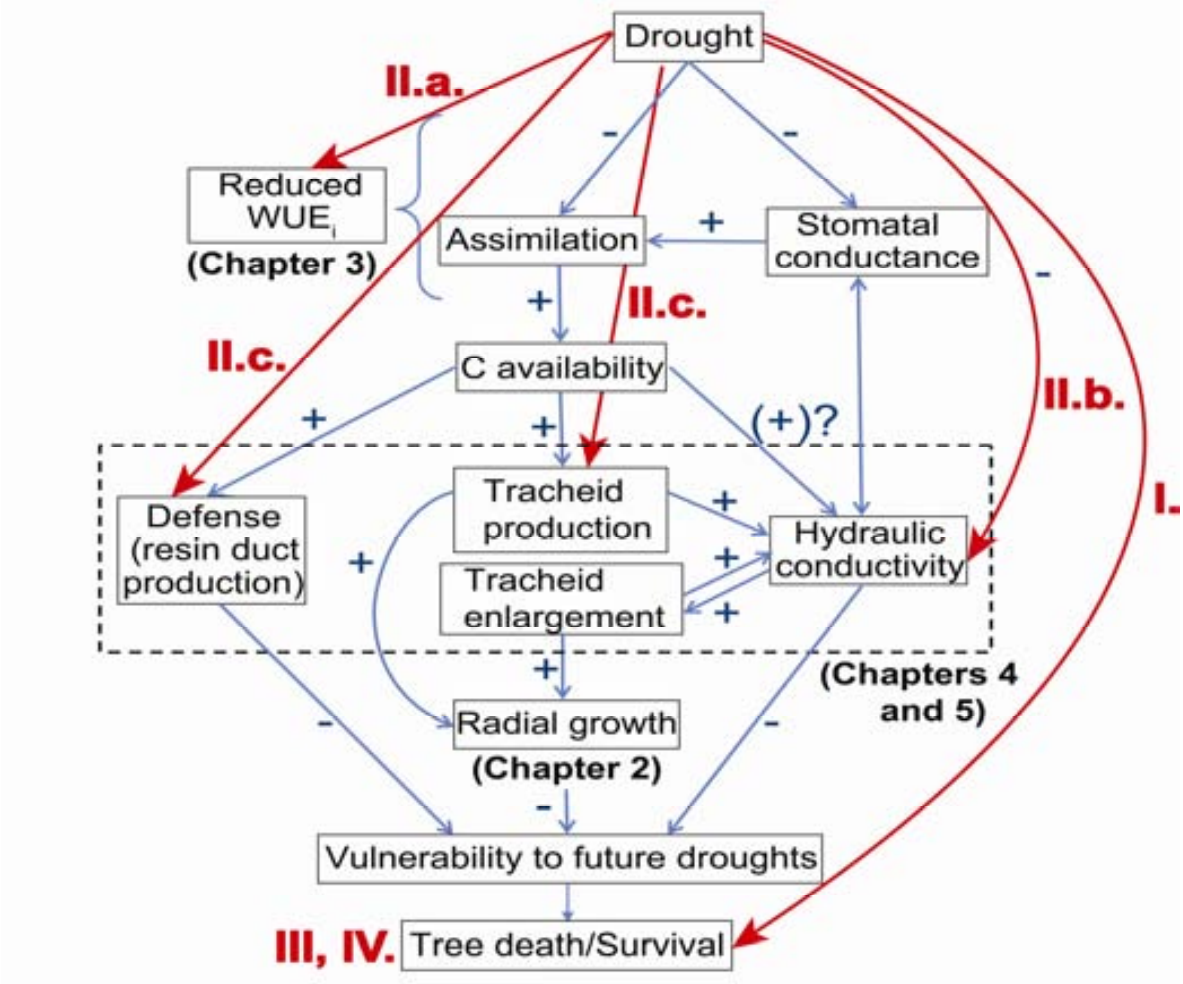

I. SEVERE DROUGHT IS ASSOCIATED WITH SCOTS PINE MORTALITY

Scots pine mortality in Prades and Arcalís was directly associated with severe drought events characterized by low summer water availability. Dendrochronological studies comparing living trees with coexisting now-dead individuals are relatively rare and this study is among the few ones showing a direct association between severe drought and mortality. Our results here confirm observational accounts indicating that Scots pine has started to register important mortality rates at the two study sites since the 1990s and 2000s, especially following drought events (Martínez-Vilalta and Piñol 2002; Galiano *et al.* 2010). Although drought-induced tree mortality is a widespread phenomenon documented all over the world (for a review see Allan *et al.* 2010), the direct link between periods of low water availability and tree death is still poorly documented (but see Villalba and Veblen 1998; Guarín and Taylor 2005; Bigler *et al.* 2007). One explanation for this is the fact that this type of temporal associations requires long-term studies, which are necessarily scarce, or retrospective approaches, like the one used here.

In addition, causality between drought and mortality might be difficult to establish because drought-induced tree death may not occur immediately, but years after the drought event, as documented here (**Chapter 2**). During this lagged period other factors may interfere (Bréda *et al.* 2006), blurring the link between drought and mortality. Scots pine mortality in Prades and Arcalís had an episodic character, faithfully coinciding or following severe drought events. In our case, the effect of additional factors such as insect attack can be discarded, as insect outbreaks were rare and never occurred before mortality was observed. On the other hand, however, fungal pathogens might have had a role in the studied mortality process, at least in Prades, where a root pathogen (*Onnia cf. tomentosa*) has been recently identified (J Oliva, com. pers.).

II. NOW-DEAD SCOTS PINES SHOWED DISTINCTIVE PHYSIOLOGICAL AND GROWTH PATTERNS COMPARED WITH SURVIVING INDIVIDUALS

Overall, the results of this thesis show that now-dead Scots pines from Prades and Arcalís had different growth, WUE_i and wood anatomical features than their surviving

neighbours. These findings can be used as tools to identify vulnerable trees that are more prone to suffer from stressful conditions and eventually die in the future.

a. Now-dead trees showed limited increase of intrinsic water-use efficiency (WUE_i) in response to rising atmospheric CO_2

Now-dead and living Scots pine trees from Prades and Arcalís registered a significant increase of their WUE_i over the studied period. However, for now-dead individuals this increase was significantly lower than for surviving trees. At the same time, no positive effect of the rising atmospheric CO_2 concentrations was found on the trees' growth rates, as illustrated by the negative relationship between WUE_i and growth (BAI). The constant C_i/C_a scenario to which the WUE_i increase of the now-dead trees was closer, involves a proportional regulation of the stomatal conductance and photosynthesis (Wong *et al.* 1979; Saurer *et al.* 2004). Under drought conditions, isohydric species like Scots pine reduce their stomatal conductance by closing stomata in order to avoid water loss and cavitation (Irvine *et al.* 1998; Poyatos *et al.* 2013), and this affects both carbon uptake and photosynthesis (Bréda *et al.* 2006; McDowell *et al*. 2010). WUE_i usually increases under conditions of stomatal limitation of photosynthesis due to low intercellular CO_2 concentrations (Saurer *et al.* 2004). Nevertheless, in trees weakened over a long time period by stressful climatic conditions (e.g. drought), this WUE_i increase seems to be finally limited despite rising CO_2 concentrations. This decoupling is not well understood, but points towards a threshold in the capacity of trees to cope with stressful drought conditions (Linares and Camarero 2012 and references therein).

b. Now-dead trees had lower hydraulic capacity before death

Now-dead Scots pines from Prades and Arcalís were also characterized by reduced hydraulic conductance of their xylem, compared to their surviving neighbours. This reduced hydraulic capacity was related, in part, with the low lumen diameter of their tracheids, as hydraulic conductance is proportional to the fourth power of conduit diameter (Tyree and Zimmermann 2002). Cell size largely depends on climatic conditions and a reduced lumen diameter is frequently an indicator of water scarcity at the time of tracheid enlargement (Vaganov 1990). In parallel with the lumen reduction, the production of tracheids per tree-ring was also low in now-dead Scots

pines, determining narrow annual rings. Pines in general, and Scots pine in particular, try to compensate the formation of narrow rings by transporting water through several adjacent tree-rings (Eilmann *et al.* 2009). In our case, however, measurements comparing healthy and defoliated Scots pines at the same Prades site studied here show that sapwood depth was similar between crown defoliation classes (Poyatos *et al*. 2003). Similarly, the vulnerability to xylem embolism in the stem, estimated from the ratio between cell-wall thickness and radial lumen diameter (Hacke *et al.* 2001), was similar between surviving and now-dead trees, in agreement with our own measurements at the Prades site (Poyatos *et al.* 2013; M Gómez, unpublished data).

Now-dead individuals showed low growth rates over many years before their death, indicating that the hydraulic conductance of their xylem had been long-time severely diminished. The formation of a low number of tracheids is consistent with the carbon balance dysfunction perspective (Bréda *et al.* 2006). Low assimilation rates and reduced leaf area have been shown to occur in Scots pine in the time period prior to death (Galiano *et al.* 2011; Poyatos *et al.* 2013). This low carbon uptake could result in reduced internal carbon pools, which could explain both the reduction in stored carbohydrates and the decline in radial growth in dying trees (Galiano *et al.* 2011; Poyatos *et al.* 2013). In addition, carbon pools may become unavailable under extreme drought (Sala *et al.* 2012) or might be preferentially allocated to tissues other than xylem (Waring 1987).

c. Now-dead trees showed lower investment of carbon in growth and defence

The hypothesis that now-dead Scots pines from Prades and Arcalís were carbon limited, probably due to constraining drought effects on carbon assimilation (Bréda *et al.* 2006), is sustained by their low carbon investment, as reflected in the low tracheid and resin duct production, with consequences on the hydraulic performance and defence, respectively. Mainly as a result of a low tracheid production per annual growth ring, now-dead individuals showed a reduced radial growth (e.g. BAI) before dying. More precisely, now-dead Scots pines from Prades and Arcalís started to grow less than their surviving neighbours 40 to 15 years before their death, respectively, suggesting a slow process of growth decline preceding mortality. Reduced growth rates are a frequent response to drought events (Bréda *et al.* 2006) and a common

characteristic of dying trees (Pedersen 1998; Bigler *et al.* 2006). The impact of droughts on carbon uptake probably increases the dependency on stored carbon reserves for processes such as growth or defence. In any case, lower investment in growth, particularly when it involves a reduction in leaf area and hydraulic capacity, has carry over effects on the carbon economy of trees, which could explain the long-term decline processes characterized in this thesis (**Chapters 2-4**). The presence of long–term decline processes and time lags between drought and tree death has been documented in previous studies (e.g. Guarín and Taylor 2005; Bigler *et al.* 2006, 2007). Similarly, the low number of resin ducts in now-dead trees observed in this thesis is consistent with published results (Kane and Kolb 2010; Gaylord *et al.* 2013). Although in our case there was no evidence of insect attack, the reduced defence found for these trees must be included as an additional factor of vulnerability that might be involved in the mortality processes.

III. MECHANISMS OF DROUGHT-INDUCED MORTALITY LIKELY DIFFER BETWEEN SITES

Overall, the results of this thesis show that the physiological and growth patterns considered here differed between now-dead and surviving Scots pines. Nevertheless, it must be stressed out that the two sites we studied showed two different stories: living and dead trees had a long-term divergent growth and hydraulic performance in Prades, whereas this divergence was less accentuated and more recent in Arcalís. Altogether, now-dead Scots pines showed both carbon- and hydraulic-related limitations, bringing support to the idea that tree mortality is determined by a complex set of interrelated changes in the carbon and water economy of plants (McDowell 2011; McDowell *et al.* 2011; Sevanto *et al.* 2013). The fact that the timing and characteristics of the decline process differed substantially between the two sites studied in this thesis indicates that the detailed physiological mechanism of drought-induced mortality might differ even among populations of the same species.

IV. IMPLICATIONS FOR SOUTHERN SCOTS PINE POPULATIONS UNDER CLIMATE CHANGE

Climatic models predict that climate in the Mediterranean region will get warmer and drier (Giorgi 2006; IPCC 2007). Since the Iberian Scots pine populations are at their

south-western (and dry) limits of distribution, episodes of drought-induced mortality are likely to become more frequent and widespread in the future. This thesis and other studies suggest that Scots pine may have serious difficulties in coping with ongoing climate change in southern populations (Reich and Oleksyn 2008; Matías and Jump 2012), leading to a reduction in its range (Benito Garzón *et al.* 2008, 2011). Although stand factors have a key role in modulating Scots pine mortality at regional scales (Vilà-Cabrera et al. 2011), the overall scenario is worsened by the fact that Scots pine regeneration is low (Castro *et al.* 2004; Mendoza *et al.* 2009; Galiano *et al.* 2010), especially in areas where it registers higher mortality (Vilà-Cabrera *et al.* 2011). In addition, the regeneration of trees from the *Quercus* genus seems to be favoured in many areas currently dominated by Scots pine (e.g. Galiano *et al.* 2010, 2013), which could lead to a progressive replacement of some Scots pine forests by *Quercus* sp. woodlands, as already observed in some areas (Galiano *et al*. 2010; Poyatos *et al*. 2013). Although it is clear that this process is driven mostly by historical changes in forest management and stand structure (e.g. Vayreda *et al*. 2012*b*), it also seems clear that increased drought has the potential to accelerate the process and that important ecosystem functions will be affected.

V. CONCLUSIONS

i. Scots pine mortality in Prades and Arcalís was directly associated with severe drought events characterized by low summer water availability.

ii. Radial growth, intrinsic water-use efficiency (WUE_i) and wood anatomical features of now-dead Scots pines were different from those of the pines that survived. These findings offer a way of identifying the trees that are more predisposed to die in the future.

iii. The trees that died showed lower hydraulic capacity and lower investment of carbon for growth and defence, bringing support to the idea that drought-induced tree mortality is determined by a complex set of interrelated changes in the carbon and water economy of plants. Lower carbon availability in dying trees is consistent with depleted carbohydrate reserves observed in Scots pines from the same study sites prior to mortality.

iv. Although the qualitative responses were similar between sites, the timing and fine characteristics of the decline process differed substantially between them, suggesting a long-term decline process at Prades and more recent and sudden process at Arcalís. This result suggests that the detailed physiological mechanism of drought-induced mortality might differ even among populations of the same species.

v. This thesis adds to the evidence suggesting that if the projections of more frequent and intense drought events come true, episodes of Scots pine mortality are likely to continue, leading eventually to a shift in the dominant vegetation in some areas.

BIBLIOGRAPHY

Aguilera M, Ferrio JP, Araus JL, Tarrús J, Voltas J (2011) Climate at the onset of Western Mediterranean agriculture expansion: Evidence from stable isotopes of sub-fossil oak tree rings in Spain. *Palaeogeography, Palaeoclimatology, Palaeoecology* **299**, 541-551.

Allen CD, Breshears DD (1998) Drought-induced shift of a forest-woodland ecotone: Rapid landscape response to climate variation. *Proceedings of the National Academy of Sciences of the Unites States of America* **95**, 14839-14842.

Allen CD, Macalady AK, Chenchouni H, Bachelet D, McDowell N, Vennetier M, Kitzberger T, Rigling A, Breshears DD, Hogg EH, Gonzalez P, Fensham R, Zhang Z, Castro J, Demidova N, Lim JH, Allard G, Running SW, Semerci A, Cobb N (2010) A global overview of drought and heat-induced tree mortality reveals emerging climate change risks for forests. *Forest Ecology and Management* **259**, 660-684.

Amoroso MM, Daniels LD (2010) Cambial mortality in declining *Austrocedrus chilensis* forests: implications for stand dynamics. *Canadian Journal of Forest Research* **40**, 885-893.

Anderegg WRL, Berry JA, Field CB (2012) Linking definitions, mechanisms, and modelling of drought-induced tree death. *Trends in Plant Science* **17**, 693-700.

Anderegg WRL, Kane JM, Anderegg LDL (2013*a*) Consequences of widespread trees mortality triggered by drought and temperatures stress. *Nature Climate Change* **3**, 30-36.

Anderegg WRL, Plavcova L, Anderegg LDL, Hacke UG, Berry JA, Field CB (2013*b*) Drought's legacy: multiyear hydraulic deterioration underlies widespread aspen forest die-off and portends increased future risk. *Global Change Biology* **19**, 1188-1196.

Anderson RG, Canadell JG, Randerson JT, Jackson RB, Hungate BA, Baldocchi DD, Ban-Weiss GA, Bonan GB, Caldeira K, Cao L, Diffenbaugh NS, Gurney KR, Kueppers LM, Law BE, Luyssaert S, O'Halloran TL (2011) Biophysical considerations in forestry for climate protection. *Frontiers in Ecology and the Environment* **9,** 174–182.

Andreu L, Gutiérrez E, Macias M, Ribas M, Bosch O, Camarero JJ (2007) Climate increases regional tree-growth variability in Iberian pine forests. *Global Change Biology* **13**, 804-815.

Andreu L, Planells O, Gutiérrez E, Helle G, Schleser GH (2008) Climatic significance of tree-ring width and $\delta^{13}C$ in a Spanish pine forest network. *Tellus B* **60**, 771-781.

Andreu-Hayles L, Planells O, Gutiérrez E, Muntan E, Helle G, Anchukaitis KJ, Schleser GH (2011) Long tree-ring chronologies reveal 20th century increases in water-use efficiency but no enhancement of tree growth at five Iberian pine forests. *Global Change Biology* **17**, 2095-2112.

Bakkenes M, Alkemade JRM, Ihle F, Leemans R, Latour JB (2002) Assessing effects of forecast climate change on the diversity and distribution of European higher plants for 2050. *Global Change Biology* **8**, 390-407.

Barbéro M, Loisel R, Quézel P, Richardson DM, Romane F (1998) Pines of the Mediterranean Basin. In 'Ecology and Biogeography of *Pinus*'. (Ed. DM Richardson) pp. 153-170. (Cambridge University Press: Cambridge).

Bates BC, Kundzewicz ZW, Wu S, Palutikof JP (2008) Climate change and water. Technical paper VI of the intergovernmental panel on climate change. IPCC Secretariat, Geneva, 210 p.

Barbéro M, Loisel R, Quézel P, Richardson DM, Romane F (1998) Pines of the Mediterranean Basin. In 'Ecology and Biogeography of *Pinus*'. (Ed. DM Richardson) pp. 153-170. (Cambridge University, Cambridge, UK).

Beerling DJ (1997) Carbon isotope discrimination and stomatal responses of mature *Pinus sylvestris* L. trees exposed *in situ* for three years to elevated CO_2 and temperature. *Acta Oecologica* **18**, 697-712.

Beniston M, Innes JL (1998) Impacts of climatic variability and extreme on forest: synthesis. In: 'The impacts of climate variability and forests'. (Eds. M Beniston, JL Innes) pp. 309–318, 329 p. (*Lecture notes in Earth Sciences* 74, Springer).

Benito Garzón M, Sánchez de Dios R, Sainz Ollero H (2008) Effects of climate change on the distribution of Iberian tree species. *Applied Vegetation Science* **11**, 169-178.

Benito Garzón M, Alía R, Robson TM, Zavala MA (2011) Intra-specific variability and plasticity influence potential tree species distributions under climate change. *Global Ecology and Biogeography* **20**, 766-778.

Bigler C, Bugmann H (2003) Growth-dependent tree mortality models based on tree rings. *Canadian Journal of Forest Research* **33**, 210-221.

Bigler C, Kulakowski D, Veblen TT (2005) Multiple disturbance interactions and drought influence fire severity in rocky mountain subalpine forests. *Ecology* **86,** 3018–3029.

Bigler C, Bräker OU, Bugmann H, Dobbertin M, Rigling A (2006) Drought as an inciting mortality factor in Scots pine stands of the Valais, Switzerland. *Ecosystems* **9**, 330–343.

Bigler C, Gavin DG, Gunning C, Veblen TT (2007) Drought induces lagged tree mortality in a subalpine forest in the Rocky Mountains. *Oikos* **116**, 1983-1994.

Biondi F (1999) Comparing tree-ring chronologies and repeated timber inventories as forest monitoring tools. *Ecological Applications* **9**, 216–227.

Bonan GB (2008) Forests and Climate Change: Forcings, Feedbacks, and the Climate Benefits of Forests. *Science* **320**, 1444-1449.

Boratynski A (1991) Range of natural distribution. In: 'Genetics of Scots pine'. (Eds. M Giertych, C Mátyás), pp. 19–30. (Akadémiai Kiadó, Budapest, Hungary).

Boyer JS (1985) Water transport. *Annual Review of Plant Physiology and Plant Molecular Biology* **36**, 473–516.

Bréda N, Huc R, Granier A, Dreyer E (2006) Temperate forest trees and stands under severe drought: a review of ecophysiological responses, adaptation processes and long-term consequences. *Annals of Forest Science* **63**, 625–644.

Bréda N, Badeau V (2008) Forest tree responses to extreme drought and some biotic events: Towards a selection according to hazard tolerance? *Comptes Rendus Geoscience* **340**, 651-662.

Brendel O, Iannetta PPM, Stewart D (2000) A Rapid and Simple Method to Isolate Pure Alpha-cellulose. *Phytochemical Analysis* **11**, 7-10.

Brodribb TJ, Cochard H (2009) Hydraulic failure defines the recovery and point of death in water-stressed conifers. *Plant Physiology* **149**, 575-584.

Camarero JJ, Guerrero-Campo J, Gutiérrez E (1998) Tree-ring growth and structure of *Pinus uncinata* and *Pinus sylvestris* in the Central Spanish Pyrenees. *Arctic and Alpine Research* **30**, 1-10.

Camarero JJ, Olano JM, Parras A (2010) Plastic bimodal xylogenesis in conifers from continental Mediterranean climates. *New Phytologist* **185**, 471-480.

Carlisle A, Brown AHF (1968) *Pinus sylvestris* L. *Journal of Ecology* **56**, 269-307.

Castro J, Zamora R, Hódar JA, Gómez JM (2004) Seedling establishment of a boreal tree species (*Pinus sylvestris*) at its southernmost distribution limit: consequences of being in a marginal Mediterranean habit. *Journal of Ecology* **92**, 266-277.

Catalan Bachiller G, Muñoz PG, Galera Peral RM, Martin Albertos S, Agundez Leal D, Alia Miranda R (1991) Las regiones de procedencia de *Pinus sylvestris* L. y *Pinus nigra* Arn. subsp. *salzmannii* (Dunal) Franco en España. INIA, departamento de sistemas forestales, ICONA, servicio e material genético, Madrid.

Ceballos L, Ruiz de la Torre J (1971) Árboles Y Arbustos de la España Peninsular. Instituto Forestal de Investigaciones y Experiencias, Madrid.

Cherubini P, Gartner BL, Tognetti R, Bräker OU, Schoch W, Innes JL (2003) Identification, measurement and interpretation of tree rings in woody species from Mediterranean climates. *Biological Reviews* **78**, 119-148.

Christensen JH, Hewitson B, Busuioc A, Chen A, Gao X, Held I, Jones R, Kolli RK, Kwon WT, Laprise R, Magaña Rueda V, Mearns L, Menéndez CG, Räisänen J, Rinke A, Sarr A, Whetton P (2007) Regional climate projections. In 'Climate change 2007: The physical science basis. Contribution of Working Group I to the fourth assessment report of the intergovernmental panel on climate change'. (Eds. S Solomon, D Qin, M Manning, Z Chen, M Marquis, KB Averyt, M Tignor, HL Miller) pp. 847–940. (Cambridge University Press: Cambridge).

Cochard H (1992) Vulnerability of several conifers to air embolism. *Tree Physiology* **11**, 73-83.

Cochard H, Froux F, Mayr S, Coutand C (2004) Xylem wall collapse in water-stressed pine needles. *Plant Physiology* **134**, 401-408.

Corcuera L, Camarero JJ, Sisó S, Gil-Pelegrín E (2006) Radial-growth and wood-anatomical changes in overaged *Quercus pyrenaica* coppice stands: functional

responses in a new Mediterranean landscape. *Trees Structure and Function* **20**, 91-98.

Cherubini P, Gartner BL, Tognetti R, Bräker OU, Schoch W, Innes JL (2003) Identificantion, measurement and interpretation of tree rings in woody species from Mediterranean climates. *Biological Reviews* **78**,119-148.

Choat B, Jansen S, Brodribb TJ, Cochard H, Delzon S, Bhaskar R, Bucci SJ, Feild TS, Gleason SM, Hacke UG, Jacobsen AL, Lens F, Maherali H, Martínez-Vilalta J, Mayr S, Mencuccini M, Mitchell PJ, Nardini A, Pittermann J, Pratt RB, Sperry JS, Westoby M, Wright IJ, Zanne AE (2012) Global convergence in the vulnerability of forests to drought. *Nature* **491**, 752-755.

Das AJ, Battles JJ, Stephenson NL, van Mantgem PJ (2007) The relationship between tree growth patterns and likelihood of mortality: a study of two tree species in the Sierra Nevada. *Canadian Journal of Forest Research* **37**, 580-597.

Denne MP, Dodd RS (1981) The environmental control of xylem differentiation. In 'Xylem cell development'. (Ed. JR Barnett) pp. 236-255. (Kent, Castle House, UK).

Denne MP (1988) Definition of latewood according to Mork (1928). *IAWA Bulletin* **10**, 59-62.

Deslauriers A, Morin H, Urbinati C, Carrer M (2003) Daily weather responses of balsam fir (*Abies balsamea* (L.) Mill.) stem radius increment from dendrometer analysis in the boreal forests of Québec (Canada). *Trees Structure and Function* **17**, 477-484.

DeSoto L, De la Cruz M, Fonti P (2011) Intra-annual patterns of tracheid size in the Mediterranean tree *Juniperus thurifera* as an indicator of seasonal water stress. *Canadian Journal of Forest Research* **41**, 1280-1294.

Dobbertin M (2005) Tree growth as indicator of tree vitality and of tree reaction to environmental stress: a review. *European Journal of Forest Research* **124**, 319-333.

Dorado Liñán I, Gutiérrez E, Helle G, Heinrich I, Andreu-Hayles L, Planells O, Leuenberger M, Bürger C, Schleser G (2011) Pooled versus separate measurements of tree-ring stable isotopes. *Science of the Total Environment* **409**, 2244-2251.

Douville H, Chauvin F, Planton S, Royer JF, Salas-Mélia D, Tyteca S (2002) Sensitivity of the hydrological cycle to increasing amounts of greenhouse gases and aerosols. *Climate Dynamics* **20**, 45–68.

Drobyshev I, Linderson H, Sonesson K (2007) Temporal mortality pattern of pedunculate oaks in southern Sweden. *Dendrochronologia* **24**, 97-108.

Duquesnay A, Bréda N, Stievenard M, Dupouey JL (1998) Changes of tree-ring $\delta^{13}C$ and water-use efficiency of beech (*Fagus sylvatica* L.) in north-east France during the past century. *Plant, Cell and Environment* **21**, 565–572.

Eamus D (1991) The interaction of rising CO_2 and temperatures with water use efficiency. *Plant, Cell and Environment* **14**, 843-852.

Eckstein D, Frisse E, Liese W (1974) Holzanatomische Untersuchungen an umweltgeschädigten Strassenbäumen der Hamburger Innenstadt. *European Journal of Forest Pathology* **4**, 232–244.

Eilmann B, Weber P, Rigling A, Eckstein D (2006) Growth reactions of *Pinus sylvestris* L. and *Quercus pubescens* Willd. to drought years at a xeric site in Valais, Switzerland. *Dendrochronologia* **23**, 121–132.

Eilmann B, Zweifel R, Buchmann N, Fonti P, Rigling A (2009) Drought-induced adaptation of the xylem in Scots pine and pubescent oak. *Tree Physiology* **29**, 1011-1020.

Eilmann B, Buchmann N, Siegwolf R, Saurer M, Cherubini P, Rigling A (2010) Fast response of Scots pine to improved water availability reflected in tree-ring width and $\delta^{13}C$. *Plant, Cell and Environment* **33**, 1351-1360.

Eilmann B, Rigling A (2012) Tree-growth analyses to estimate tree species' drought tolerance. *Tree Physiology* **32**, 178-187.

Ellenberg H (1988) Vegetation ecology of Central Europe. (Cambridge University, Cambridge, UK).

Farquhar GD, O'Leary MH, Berry JA (1982) On the Relationship between Carbon Isotope Discrimination and the Intercellular Carbon Dioxide Concentration in Leaves. *Australian Journal of Plant Physiology* **9**, 121-137.

Farquhar GD, Richards RA (1984) Isotopic composition of plant carbon correlates with water-use efficiency of wheat genotypes. *Australian Journal of Plant Physiology* **11**, 539-552.

Farquhar GD, Ehleringer JR, Hubick KT (1989) Carbon isotope discrimination and photosynthesis. *Annual Review of Plant Physiology and Plant Molecular Biology* **40**, 503-537.

Ferreira T, Rasband WS (2010-2012), ImageJ User GuideIJ 1.46, imagej.nih.gov/ij/docs/guide/

Ferrio JP, Florit A, Vega A, Serrano L, Voltas J (2003) $\Delta^{13}C$ and tree-ring width reflect different drought responses in *Quercus ilex* and *Pinus halepensis*. *Oecologia* **137**, 512-518.

Ferrio JP, Araus JL, Buxó R, Voltas J, Bort J (2005*b*) Water management practices and climate in ancient agriculture: inferences from the stable isotope composition of archaeobotanical remains. *Vegetation History and Archaeobotany* **14**, 510-517. Database: CU-INSTAAR/NOAA-CMDL. Available on internet: http://web.udl.es/usuaris/x3845331/AIRCO2_LOESS.xls.

Fischer TM, Gilmour AR, Werf JHJ (2004) Computing approximate standard errors for genetic parameters derived from random regression models fitted by average information REML. *Genetics Selection Evolution* **36**, 363-369.

Flexas J, Barbour MM, Brendel O, Cabrera HM, Carriquí M, Díaz-Espejo A, Douthe C, Dreyer E, Ferrio JP, Gago J, Gallé A, Galmés J, Kodama N, Medrano H, Niinemets Ü, Peguero-Pina JJ, Pou A, Ribas-Carbó M, Tomás M, Tosens T, Warren CR (2012) Mesophyll diffusion conductance to CO2: An unappreciated central player in photosynthesis. *Plant Science* **193-194**, 70-84.

Fonti P, Eilmann B, García-Gonzáles I, von Arx G (2009) Expeditious building of ring-porous earlywood vessel chronologies without loosing signal information. *Trees Structure and Function* **23**, 665-671.

Fonti P, von Arx G, García-González I, Eilmann B, Sass-Klaassen U, Gärtner H, Eckstein D (2010) Studying global change through investigation of the plastic responses of xylem anatomy in tree rings. *New Phytologist* **185**, 42-53.

Franklin JF, Shugart HH, Harmon ME (1987) Tree death as an ecological process. *Bioscience* **37,** 550–556.

Fritts HC (2001) Tree rings and climate (Reprint of second printing). (Blackburn Press: New Jersey).

Gagen M, McCarroll D, Edouard JL (2004) Latewood width, maximum density, and stable carbon isotope ratios of pine as climate indicators in a dry subalpine environment, French Alps. *Arctic, Antarctic, and Alpine Research* **36**, 166–171.

Galiano L, Martínez-Vilalta J, Lloret F (2010) Drought-induced multifactor decline of Scots pine in the Pyrenees and potential vegetation change by the expansion of co-occurring oak species. *Ecosystems* **13**, 978-991.

Galiano L, Martínez-Vilalta J, Lloret F (2011) Carbon reserves and canopy defoliation determine the recovery of Scots pine 4 yr after a drought episode. *New Phytologist* **190**, 750-759.

Galiano L, Martínez-Vilalta J, Eugenio M, Granzow de La Cerda I, Lloret F (2013) Seedling emergence and growth of *Quercus* spp. following severe drought effects on a *Pinus sylvestris* canopy. *Journal of Vegetation Science* **24**, 580-588.

Galmés J, Medrano H, Flexas J (2007) Photosynthetic limitations in response to water stress and recovery in Mediterranean plants with different growth forms. *New Phytologist* **175**, 81-93.

García López JM, Allué Camacho C (2010) Effects of climate change on the distribution of *Pinus sylvestris* L. stands in Spain. A phytoclimatic approach to defining management alternatives. *Forest Systems* **19**, 329-339.

Gaudinski JB, Dawson TE, Quideau S, Schuur EAG, Roden JS, Trumbore SE, Sandquist DR, Oh SW, Wasylishen RE (2005) Comparative Analysis of Cellulose Preparation Techniques for Use with ^{13}C, ^{14}C, and ^{18}O Isotopic Measurements. *Analytical Chemistry* **77**, 7212-7224.

Gaylord ML, Kolb TE, Pockman WT, Plaut JA, Yepez EA, Macalady AK, Pangle RE, McDowell N (2013) Drought predisposes piñon-juniper woodlands to insect attack and mortality. *New Phytologist* **198**, 567-578.

Giorgi F (2006) Climate change Hot-spots. *Geophysical Research Letters* **33**, L08707.

Giorgi F, Lionello P (2008) Climate change projections for the Mediterranean region. *Global and Planetary Change* **63**, 90-104.

Giuggiola A, Kuster TM, Saha S (2010) Drought-induced mortality of Scots pines at the southern limits of its distribution in Europe: causes and consequences. *Forest Biosciences and Forestry* **3**, 95-97.

Gruber A, Strobl S, Veit B, Oberhuber W (2010) Impact of drought on the temporal dynamics of wood formation in *Pinus sylvestris*. *Tree Physiology* **30**, 490-501.

Grudd H, Briffa KR, Karlén W, Bartholin TS, Jones PD, Kromer B (2002) A 7400-year tree-ring chronology in northern Swedish Lapland: natural climatic variability expressed on annual to millennial timescales. *The Holocene* **12**, 657-665.

Guarín A, Taylor AH (2005) Drought triggered tree mortality in mixed conifer forests in Yosemite National Park, California, USA. *Forest Ecology and Management* **218**, 229-244.

Gutiérrez E (1989) Dendroclimatological study of *Pinus sylvestris* L. in Southern Catalonia (Spain). *Tree-Ring Bulletin* **49**, 1-9.

Gutschick VP, BassiriRad H (2003) Extreme events as shaping physiology, ecology, and evolution of plants: toward a unified definition and evaluation of their consequences. *New Phytologist* **160**, 21-42.

Hacke UG, Sperry JS, Pockman WT, Davis SD, McCulloh KA (2001) Trends in wood density and structure are linked to prevention of xylem implosion by negative pressure. *Oecologia* **126**, 457–461.

Hampe A, Petit RJ (2005) Conserving biodiversity under climate change: the rear edge matters. *Ecology Letters* **8**, 461-467.

Hargreaves GH, Samani ZA (1982) Estimating potential evapotranspiration. *Journal of the Irrigation and Drainage Division ASCE* **108**, 225–230.

Helama S, Lindholm M, Timonen M, Meriläinen J, Eronen M (2002) The supra-long Scots pine tree-ring record for Finnish Lapland: Part 2, interannual to centennial variability in summer temperatures for 7500 years. *The Holocene* **12**, 681-687.

Helama S, Timonen M, Holopainen J, Ogurtsov MG, Mielikäinen K, Eronen M, Lindholm M, Meriläinen J (2009) Summer temperature variations in Lapland during the Medieval Warm Period and the Little Ice Age relative to natural instability of thermohaline circulation on multi-decadal and multi-centennial scales. *Journal of Quaternary Science* **24**, 450-456.

Hereş AM, Martínez-Vilalta J, Claramunt López B (2012) Growth patterns in relation to drought-induced mortality at two Scots pine (*Pinus sylvestris* L.) sites in NE Iberian Peninsula. *Trees Structure and Function* **26**, 621-630.

Hereter A, Sánchez JR (1999) Experimental areas of Prades and Montseny. In 'Ecology of Mediterranean Evergreen Oak Forests'. (Eds. F Rodà, J Retana, CA Gracia, J Bellot) pp. 15-27. (Springer Press, Berlin, Germany).

Hewitt GM (2004) Genetic consequences of climatic oscillations in the Quaternary. *Philosophical Transactions of The Royal Society Biological Sciences* **359**, 183-195.

Holmes RL (1983) Computer-assisted quality control in tree-ring dating and measurement. *Tree-ring Bulletin* **43,** 69-78.

Hsiao TC (1973) Plant responses to water stress. *Annual Review of Plant Physiology* **24**, 519–570.

Hsiao TC, Acevedo E (1974) Plant responses to water deficits, water-use efficiency, and drought resistance. *Agricultural Meteorology* **14**, 59-84.

Hughes MK, Kelly PM, Pilcher JR, Lamarche VC (1982) Climate from Tree Rings. 223 p. (Cambridge University Press: Cambridge).

Image-Pro Plus Media Cybernetics Inc. (2012) v6.1-7. (Rockville, USA).

IPCC (2007) Climate Change 2007: The Physical Science Basis. Contribution of Working Group I to the Fourth Assessment Report of the Intergovernmental Panel on Climate Change. (Eds. S Solomon, D Qin, M Manning, Z Chen, M Marquis, KB Averyt, M Tignor, HL Miller). (Cambridge University Press: Cambridge).

Irvine J, Perks MP, Magnani F, Grace J (1998) The response of *Pinus sylvestris* to drought: stomatal control of transpiration and hydraulic conductance. *Tree Physiology* **18**, 393-402.

Kane JM, Kolb TE (2010) Importance of resin ducts in reducing ponderosa pine mortality from bark beetle attack. *Oecologia* **164**, 601-609.

Keeling CD, Bacastow RB, Carter AF, Piper SC, Whorf TP, Heimann M, Mook WG, Roeloffzen H (1989) A three dimensional model of atmospheric CO_2 transport based on observed winds. 1. Analysis of observational data. In 'Geophysical Monograph'. (Ed. DH Peterson) pp. 165-236. (American Geophysical Union: Washington DC).

Keenan T, Sabate S, Gracia C (2010) The importance of mesophyll conductance in regulating forest ecosystem productivity during drought periods. *Global Change Biology* **16**, 1019-1034.

Keenan TF, Hollinger DY, Bohrer G, Dragoni D, Munger JW, Schmid HP, Richardson AD (2013) Increase in forest water-use efficiency as atmospheric carbon dioxide concentrations rise. *Nature* **499**, 324-327.

Knigge W, Schulz H (1961) Einfluss der Jahreswitterung 1959 auf Zellartverteilung, Faserlänge und Gefässweite verschiedener Holzarten. *Holz als Roh- und Werkstoff* **19**, 293–303.

Köppen W (1936) Das Geographische System der Klimate. In 'Handbuch der Klimatologie, Vol. 1, part C'. (Eds. W Köppen, R Geiger) pp. 1-44. (Gebrüder Borntraeger: Berlin).

Laumer W, Andreu L, Helle G, Schleser GH, Wieloch T, Wissel H (2009) A novel approach for the homogenization of cellulose to use micro-amounts for stable isotope analyses. *Rapid Communications in Mass Spectrometry* **23**, 1934-1940.

Le Houerou HN (2004) An Agro-Bioclimatic Classification of Arid and Semiarid Lands in the Isoclimatic Mediterranean Zones. *Arid Land Research and Management* **18**, 301-346.

Leavitt SW (2010) Tree-ring C-H-O isotope variability and sampling. *Science of the Total Environment* **408**, 5244-5253.

Levanič T, Čater M, McDowell N (2011) Associations between growth, wood anatomy, carbon isotope discrimination and mortality in a *Quercus robur* forest. *Tree Physiology* **31**, 298-308.

Linares JC, Delgado-Huertas A, Camarero JJ, Merino J, Carreira JA (2009) Competition and drought limit the response of water-use efficiency to rising atmospheric carbon dioxide in the Mediterranean fir *Abies pinsapo*. *Oecologia* **161**, 611-624.

Linares JC, Camarero JJ, Carreira JA (2010) Competition modulates the adaptation capacity of forests to climatic stress: insights from recent growth decline and death in relict stands of the Mediterranean fir *Abies pinsapo*. *Journal of Ecology* **98**, 592-603.

Linares JC, Camarero JJ (2012) From pattern to process: linking intrinsic water-use efficiency to drought-induced forest decline. *Global Change Biology* **18**, 1000-1015.

Lloret F, Escudero A, Iriondo JM, Martínez-Vilalta J, Valladares F (2012) Extreme climatic events and vegetation: the role of stabilizing processes. *Global Change Biology* **18**, 797-805.

Loader NJ, McCarroll D, Gagen M, Robertson I, Jalkanen R (2007) Extracting climatic information from stable isotopes in tree rings. In 'Stable Isotopes as Indicators of Ecological Change'. (Eds. TE Dawson, RTW Siegwolf) pp. 23-44. (Elsevier: The Netherlands).

Long SP (1991) Modification of the response of photosynthetic productivity to rising temperature by atmospheric CO_2: has its importance been underestimated? *Plant, Cell and Environment* **14**, 729-739.

Manion PD (1991) Tree Disease Concepts (2nd ed.). (Prentice Hall, Upper Saddle River: New Jersey).

Martín JA, Esteban LG, de Palacios P, García Fernández F (2010) Variation in wood anatomical traits of *Pinus sylvestris* L. between Spanish regions of provenance. *Trees Structure and Function* **24**, 1017–1028.

Martín Benito D, Cherubini P, del Río M, Cañellas I (2008) Growth response to climate and drought in *Pinus nigra* Arn. trees of different crown classes. *Trees Structure and Function* **22**, 363-373.

Martín Benito D, Beeckman H, Cañellas I (2013) Influence of drought on tree rings and tracheid features of *Pinus nigra* and *Pinus sylvestris* in a mesic Mediterranean forest. *European Journal of Forest Research* **132**, 33-45.

Martínez-Vilalta J, Piñol J (2002) Drought-induced mortality and hydraulic architecture in pine populations of the NE Iberian Peninsula. *Forest Ecology and Management* **161**, 247-256.

Martínez-Vilalta J, López BC, Adell N, Badiella L, Ninyerola M (2008) Twentieth century increase of Scots pine radial growth in NE Spain shows strong climate interactions. *Glob Change Biology* **14**, 1-14.

Martínez-Vilalta J, Cochard H, Mencuccini M, Sterck F, Herrero A, Korhonen JFJ, Llorens P, Nikinmaa E, Nolè A, Poyatos R, Ripullone F, Sass-Klaassen U, Zweifel R (2009) Hydraulic adjustment of Scots pine across Europe. *New Phytologist* **184**, 353-364.

Martínez-Vilalta J, Aguadé D, Banqué M, Barba J, Curiel Yuste J, Galiano L, Garcia N, Gómez M, Hereş AM, López BC, Lloret F, Poyatos R, Retana J, Sus O, Vayreda J, Vilà-Cabrera A (2012) Las poblaciones ibéricas de pino albar ante el cambio climático: con la muerte en los talones. *Ecosistemas* **21**, 15-21.

Maseyk K, Hemming D, Angert A, Leavitt SW, Yakir D (2011) Increase in water-use efficiency and underlying processes in pine forests across a precipitation gradient in the dry Mediterranean region over the past 30 years. *Oecologia* **167**, 573-585.

Matías L, Gómez-Aparicio L, Zamora R, Castro J (2011*b*) Effects of resource availability on plant recruitment at community level: an integrated analysis using structural equation modelling. *Perspectives in Plant Ecology, Evolution and Systematics* **13**, 277–285.

Matías L, Jump AS (2012) Interactions between growth, demography and biotic interactions in determining species range limits in a warming world: The case of *Pinus sylvestris*. *Forest Ecology and Management* **282**, 10-22.

McCarroll D, Pawellek F (1998) Stable carbon isotope content of latewood cellulose in *Pinus sylvestris* from northern Finland: variability and signal-strength. *The Holocene* **8**:675–684.

McCarroll D, Loader NJ (2004) Stable isotopes in tree rings. *Quaternary Science Review* **23**, 771-801.

McDowell N, Pockman WT, Allen CD, Breshears DD, Cobb N, Kolb T, Plaut J, Sperry J, West A, Williams DG, Yepez EA (2008) Mechanisms of plant survival and mortality during drought: why do some plants survive while others succumb to drought? *New Phytologist* **178**, 719-739.

McDowell N, Sevanto S (2010) The mechanisms of carbon starvation: how, when, or does it occur at all? *New Phytologist* **186**, 264-266.

McDowell N, Allen CD, Marshall L (2010) Growth, carbon-isotope discrimination, and drought-associated mortality across a *Pinus ponderosa* elevational transect. *Global Change Biology* **16**, 399-415.

McDowell N (2011) Mechanisms linking drought, hydraulics, carbon metabolism, and vegetation mortality. *Plant Physiology* **155**, 1051–1059.

McDowell N, Beerling DJ, Breshears DD, Fisher RA, Raffa KF, Stitt M (2011) The interdependence of mechanisms underlying climate-driven vegetation mortality. *Trends in Ecology and Evolution* **26**, 523-532.

Mendoza I, Gómez-Aparicio L, Zamora R, Matías L (2009) Recruitment limitation of forest communities in a degraded Mediterranean landscape. *Journal of Vegetation Science* **20**, 367-376.

Nikolov N, Helmisaari H (1992) Silvics of the circumpolar boreal forest tree species. In: 'A Systems Analysis of the Global Boreal Forest'. (Eds. H Shugart, R Leemans, G Bowan) pp. 13-84. (Cambridge University Press, Cambridge, UK).

Ninyerola M, Pons X, Roure JM (2000) A methodological approach of climatological modeling of air temperature and precipitation through GIS techniques. *International Journal of Climatology* **20**, 1823-1841.

Ninyerola M, Pons X, Roure JM (2007*a*) Monthly precipitation mapping of the Iberian Peninsula using spatial interpolation tools implemented in a Geographic Information System. *Theoretical and Applied Climatology* **89**, 195-209.

Ninyerola M, Pons X, Roure JM (2007*b*) Objective air temperature mapping for the Iberian Peninsula using spatial interpolation and GIS. *International Journal of Climatology* **27**, 1231-1242.

Ogle K, Whitham TG, Cobb NS (2000) Tree-ring variation in pinyon predicts likelihood of death following severe drought. *Ecology* **81**, 3237–3243.

O'Leary MH (1981) Carbon isotope fractionation in plants. *Phytochemistry* **20**, 553-567.

Pedersen BS (1992) Tree mortality in Midwestern oak–hickory forests: rates and processes. Dissertation. (Oregon State University, Corvallis, Oregon, USA).

Pedersen BS (1998) The role of stress in the mortality of Midwestern oaks as indicated by growth prior to death. *Ecology* **79**, 79–93.

Pedersen BS (1999) The mortality of Midwestern overstory oaks as a bioindicator of environmental stress. *Ecological Applications* **9,** 1017-1027.

Peñuelas J, Filella I, Lloret F, Piñol J, Siscart D (2000) Effects of a severe drought on water and nitrogen use by *Quercus ilex* and *Phyllirea latifolia*. *Biologia Plantarium* **43**, 47-53.

Peñuelas J, Hunt JM, Ogaya R, Jump AS (2008) Twentieth century changes of tree-ring $\delta^{13}C$ at the southern range-edge of *Fagus sylvatica*: increasing water-use efficiency does not avoid the growth decline induced by warming at low altitudes. *Global Change Biology* **14**, 1076-1088.

Peñuelas J, Canadell JG, Ogaya R (2011) Increased water-use efficiency during the 20th century did not translate into enhanced tree growth. *Global Ecology and Biogeography* **20**, 597-608.

Petit RJ, Aguinagalde I, de Beaulieu JL, Bittkau C. Brewer S, Cheddadi R *et al.* (2003) Glacial refugia: hotspots but not melting pots of genetic diversity. *Science* **300**, 1563-1565.

Pías B, Matesanz S, Herrero A, Gimeno TE, Escudero A, Valladares F (2010) Trangenerational effects of three global change drivers on an endemic Mediterranean plant. *Oikos* **119**, 1435-1444.

Pilcher JR (1990) Sample Preparation, Cross-dating, and Measurements. In 'Methods of Dendrochronology – Applications in the Environmental Sciences' (Eds. ER Cook, LA Kairiukstis) pp. 40-50. (Kluwer Academic Publishers, Dordrecht, the Netherlands).

Piñol J, Lledó MJ, Escarré A (1991) Hydrological balance of two Mediterranean forested catchments (Prades, northeast Spain). *Hydrological Sciences Journal* **36**, 95-107.

Piñol J, Terradas J, Lloret F (1998) Climate warming, wildfire hazard, and wildfire occurrence in coastal eastern Spain. *Climate Change* **38**, 345-357.

Planells O, Gutiérrez E, Helle G, Schleser GH (2009) A forced response to twenty century climate conditions of two Spanish forests inferred from widths and stable isotopes of tree rings. *Climatic Change* **97**, 229-252.

Pons X (1996) Estimación de la radiación solar a partir de modelos digitales de elevaciones. Propuesta metodológica. In 'VII Coloquio de Geografía Cuantitativa, Sistemas de Información Geográfica y Teledetección'. (Eds. J Juaristi, I Moro) pp. 87-97. (Vitoria-Gasteiz: Spain).

Poyatos R, Latron J, Llorens P (2003) Land use and land cover change after agricultural abandonment – The case of a Mediterranean mountain area (Catalan Pre-Pyrenees). *Mountain Research and Development* **23**, 362-368.

Poyatos R, Aguadé D, Galiano L, Mencuccini M, Martínez-Vilalta J (2013) Drought-induced defoliation and long periods of near-zero gas exchange play a key role in accentuating metabolic decline of Scots pine. *New Phytologist* doi: 10.1111/nph.12278.

R Development Core Team R v.3.0 (2013) R: A Language and Environment for Statistical Computing. R Foundation for Statistical Computing, Vienna, Austria. URL http://www.r-project.org/

Ramírez-Valiente JA, Valladares F, Gil L, Aranda I (2009) Population differences in juvenile survival under increasing drought are mediated by seed size in cork oak (*Quercus suber* L.). *Forest Ecology and Management* **257**, 1676-1683.

Régent Instruments Inc (2004*c*) WinDendro for Tree-rings analysis, Régent Instruments Quebec, Canada.

Régent Instruments Inc (2013) WinCELL for Wood Cell aanalysis, Régent Instruments Quebec, Canada.

Régent Instruments Inc (2013) XLCELL for Wood Cell aanalysis, Régent Instruments Quebec, Canada.

Reich PB, Oleksyn J (2008) Climate warming will reduce growth and survival of Scots pine except in the far north. *Ecology Letters* **11**, 588-597.

Rigling A, Waldner PO, Forster T, Bräker OU, Pouttu A (2001) Ecological interpretation of tree-ring width and intraannual density fluctuations in *Pinus sylvestris* on dry sites in the central Alps and Siberia. *Canadian Journal of Forest Research* **31**, 18-31.

Rigling A, Bräker O, Schneiter G, Schweingruber F (2002) Intra-annual tree-ring parameters indicating differences in drought stress of *Pinus sylvestris* forests within the Erico-Pinion in the Valais (Switzerland). *Plant Ecology* **163**, 105-121.

Rigling A, Bigler C, Eilmann B, Feldmeyer-Christe E, Gimmi U, Ginzler C, Graf U, Mayer P, Vacchiano G, Weber P, Wohlgemuth T, Zweifel R, Dobbertin M (2013) Driving factors of a vegetation shift from Scots pine to pubescent oak in dry Alpine forests. *Global Change Biology* **19**, 229-240.

Rigling A, Bigler C, Eilmann B, Feldmeyer-Christe E, Gimmi U, Ginzler C, Graf U, Mayer P, Vacchiano G, Weber P, Wohlgemuth T, Zweifel R, Dobbertin M (2013) Driving factors of a vegetation shift from Scots pine to pubescent oak in dry Alpine forests. *Global Change Biology* **19**, 229-240.

Robertson A, Overpeck J, Rind D, Mosley-Thompson E, Zielinski G, Lean J, Koch D, Penner J, Tegen I, Healy R (2001*a*) Hypothesized climate forcing time series for the last 500 years. *Journal of Geophysical Research* **106**, 14783-14803.

Sage RF, Santrucek J, Grise DJ (1995) Temperature effects on the photosynthetic response of C_3 plants to long-term CO_2 enrichment. *Vegetatio* **121**, 67-77.

Sala A, Piper F, Hoch G (2010) Physiological mechanisms of drought-induced tree mortality are far from being resolved. *New Phytologist* **186**, 274-281.

Sala A, Woodruff DR, Meinzer FC (2012) Carbon dynamics in trees: feast or famine? *Tree Physiology* **32**, 764-775.

SAS Institute Inc. (2012) Version 9.3. (SAS Inc. Cary NC: USA).

Saurer M, Siegenthaler U, Schweingruber F (1995) The climate-carbon isotope relationship in tree rings and the significance of site conditions. *Tellus B* **47**, 320-330.

Saurer M, Siegwolf RTW, Schweingruber FH (2004) Carbon isotope discrimination indicates improving water-use efficiency of trees in northern Eurasia over the last 100 years. *Global Change Biology* **10**, 2109-2120.

Savolainen O, Kujala ST, Sokol C, Pyhäjärvi T, Avia K, Knürr T, Kärkkäinen K, Hicks S (2011) Adaptive potential of northernmost tree populations to climate change, with emphasis on Scots pine (*Pinus sylvestris* L.). *Journal of Heredity* **102**, 526–536.

Schweingruber FH (2007) Wood Structure and Environment. In 'Wood Science'. (Springer-Verlag, Berlin, Germany).

Sevanto S, McDowell N, Dickman LT, Pangle R, Pockman WT (2013) How do trees die? A test of the hydraulic failure and carbon starvation hypotheses. *Plant, Cell and Environment* doi: 10.1111/pce.12141.

SPSS Inc (2006) Version 15.0 for Windows. (SPSS Inc. Chicago IL: USA).

SPSS Inc. IBM Company (2010) Version 19.0 for Windows. (SPSS Inc. Chicago IL: USA).

Suarez ML, Ghermandi L, Kitzberger T (2004) Factors predisposing episodic drought-induced tree mortality in *Nothofagus* – site, climatic sensitivity and growth trends. *Journal of Ecology* **92**, 954-966.

Tardif J, Camarero JJ, Ribas M, Gutiérrez E (2003) Spatiotemporal variability in tree growth in the Central Pyrenees: climatic and site influences. *Ecological Monographs* **73**, 241–257.

Thornthwaite CW (1948) An approach toward a rational classification of climate. *Geographical Review* **38**, 55-94.

Tyree MT, Zimmerman MH (2002) Xylem structure and the ascent of sap (2nd ed.). (Springer-Verlag, New York, USA).

UNESCO (1979) Map of the world distribution of arid regions: explanatory note. MAB technical notes. (Paris, UNESCO: France).

Vaganov EA (1990) The tracheidogram method in tree-ring analysis and its application. In 'Methods of dendrochronology: applications in the environmental

sciences'. (Eds. ER Cook, LA Kairiukstis) pp. 63-76. (Kluwer Academic Publishers, Dordrecht, the Netherlands).

Vaganov EA, Hughes MK, Shashkin AV (2006) Growth dynamics of conifer tree rings: Images of past and future environments. (Springer: Berlin).

van Mantgem PJ, Stephenson NL, Byrne JC, Daniels LD, Franklin JF, Fulé PZ, Harmon ME, Larson AJ, Smith JM, Taylor AH, Veblen TT (2009) Widespread Increase of Tree Mortality Rates in the Western United States. *Science* **323**, 521-524.

Vayreda J, Martínez-Vilalta J, Gracia M, Retana J (2012*b*) Recent climate changes interact with stand structure and management to determine changes in tree carbon stocks in Spanish forests. *Global Change Biology* **18**, 1028-1041.

von Arx G, Dietz H (2005) Automated image analysis of annual rings in the roots of perennial forbs. *International Journal of Plant Sciences* **166**, 723-732.

von Arx G (2006) A Tool for the analysis of Annual Root Rings in Perennial Forbs. *Media Cybernetics' Application Note*.

von Arx G, Archer SR, Hughes MK (2012) Long-term functional plasticity in plant hydraulic architecture in response to supplemental moisture. *Annals of Botany* **109**, 1091-1100.

Vicente-Serrano SM, Beguería S, López-Moreno JI (2010*a*) A multi-scalar drought index sensitive to global warming: the standardized precipitation evapotranspiration index. *Journal of Climate* **23**, 1696-1718.

Vicente-Serrano SM, Beguería S, López-Moreno JI, Angulo M, El Kenawy A (2010*b*) A new global 0.5° gridded dataset (1901-2006) of a multiscalar drought index: comparison with current drought index datasets based on the Palmer drought severity index. *Journal of Hydrometeorology* **11**, 1033-1043.

Vilà-Cabrera A, Martínez-Vilalta J, Vayreda J, Retana J (2011) Structural and climatic determinants of demographic rates of Scots pine forests across the Iberian Península. *Ecological Applications* **21**, 1162–1172.

Vilà-Cabrera A, Martínez-Vilalta J, Galiano L, Retana J (2013) Patterns of forest decline and regeneration across Scots pine populations. *Ecosystems* **16**, 323-335.

Villalba R, Veblen TT (1998) Influences of large-scale climatic variability on episodic tree mortality in northern Patagonia. *Ecology* **79**, 2624-2640.

Voltas J, Camarero JJ, Carulla D, Aguilera M, Ortiz A, Ferrio JP (2013) A retrospective, dual-isotope approach reveals individual predispositions to winter-

drought induced tree dieback in the southernmost distribution limit of Scots pine. *Plant, Cell and Environment* **36**, 1435-1448.

von Wilpert K (1991) Intraannual variation of radial tracheid diameters as monitor of site specific water stress. *Dendrochronologia* **9**, 95–113.

Vysotskaya LG, Vaganov EA (1989) Components of the variability of radial cell size in tree rings of conifers. *IAWA Bulletin* **10**, 417-428.

Waring RH, Pitman GB (1985) Modifying lodgepole pine stands to change susceptibility to mountain pine beetle attack. *Ecology* **66**, 889–897.

Waring RH (1987) Characteristics of trees predisposed to die. *Bioscience* **37**, 569–574.

Warren CR, McGrath JF, Adams MA (2001) Water availability and carbon isotope discrimination in conifers. *Oecologia* **127**, 476-486.

Waterhouse JS, Switsur VR, Barker AC, Carter AHC, Hemming DL, Loader NJ, Robertson I (2004) Northern European trees show a progressively diminishing response to increasing atmospheric carbon dioxide concentration. *Quaternary Science Reviews* **23**, 803-810.

Weber P, Bugmann H, Rigling A (2007) Radial growth responses to drought of *Pinus sylvestris* and *Quercus pubescens* in an inner-Alpine dry valley. *Journal of Vegetation Science* **18**, 777-792.

Wigley TML, Briffa KR, Jones PD (1984) On the average value of correlated time series, with applications in dendroclimatology and hydrometeorology. *Journal of Climate and Applied Meteorology* **23**, 201–213.

Williams AP, Allen CD, Macalady AK, Griffin D, Woodhouse CA, Meko DM, Swetnam TW, Rauscher SA, Seager R, Grissino-Mayer HD, Dean JS, Cook ER, Gangodagamage C, Cai M, McDowell N (2013) Temperature as a potent driver of regional forest drought stress and tree mortality. *Nature Climate Change* **3**, 292-297.

Wimmer R (2002) Wood anatomical features in tree-rings as indicators of environmental change. *Dendrochronologia* **20**, 21-36.

Woodward FI (1987) Climate and Plant Distribution. (Cambridge University Press, Cambridge, UK).

Wong SC, Cowan IR, Farquhar GD (1979) Stomatal conductance correlates with photosynthetic capacity. *Nature* **282**, 424–426.

Zweifel R, Zimmermann L, Zeugin F, Newbery DM (2006) Intra-annual radial growth and water relations of trees: implications towards a growth mechanism. *Journal of Experimental Botany* **57**, 1445-1459.

ACKNOWLEDGEMENTS

I would like to thank my teachers Jordi and Bernat that made possible this doctorate and from whom I learned so many things. First of all, for the opportunity they gave me to win a scholarship and get out from Romania. Then, for the huge patience with the statistics, as when they first said this word, although they pronounced it in English, I thought they were saying something in a strange language I never heard before. Thanks a lot for teaching me how to write a scientific paper although you had to spend so much time sending me hundreds of versions of the discussions (sorry for that!). Not to mention the intense field campaigns.

Many thanks to Jordi Voltas and Chechu Camarero for accepting me in their laboratories and for introducing me in the interesting world of the isotopes and wood anatomy studies. Also, to all the people in your labs that have helped me with the thousands of samples I had and that have taken care of me not only inside the lab but also outside it. Thanks to them I had the opportunity to visit places and to get in contact with curious cultural customs like eating snails and dancing “La Jota”. I will never forget you guys: Mara, Mònica, Pitter, Pilar, Ángela, Arben, Edmond.

Thanks to all the people in CREAF. For the field work assistance and interesting discussions related with my thesis (Maurizio, Albert) or the logistics and chocolate (Magda, Marta). For the special moments and interesting/strange discussions spent during lunch time and sky weekends: Ana, Monica, Vir, Xavi, Gerardo, Rafa, Eli, Roberto, Lucie, Oliver. Thanks to Ana for putting into my hands one day the very helpful and *heavy* statistics book of Andy … this helped me to understand the strange language Jordi and Bernat were talking.

Mulțumesc familiei mele, fără de care nu aş fi reuşit să fac un doctorat şi care m-au susținut mereu fiind încrezători în mine: mami, moşica, Vasi, Luminița, bunicii şi toată trupa de la Cîțcău. Mulțmesc prietenei mele Carmen pentru ca m-a primit în căsuța ei unde m-am simțit ca acasa şi care mi-a trimis frecvent mesaje de încurajare şi şuturi ajutătoare. Mulțumesc prietenilor de la Cluj are au făcut ca vacanțele petrecute în țară

să fie intense şi plăcute. Mulțumesc Corinei şi lui Romà pentru că prin intermediul lor am avut parte de un colț din Romînia in CREAF.

No tinc prou paraules per agrair a la meva estimada família catalana: Alícia, Santi, Carme, Dolors, Josep, Cris (:P). Gràcies a vosaltres la meva vida a Cardedeu ha sigut i es molt feliç. Vosaltres m'heu ensenyat el significat i la importància de la tranquil·litat en la vida d'una persona i que mirar las coses amb optimisme sempre ajuda. Gràcies per cuidar-me i per estar sempre el meu costat en els moments difícils. Per fer-me sempre sentir com una persona mes de la casa. I per tot lo altre que no puc escriure aquí ...

Moltes gràcies també a la Pepa i en Quico per acollir-me el seu pis, en Flama per la seva ajuda amb la informàtica i a tots els alters amics de Cardedeu per la bona companya i els moments agradables passats junts.

Muchas gracias a Jorge y toda su familia de Madrid por quererme, haberme integrado en sus vidas y haber estado a mi lado apoyándome tanto sobre todo en los últimos meses de la tesis cuando el estrés y los nervios han sido máximos.